THE CORDILLERAN LITHOSPHERE IN SOUTH-CENTRAL BRITISH COLUMBIA: INSIGHTS FROM TWO XENOLITH SUITES

by

Ryan Keith Kroner

B.A., Colorado College, 2016

A THESIS SUBMITTED IN PARTIAL FULFILLMENT OF THE REQUIREMENTS FOR THE DEGREE OF

MASTER OF SCIENCE

in

THE FACULTY OF GRADUATE AND POSTDOCTORAL STUDIES

(Geological Sciences)

THE UNIVERSITY OF BRITISH COLUMBIA

(Vancouver)

June 2019

The following individuals certify that they have read, and recommend to the Faculty of Graduate and Postdoctoral Studies for acceptance, a thesis/dissertation entitled:

The Cordilleran lithosphere beneath south-central British Columbia: insights from two xenolith suites

submitted by Ryan Kroner in partial fulfillment of the requirements for

the degree of Master of Science

in Geological Sciences

Examining Committee:

James Kelly Russell, Geological Sciences
Supervisor

Maya Kopylova, Geological Sciences
Supervisory Committee Member

Lori Kennedy, Geological Sciences
Supervisory Committee Member

Lee Groat, Geological Sciences
Additional Examiner

ABSTRACT

Mantle-derived peridotite xenoliths represent a valuable source of information about the structure, chemistry, origin, and evolution of the mantle lithosphere underlying various tectonic environments. Xenolith-bearing volcanic suites at Mt. Timothy and Summit Lake in south-central British Columbia are two particularly intriguing sites for evaluating the nature of the lithosphere beneath the southern Canadian Cordillera. The peridotite xenoliths at Mt. Timothy are texturally and mineralogically homogenous, while the xenoliths from Summit Lake contain a greater variety of textures and rock types, both mantle-derived and crustal. These peridotites are similar geochemically to other peridotite datasets from the Canadian Cordillera, indicating a geochemically homogenous mantle lithosphere and evolution from a fertile peridotite source. Enrichments of MREEs and LREEs in certain samples may indicate that these rocks were subject to a small degree of metasomatism. The geochemical signatures of the pyroxenes in these xenoliths are indicative of an orogenic lithospheric mantle. Temperatures and depths of equilibration for these peridotites have been determined by combining a two-pyroxene geothermometer with a geotherm constructed from several regional geophysical parameters. The Mt. Timothy peridotites sample an extensive window of mantle lithosphere ranging from the Moho (813 °C; 33 km) to relatively deep within the mantle lithosphere (1091 °C; 50.9 km), while the Summit Lake peridotites sample a very deep and narrow window of mantle lithosphere (1061 °C to 1119 °C; 49.0 km to 52.7 km). The window sampled by Mt. Timothy is most similar to a number of other xenolith suites scattered across the southern Cordillera, while the comparatively unique sampling range of the Summit Lake suite shares certain mineralogical characteristics with other xenolith suites straddling the boundary between the Cordillera and the North American craton.

LAY SUMMARY

Peridotite xenoliths brought to the surface from the mantle by magma can be used as proxies for studying the physical and chemical conditions of the lithospheric mantle underlying the Canadian Cordillera in south and central British Columbia. This study describes xenoliths collected at two volcanic units at Summit Lake and Mt. Timothy. They are broadly similar to each other and to other sites around British Columbia in terms of geochemistry, and they both suggest that the lithospheric mantle they sample is genetically tied to Cordilleran arc terranes rather than older material in the North American craton to the east. The two sites do represent very different mantle conditions, with the Mt. Timothy samples recording a very broad range of temperatures and depths and the Summit Lake samples recording a narrow range of deep and hot conditions. This may reflect the differing tectonic settings the two sites occupy.

PREFACE

This thesis was written and researched by myself with significant editorial input in multiple stages from J. K. Russell. John Chapman, formerly of the Geological Survey of Canada, provided significant assistance with the early stages of this research and with the requisite fieldwork.

TABLE OF CONTENTS

LIST OF TABLES

LIST OF FIGURES

ACKNOWLEDGEMENTS

This research was funded by the Geological Survey of Canada under Targeted Geoscience Initiative (TGI) P-1.4, “Temporal and spatial controls on the nature and distribution of porphyry-style deposits,” a subsection led by John Chapman. I would like to thank John and his colleagues at the GSC for providing invaluable guidance and advisement during the first stages of this research and Neil Rogers for providing guidance especially during its later stages.

I would like to thank my UBC advisor Kelly Russell for being the driving force behind this research and for the wisdom and nearly infinite patience he lent me over this entire process. Sincere thanks go to rest of my advisory committee – Lori Kennedy and Maya Kopylova – for lending their time and effort to guide this research and help revise this thesis, and additionally to Lee Groat for being my external examiner. I would also like to thank my fellow VPL lab members Alex Wilson and Amy Ryan for their valuable assistance and advice during all stages of this research.

My sincere gratitude also goes to Christopher Lawley at the Geological Survey of Canada in Ottawa for the time and effort he generously donated to this project in analyzing the bulk geochemistry of these xenoliths through his pressed nanoparticulate powder pellets methodology.

1. INTRODUCTION

Lithospheric xenoliths, both crustal and mantle-derived, are commonly present as inclusions in mafic volcanic centers across the globe. The magmas sample, entrain, and erupt fragments of the lower crust and upper mantle. These xenoliths provide a unique opportunity to study the properties of the lithosphere associated with various tectonic environments. By using these samples as proxies for the lithosphere, it is possible to quantify the physical and chemical properties of the underlying lithospheric mantle, including its geochemistry, structure, temperature, and rheology. Furthermore, comparing xenolith-bearing suites from across a broader tectonic region can identify vertical and lateral variations in lithospheric structure, organization, and properties that inform its origins.

The Canadian Cordillera is a tectonic region particularly rich in xenolith-bearing volcanic centers, especially in the low-lying accreted terranes of the Intermontane Belt. Many of these centers have undergone significant study in the past (Edwards and Russell, 2000; Francis et al., 2010). The thin, warm lithospheric mantle of an orogenic belt such as the Canadian Cordillera is composed primarily of olivine, orthopyroxene, clinopyroxene, and spinel. This research has included both studies of individual volcanic centers (Brearley et al., 1984; Fujii and Scarfe, 1982; Canil et al., 1987) and comprehensive accounts of variations across certain sections of the Cordillera (Peslier et al., 2002; Harder and Russell, 2006; Francis et al., 2010). These studies have thus far suggested a somewhat homogeneous lithospheric mantle in terms of geochemistry, age, and thickness (Peslier et al., 2000b).

Here, I present a detailed account of xenoliths recovered from two volcanic centers in south and central British Columbia. The first xenolith suite, located at Summit Lake (near Prince George), has been studied previously by Ross (1983), Brearley et al. (1984), and Saruwatari et al.

(2001). However, its uniqueness in terms of both the xenoliths it contains and the tectonic setting upon which it lies makes it worth re-examination. Mt. Timothy, located near 100 Mile House, is another volcanic center rich in mantle xenoliths that has not previously been studied (Schiarizza et al., 2008; Schiarizza et al., 2013).

The principal goal of this work is to use the mineral chemistry of peridotite xenoliths to estimate the temperature and depth from which these lithospheric xenoliths were sourced. These temperatures and depths are used to construct vertical profiles of the lithosphere beneath both Intermontane volcanic centers. Within the context of these vertical profiles, I have also measured bulk xenoliths for their bulk chemical compositions, modal mineralogy, mineral compositions, and their mineral fabrics. These data are used to assess variations within and between the two xenolith suites. Lastly, the results obtained from the sample collections at Summit Lake and Mt. Timothy are compared to published data from xenolith suites across British Columbia in order to illustrate the range of physical and chemical properties of the lithosphere underlying the southern Canadian Cordillera. The localities are characterized on an individual basis and then examined against each other as conclusions are drawn regarding the significance of any chemical or mineralogical variations that exist between Summit Lake and Mt. Timothy. Links between any divergent properties of the two sites and the unique geological and tectonostratigraphic settings they occupy is addressed. Finally, this research is used to address larger-scale questions regarding the tectonic structure and evolution of the Cordilleran lithosphere.

2. REGIONAL GEOLOGY

The purpose of this chapter is to (a) describe the regional and tectonic setting of the Mt. Timothy and Summit Lake localities, and (b) describe the nature and distribution of crustal and mantle xenoliths observed at both localities.

2.1 GEOLOGY OF THE SOUTHERN CANADIAN CORDILLERA

The Canadian Cordillera is a relatively young mountain belt that extends from southern British Columbia up into Alaska was primarily amalgamated between the middle Jurassic (185 ma) and the late Cretaceous (90-85 ma) (Monger and Price, 2002; Nelson and Colpron, 2007). It is comprised of four large-scale geomorphological belts, listed in order from east to west, and displayed in Figure 2.1: 1) ancestral North America, 2) the Intermontane Belt, 3) the Coast Belt (overlap between the Intermontane and Insular belts), and 4) the Insular Belt (Monger and Price, 2002). Of these, the Intermontane Belt, which in British Columbia is primarily comprised by rocks of the Quesnellia, Stikinia, and Cache Creek terranes, is the most relevant to this research, as it houses the majority of xenolith-bearing volcanic units recorded in this part of the Cordillera. These terranes are bordered to the east by ancestral North American basement material and to the west by the terranes of the Coast Belt and the Insular Belt. Scattered slivers of the upper Paleozoic Slide Mountain terrane can be found along the boundary between North American basement and the Quesnellia terrane (Nelson and Colpron, 2007).

The Quesnellia and Stikinia terranes are believed to be fragments of a late Paleozoic to early Mesozoic island arc, while the Cache Creek terrane, which lies between the two, is an early Mesozoic accretionary complex formed as the island arcs accreted onto the North American continental margin (Monger and Price, 2002).

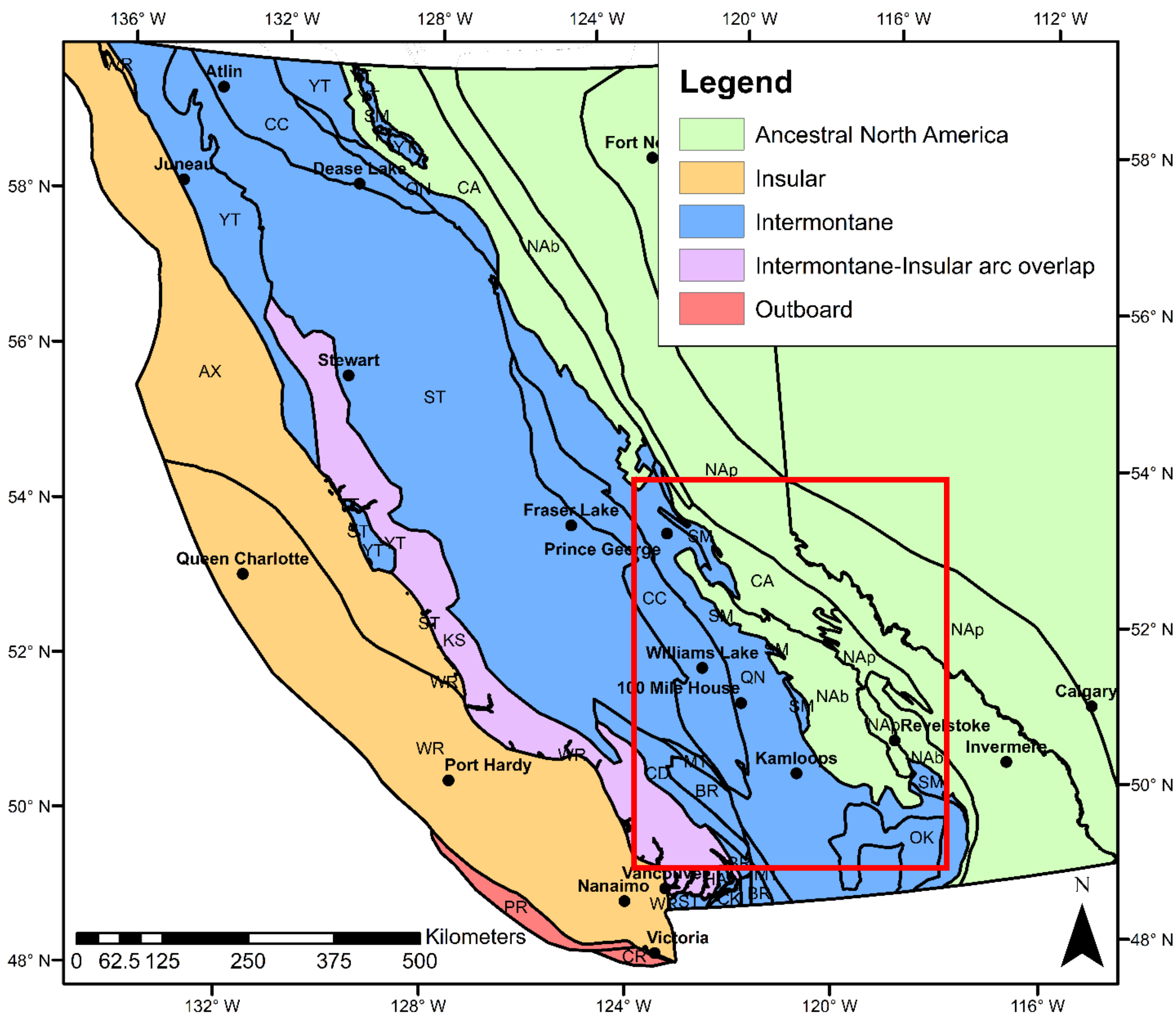

Figure 2.1 – Map of the Canadian Cordillera in British Columbia outlining boundaries of its five major tectonic realms. Major BC cities are marked with points; red box indicates the section of southern BC that is the focus of this study (see Figure 2.2). Terrane abbreviations are per the legend for Figure 2.2. Colpron and Nelson, 2007.

The Cordilleran crust comprises Phanerzoic and Mesoproterozoic material and its underlying mantle is roughly 1.1 Ga in age, based on Re-Os dating of peridotite mantle xenoliths collected from across the Cordillera (Peslier et al., 2000b). The exact relationship between the Cordilleran crust and upper mantle is one that has yet to be definitively resolved. The first school of thought posits that the Cordilleran mantle lithosphere is allochthonous: that is, the mantle material underlying the Cordilleran crust is associated with the North American craton, and lithospheric decoupling occurred during the accretion of the associated terranes (Clowes et al., 1998; Peslier et al., 2000b; Monger and Price, 2002; Cook et al., 2004). The alternative hypothesis proposes an allochthonous view of the Cordilleran lithosphere, where the mantle underlying this region is exotic material that was coupled to individual Cordilleran terranes and brought onboard as they accreted onto the continental margin (Abraham et al., 2001).

2.2 GEOLOGICAL SETTING OF XENOLITH LOCALITIES

Xenolith-bearing volcanic centers can be found scattered across the northwest-southeast trend of Canadian Cordillera's Intermontane Belt, with many predominantly Quaternary to Neogene units distributed across the Quesnel terrane in south to central British Columbia. The host volcanics are almost entirely alkaline mafic magmas including basanite, nephelinite, and alkali olivine basalt. The entrained mantle-derived peridotite xenoliths are of interest to researchers as they provide constraints on the physical and chemical conditions of the Cordilleran lithospheric mantle since the late 1960s (Soregaroli, 1968; Littlejohn and Greenwood, 1974; Fujii and Scarfe, 1982; Ross, 1983; Brearley and Scarfe, 1984; Brearley et al., 1984; Canil et al., 1987; Canil and Scarfe, 1989; Francis et al., 2010; Greenfield et al., 2013).

The two specific areas from which xenolith-bearing volcanics in this study were sampled were chosen in large part for their distinct tectonic and geographical settings. Both the Summit Lake region and the Mt. Timothy region share similar settings on a larger scale, with both being relatively young volcanic centers located in the southern part of the Canadian Cordillera's Intermontane Belt (Figure 2.2). The primary difference between the two in terms of tectonic setting lies in their relative proximities to North American cratonic basement material to the east. The Mt. Timothy field site is located atop the solely Cordilleran crust and lithosphere of the accreted Quesnel terrane. While the xenoliths from the Mt. Timothy volcanics not yet been thoroughly characterized and studied, studies of a similar nature have been undertaken for units in similar settings such as the xenolith-bearing volcanic units at Rayfield River and Big Timothy (Greenfield et al., 2013). The Summit Lake volcanics, on the other hand, lie directly atop the transition from Quesnel units to the west and rocks of the Slide Mountain and cratonic terranes to the east.

2.2.1 SUMMIT LAKE

The Summit Lake locality is a localized volcanic feature located in the Macleod Lake mapping area (NTS 93J/07), a part of the larger Northern Nechako River area within central British Columbia's Omineca Belt (Resnick et al., 1999). Detailed geological mapping for this area, located roughly 44 km north of Prince George, was largely undertaken in the early 1990s (Struik, 1994). Previous studies involving the Summit Lake xenoliths have been undertaken by Ross (1983), Brearley et al. (1984), and Peslier et al. (2002).

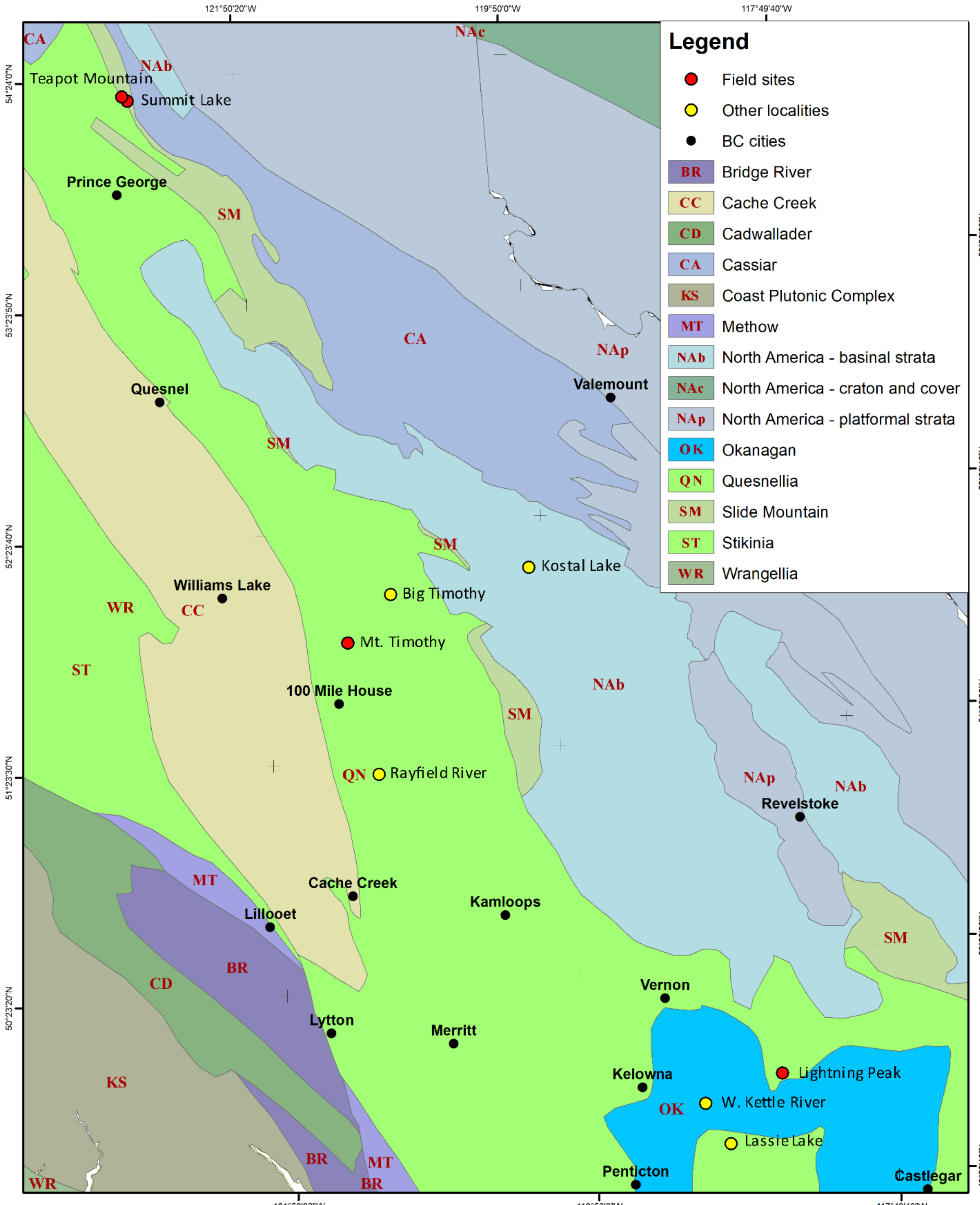

Figure 2.2 – Geological map of south-central British Columbia detailing the Intermontane terranes, and with xenolith-bearing localities marked. Terrane boundaries per Colpron and Nelson, 2011.

The Summit Lake occurrence is situated between accreted arc rocks of the intermontane Quesnel terrane to the west and the North American cratonic units to the east. The geology to the north and west of the Summit Lake volcanics is dominated by Mississippian to Permian basalts of the Antler formation, a part of the larger Slide Mountain group, while younger volcanics of the Takla group (Triassic to Jurassic) can be found to the south and west of Summit Lake (Logan et al., 2010). These two units are bisected by a northwest-southeast-trending fault and are directly overlain by the Chilcotin group basalts to which the Summit Lake locality belongs.

This region is comprised largely of low-lying hills and dense vegetation broken up by numerous water bodies and as such these Chilcotin volcanics have few surface exposures. The Summit Lake locality, located on the northeastern corner of Summit Lake itself, is a thick, columnar jointed lava flow exposed as a largely abandoned rock quarry (Figure 2.3a). A smaller exposure called Talus Quarry, still sporadically active in the work week, is located on the southwestern margin of the Summit Lake unit (Figure 2.3b). Teapot Mountain (917 m), the other prominent exposure of these xenolith-bearing Chilcotin basalts, is a topographically prominent volcanic neck located approximately 3.5 km to the northeast of the Summit Lake quarry. Another occurrence of Chilcotin volcanics exists to the north of the Summit Lake/Teapot Mountain unit, with exposures at Coffeepot mountain (1017 m) 14.8 km north of the Summit Lake quarry and a series of densely vegetated bluffs 10.5 km northwest of the quarry. These rocks were investigated and were found to be more silicic and significantly less xenolith-rich than the basalt of the Teapot/Summit Lake unit.

The unit comprising the primary quarry at Summit Lake and the peripheral semi-active Talus Quarry (coordinates for both are listed in Table 2.1) is composed of a very well-exposed and well-preserved xenolith-bearing volcanic unit. The xenolith-hosting material is a medium-

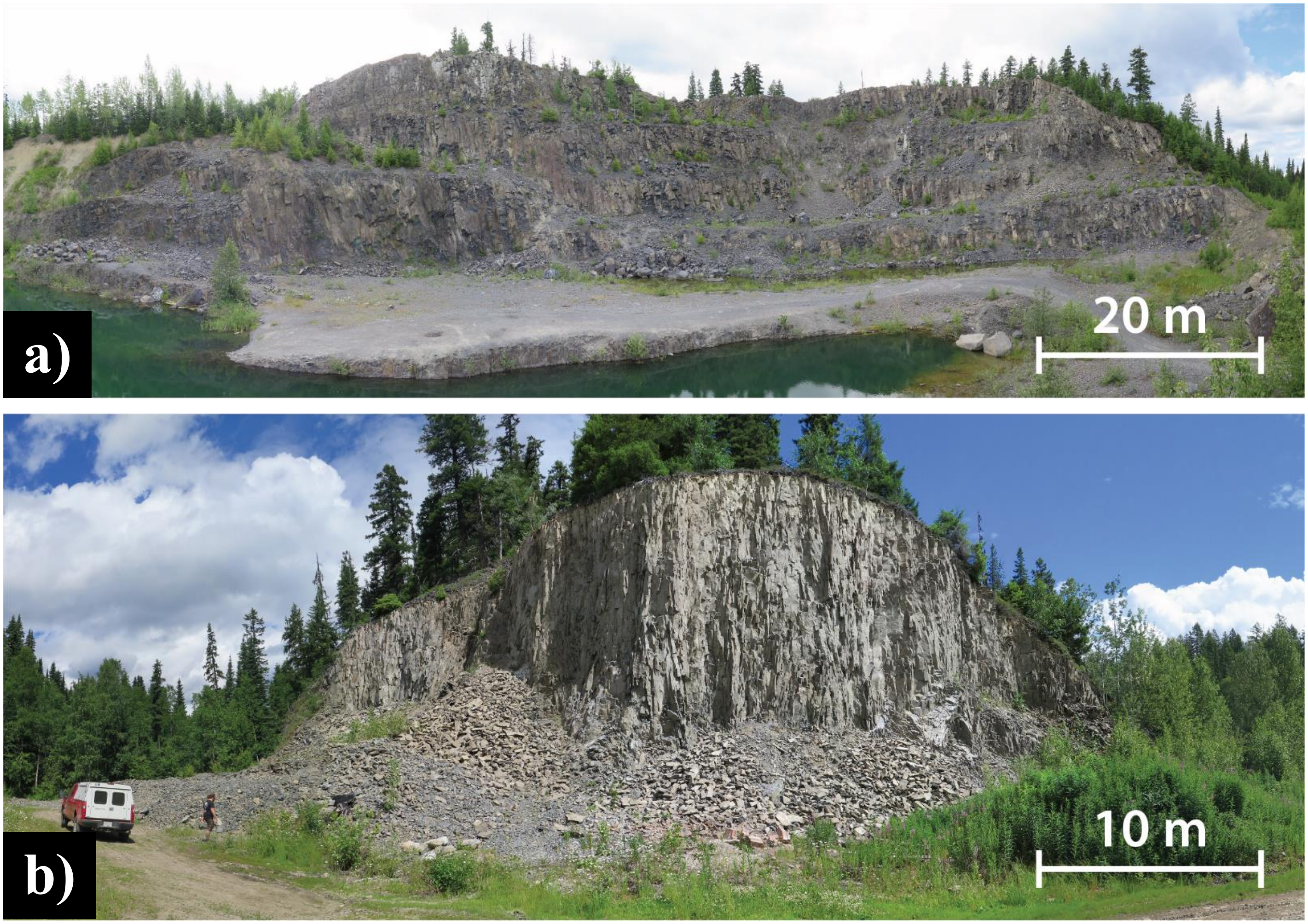

Figure 2.3 – Field photos of the Summit Lake xenolith-bearing locality. (A) The primary sampling site in the abandoned quarry; photograph looks to S/SW; (B) a smaller, semi-active talus quarry on the southwest margin of the unit; photograph looks to NE.

Table 2.1 – Coordinates and references for the primary xenolith sampling sites at Summit Lake and Mt. Timothy. Terranes are listed based on boundaries marked by Colpron and Nelson (2011). Sites marked with an asterisk were visited and sampled but were not included in this study beyond having the bulk geochemistry of their host lavas analyzed (see Chapter 4). Sites marked with a cross were visited and sampled but underwent no analyses for this study. Sample collections for these are available at UBC. See Appendix D for further details about these additional field sites and Appendix A for descriptions of the samples collected from these sites.

Locality	Latitude	Longitude	Terrane	Map reference
Prince George				
Summit Lake quarry	54° 18' 25.5"	122° 38' 24.3"	Slide Mountain	Struik, 1994
Talus quarry	54° 18' 25.9"	122° 38' 38.8"	Slide Mountain	Struik, 1994
Teapot Mountain*	54° 19' 35.5"	122° 40' 48.9"	Slide Mountain/Quesnel	Struik, 1994
Coffeepot Mountain†	54° 25' 08.2"	122° 45' 11.4"	Slide Mountain	Struik, 1994
Indigo Lake bluffs†	54° 22' 37.4"	122° 45' 05.3"	Quesnel	Struik, 1994
Mt. Timothy				
Talus slope	51° 54' 16.2"	121° 15' 52.8"	Quesnel	Schiarizza et al., 2008
Pyroclastic outcrop	51° 54' 12.2"	121° 15' 29.2"	Quesnel	Schiarizza et al., 2008
Timothy Lake flow	51° 52' 24.1"	121° 15' 18.9"	Quesnel	Schiarizza et al., 2008
Coffee Lake*	52° 00' 38.4"	121° 06' 04.5"	Quesnel	Schiarizza et al., 2013
Boss Creek†	52° 02' 37.3"	120° 51' 21.9"	Quesnel	Schiarizza and Macauley, 2007
Okanagan				
Lightning Peak*	49° 52' 44.7"	118° 31' 50.6"	Quesnel	Little, 1957
West Kettle River†	49° 46' 55.2"	119° 04' 01.2"	Okanagan	Little, 1961
Lassie Lake†	49° 35' 45.6"	118° 55' 30.0"	Quesnel	Christopher, 1978

dark grey, very fine-grained, aphanitic alkaline basalt. Xenoliths of various rock types comprise roughly 10-15% of the unit by volume, and there is little discernable vertical or lateral variation in xenolith volume across the unit. Xenoliths range in size from < 1 cm to 30 cm and are dominated by peridotites, with approximately 20% of the xenolith population consisting of various crustal rock types ranging from very fine-grained quartzites to coarse-grained, banded gabbroic material. While the majority of peridotite xenoliths from the Summit Lake unit are medium-grained, spinel-bearing lherzolites, the mantle xenoliths here display a much greater variety of textures and rock types than the corresponding units from the Mt. Timothy region. Xenoliths of all rock types are generally competent and moderately well-preserved, although some of the more heavily exposed peridotites display varying degrees of chemical weathering.

2.2.2 MOUNT TIMOTHY

Mount Timothy is a volcanic edifice located within the Timothy Lake mapping area (NTS 92P/14), which covers roughly 950 km^2 on the eastern edge of south-central British Columbia's Interior Plateau in the South Cariboo region (Schiarizza et al., 2008). Detailed mapping for this area, which comprises the communities of Lac La Hache and Forest Grove along with the western subdivision of the Canim Lake Indian Reserve, was undertaken in 2007. The mountain itself is located approximately 18 km northeast of Lac La Hache and 30 km north of 100 Mile House and sees use as a small local ski hill during the winter months (Figure 2.4a).

Mt. Timothy straddles a split in this mapping area between Middle to Upper Triassic Nicola group to its west and Early Jurassic rocks of the Takomkane batholith to its east. The underlying Nicola Group units are dominated by volcaniclastic successions of basaltic breccia, sandstone, and others along with swathes of Nicola group polylithic breccias and a red sandstone

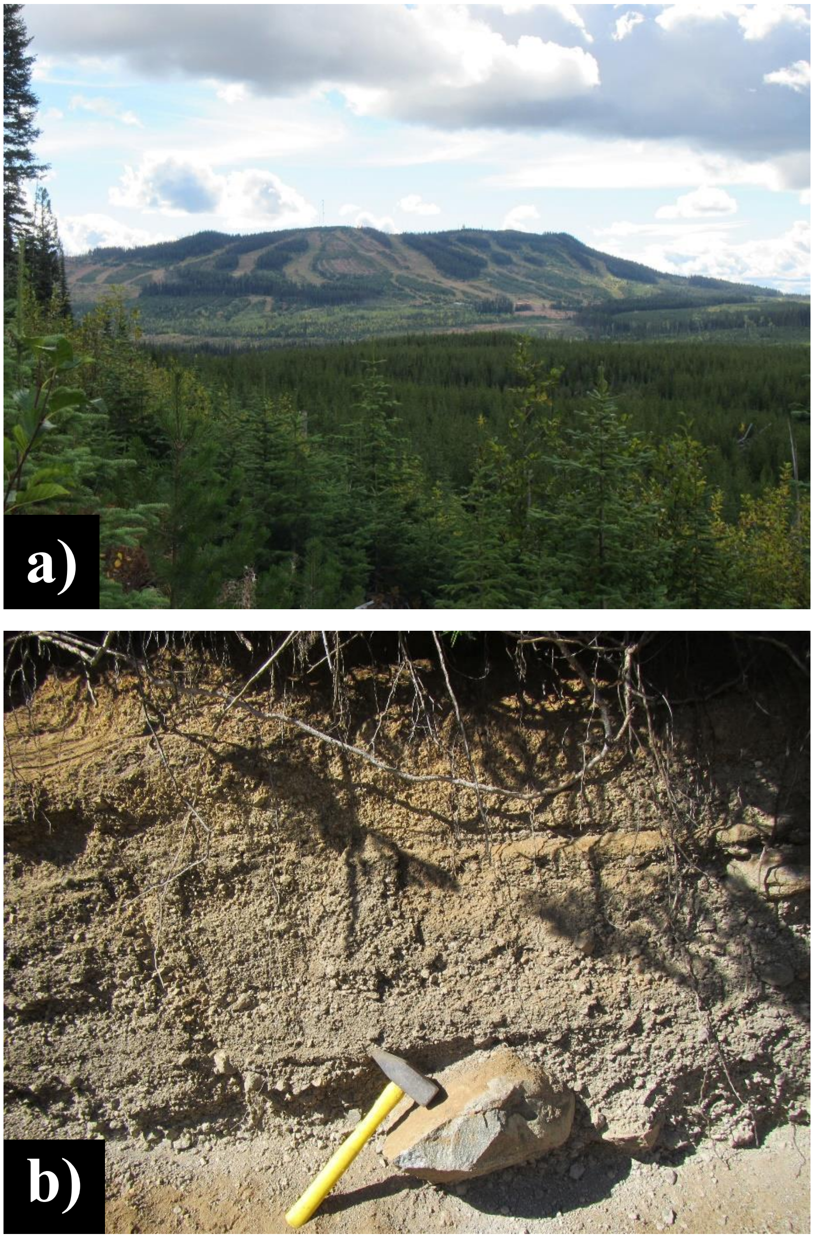

Figure 2.4 – Field photos of the Mt. Timothy xenolith-bearing locality. (A) View of Mt. Timothy's northern face; (B) close-up view of the xenolith-bearing pyroclastic unit near the summit showing stratification

conglomerate to the north of Mt. Timothy. Bedrock to the east of Mt. Timothy is entirely dominated by Takomkane batholith granodiorites and monzogranites (Schoolhouse Lake Unit).

The mountain itself primarily consists of Eocene-aged volcanic rocks from the Kamloops Group's Skull Hill formation. Most common are various andesitic and basaltic lavas, along with volcanic breccia, with less common dacites, conglomerates, and sandstones. Particularly prevalent are heavily plagioclase phyric, light- to medium-gray andesites. Mt. Timothy's lower eastern peak is mainly comprised of Eocene diorites, while its primary western peak showcases significant exposures of Quaternary xenolith-bearing lavas and pyroclastic material. These younger lavas also can be found in large swathes south of Mt. Timothy and south of Timothy Lake, and in smaller exposures to the north of Mt. Timothy.

Various xenolith-bearing sites are present on and in the vicinity of Mt. Timothy, most of which were initially mapped in detail by Schiarizza et al. (2008). None of the xenolith-bearing units at Mt. Timothy have been previously reported on. However, the xenoliths from the nearby Boss Mountain/Big Timothy volcanics were some of the first mantle xenoliths within the Canadian Cordillera to be studied in detail (Soregaroli, 1968; Littlejohn and Greenwood, 1974; Ross, 1983; Peslier et al., 2002; Greenfield et al., 2013).

Three of these xenolith-bearing sites, coordinates for which are listed in Table 2.1, were primary sampling targets for this study, while others were scouted and lightly sampled. The largest and most accessible of the three is a large, southwest-facing talus slope on the western side of Mt. Timothy consisting of medium- to coarse-grained alkaline basalt. The xenoliths hosted by this unit, of which >95% are mantle peridotites, are slightly smaller on average and sparser than at other nearby xenolith-hosting units: consequently, less time was spent sampling here than at the other sites. The second unit sampled for this study is a large, low-lying lava flow south of Mt. Timothy and directly north of Timothy Lake. This unit is extremely similar in appearance to the talus unit but with much fresher exposures of coarse alkaline basalt and, consequently, somewhat less altered peridotite xenoliths. The final unit is a smaller outcrop of pyroclastic material directly off the road to the south of Mt. Timothy's summit (Figure 2.4b). It is the only known site in the Mt. Timothy region where xenoliths are hosted by anything other than dense alkaline basalts. The xenoliths here are exposed as roughly 2-10 cm chunks of coarse-grained peridotites, usually with a partial or full shell of a very fine-grained basalt crust. These peridotites are uniformly well-preserved and are usually fragile compared to those from the other Mt. Timothy sites and those from Summit Lake.

3. XENOLITH SUITES

The xenolith suites collected at both volcanic centers are dominated by a variety of mantle peridotites. Spinel-bearing lherzolites are most common. Crustal xenoliths of various textures and mineralogies are minor in abundance. Spinel uniformly comprises <10% of the peridotites from both localities and is usually <5%. No correlations between mineralogy and sampling location are apparent within the Mt. Timothy or Summit Lake localities.

3.1 MT. TIMOTHY

The Mt. Timothy suite contains >95% peridotite xenoliths at all sampling locations, nearly all of which are chromium diopside-rich spinel lherzolites (Figure 3.1). Mt. Timothy peridotites are largely medium- to coarse-grained with highly variable grain sizes within individual samples (Figure 3.1). They usually display little to no alteration, which may partially reflect this unit's very young age compared to the much older Summit Lake xenolith suite. Mineral fabrics are very rare, if not nonexistent. Wehrlites are present but are exceedingly uncommon. Megacrystic olivine and orthopyroxene xenoliths can also be found among the lava-hosted xenoliths, but not in the pyroclastic unit. Crustal xenoliths are present in the Mt. Timothy localities, but are extremely uncommon and are generally very small, ranging from 0.5 cm to 2 cm (Figure 3.1b). They also display significantly less variety in rock types than the crustal material from Summit Lake, with most crustal xenoliths from Mt. Timothy comprising very fine-grained off-white quartzite (Figure 3.1b).

3.2 SUMMIT LAKE

The xenolith-bearing unit at Summit Lake contains ~80% peridotite xenoliths. Most common are spinel-bearing lherzolites (Figure 3.2c), similar to Mt. Timothy and other suites

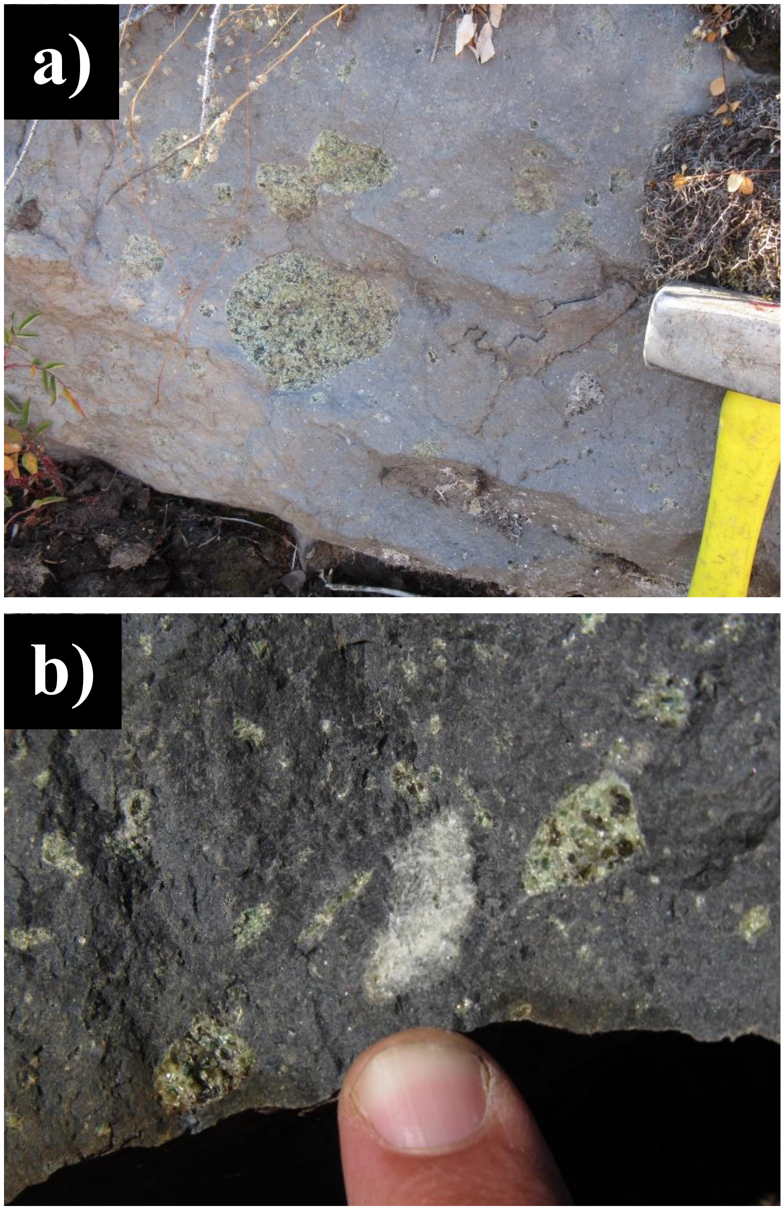

Figure 3.1 – Examples of *in situ* xenolith types present in the Mt. Timothy sample suite: (A) peridotites from the Timothy Lake lava flows; (B) quartz-rich crustal material alongside smaller peridotite xenoliths from the Timothy Lake lava flows.

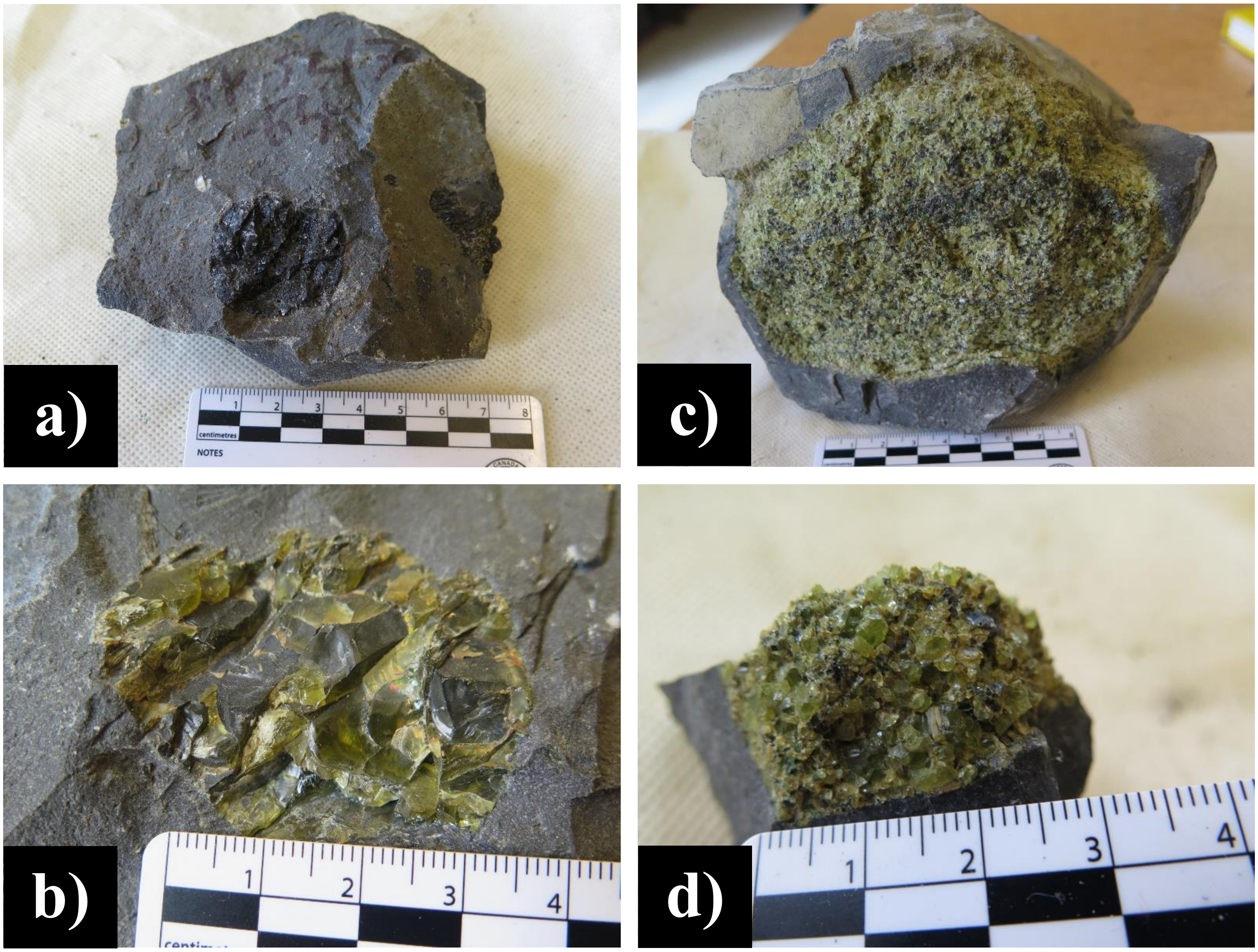

Figure 3.2 – Examples of mantle xenolith samples from the Summit Lake locality: (A) very coarse-grained clinopyroxenite; (B) megacrystic enstatite; (C); a particularly large lherzolite sample featuring a pronounced diopside-rich band; (D) coarse-grained lherzolite

across the Southern Cordillera. Also present are harzburgites, wehrlites, olivine websterites, websterites, orthopyroxenites, and clinopyroxenites, all in greater proportions than at Mt. Timothy (Figure 3.2). Summit Lake peridotite xenoliths are generally finer-grained, and more homogenous in grain sizes, than their counterparts from Mt. Timothy. Alteration is much more prevalent than in Mt. Timothy xenoliths, with iddingsitization affecting peridotites to varying degrees especially for samples more exposed to atmospheric conditions. Unlike at Mt. Timothy, they also occasionally display weak to moderate mineral fabrics, the most common of these being elongated spinel fabrics (Figure 3.4b). Dunites, megacrystic olivine, and megacrystic orthopyroxene (enstatite) are also present (Figure 3.2).

Comprising up to 20% of its xenolith population, crustal xenoliths are far more common in the Summit Lake unit than they are at Mt. Timothy. They are also significantly more diverse in size, textural features, and rock types. The small, fine-grained quartzites found sparingly at Mt. Timothy can also be found in the Summit Lake unit alongside coarse-grained granitoids, schists, and gabbroic material (Figure 3.3). The latter is of particular note due to the frequent occurrence of pronounced layering of augite and quartz in many of these xenoliths (Figure 3.3b).

3.3 MODAL MINERALOGY

Modal mineralogies for the peridotite xenoliths (based on olivine, orthopyroxene, clinopyroxene, and spinel contents) were determined using a point counting code written in MATLAB in conjunction with high-resolution scans of thick-cut thin sections from each sample. These modal mineralogies are plotted in Figure 3.5 and are listed in Table 3.1. The code and the detailed methodology can be found in Appendix C, alongside the process used to determine the

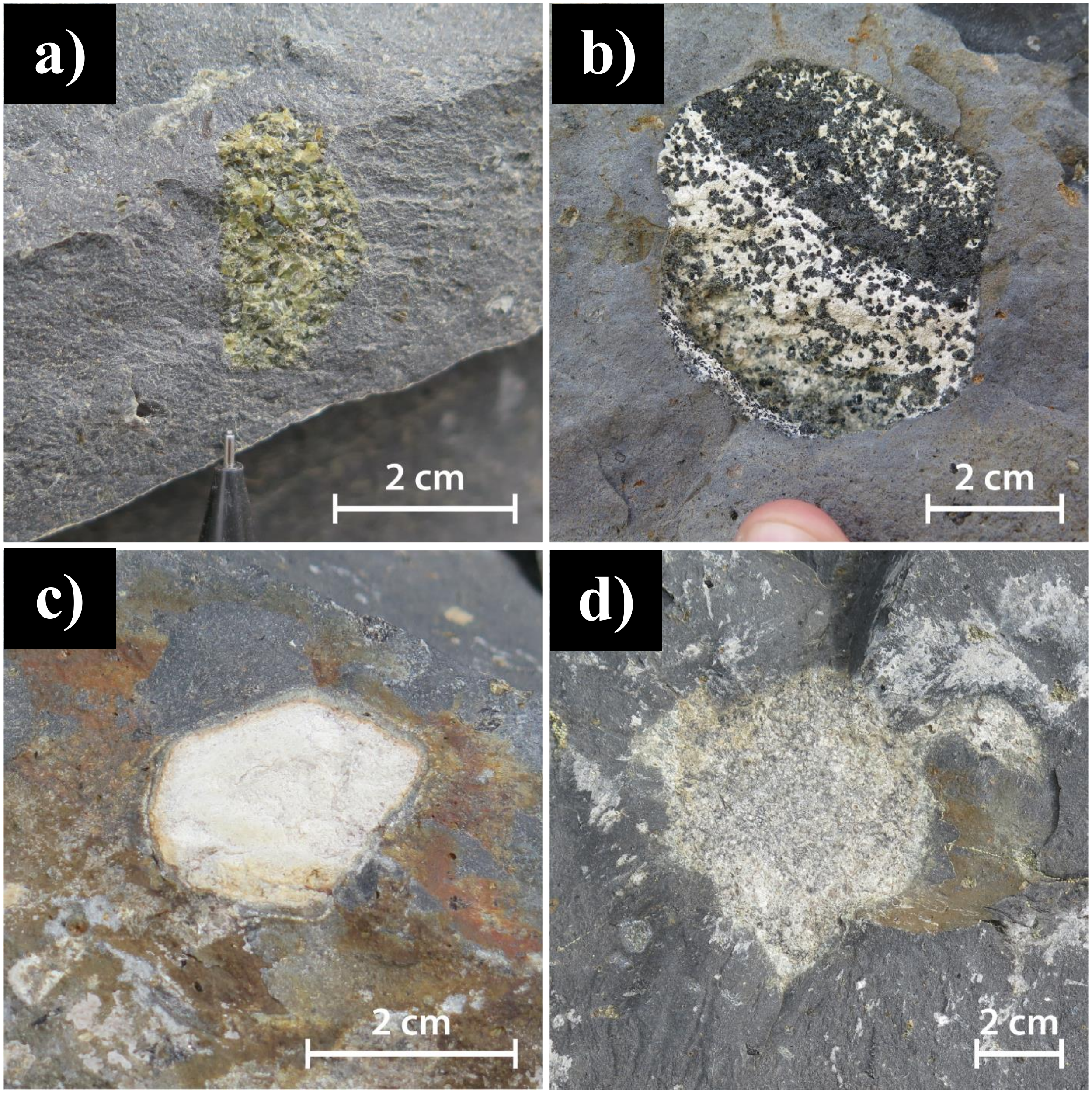

Figure 3.3 – Various *in situ* xenolith types present in the Summit Lake unit: (A) lherzolite; (B) banded gabbro; (C) fine-grained quartzite; (D) a xenolith of felsic intrusive rock.

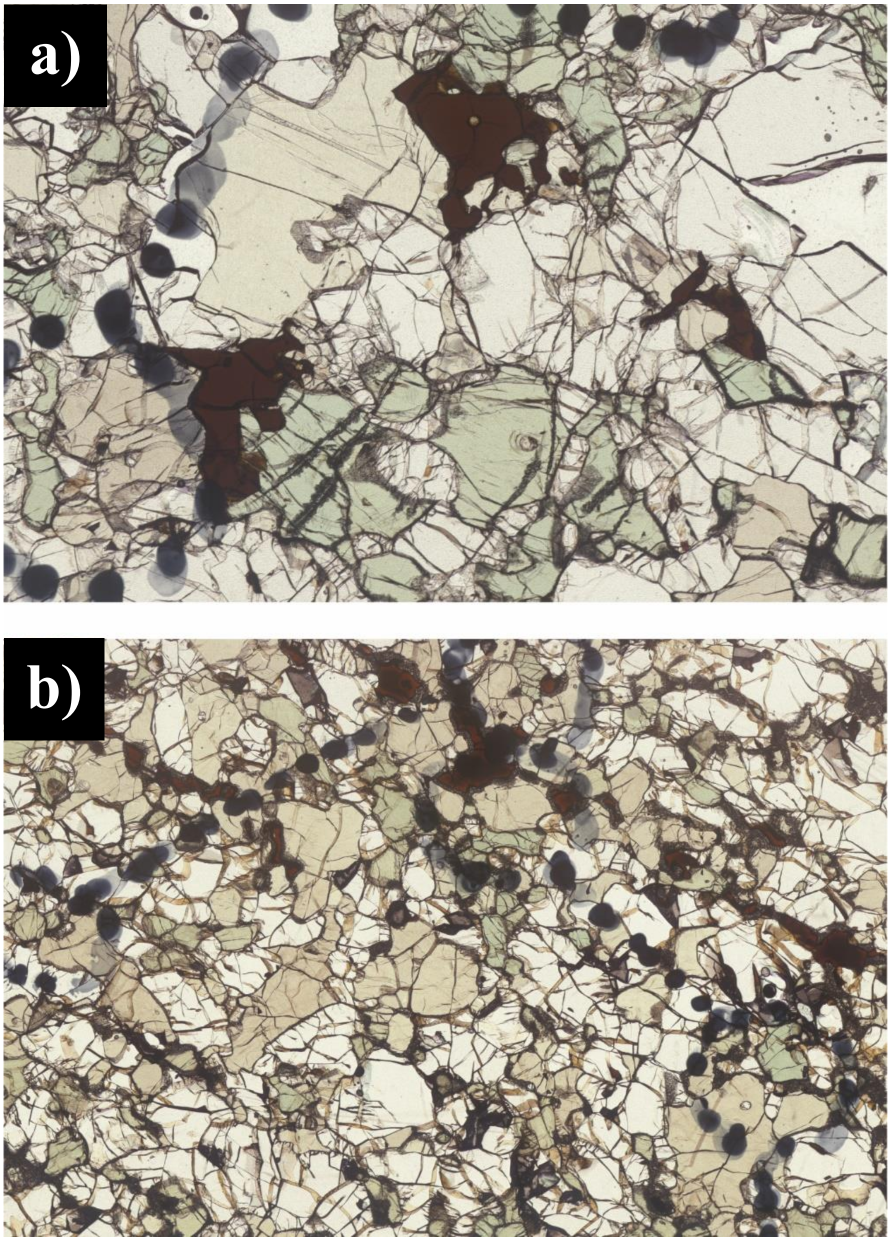

Figure 3.4 – Representative photographs of peridotites from this study. (A) A typical example of a coarse-grained spinel lherzolite from Mt. Timothy (RK-TM17-68); (B) a finer-grained spinel lherzolite from Summit Lake displaying one of the few clear examples of spinel fabrics from this collection of samples (RK-TL17-11). Both samples display grains of colorless olivine, light brown orthopyroxene (enstatite), bright green clinopyroxene (diopside), and opaque brown spinel. Marker residue was used to mark Opx-Cpx pairs for microprobe analyses. Photos were taken in plain polarized light; thin sections are uncovered and polished and are cut to a thickness of 100 μm.

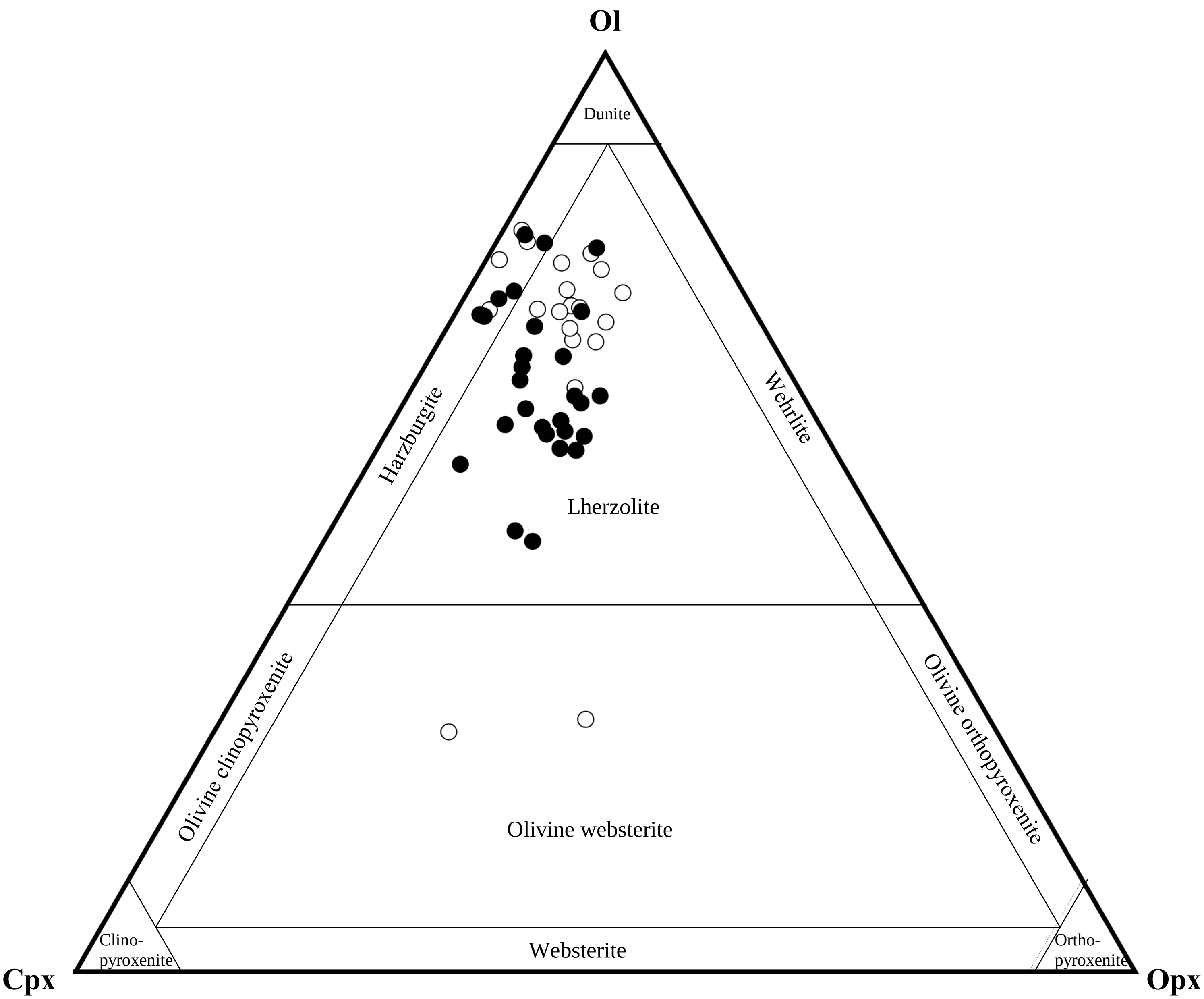

Figure 3.5 – Ternary diagram of the modal mineralogies present in the Summit Lake (open circles) and Mt. Timothy (filled circles) xenolith suites.

Table 3.1 – Modal mineralogies for all peridotite xenoliths from Summit Lake (SL & TL) and Mt. Timothy (TM). Methodology and code for these point counts is described in Appendix C. lhz = lherzolite; harz = harzburgite; ol-webs = olivine websterite. minimum number of trials needed to accurately characterize the modal mineralogy of each xenolith (Figure C.1).

Sample ID	Ol	Opx	Cpx	type
DC-SL08-02	74.3	16.5	9.3	lhz
DC-SL08-15				lhz
DC-SL08-29				lhz
DC-SL08-44				lhz
RK-SL17-10				lhz
RK-SL17-33	26.1	51.7	22.2	ol-webs
RK-SL17-41	63.6	21.1	15.3	lhz
RK-SL17-43	70.7	14.6	14.7	lhz
RK-SL17-49	68.6	16.6	14.8	lhz
RK-SL17-53	79.5	17.6	2.9	harz
RK-SL17-55A	71.9	18.4	9.8	lhz
RK-SL17-70	73.9	11.4	14.7	lhz
RK-SL17-74	72.0	24.9	3.0	harz
RK-SL17-76	27.5	38.1	34.4	ol-webs
RK-SL17-81A	70.0	18.3	11.6	lhz
RK-SL17-81B	78.2	12.2	9.6	lhz
RK-SL17-82	77.2	15.6	7.3	lhz
RK-SL17-84	72.3	16.3	11.4	lhz
RK-SL17-85	72.1	20.3	7.5	lhz
RK-SL17-91	76.5	12.2	11.4	lhz
RK-SL17-97	80.7	17.5	1.8	harz
RK-TL17-01	77.5	21.3	1.2	harz
RK-TL17-11	72.51	17.0	10.5	lhz
DC-TM08-17	60.00	24.2	15.8	lhz
DC-TM08-22	73.3	23.4	3.3	harz
DC-TM08-25C	71.9	16.3	11.8	lhz
DC-TM08-30	70.3	21.6	8.2	lhz
DC-TM08-34	80.2	17.5	2.3	harz
DC-TM08-38	71.5	26.1	2.4	harz
DC-TM08-41	55.3	36.1	8.7	lhz
DC-TM08-43	58.9	24.4	16.8	lhz
DC-TM08-48	58.5	26.3	15.2	lhz
DC-TM08-49	59.6	29.7	10.8	lhz
DC-TM08-52	61.9	21.3	16.7	lhz
DC-TM08-54	58.3	22.9	18.9	lhz
DC-TM08-63	64.4	25.9	9.8	lhz
DC-TM08-64	61.3	26.9	11.8	lhz
DC-TM08-A1	79.3	16.1	4.6	harz
DC-TM08-A2A	57.0	25.8	17.2	lhz
DC-TM08-A2A2	65.8	25.0	9.2	lhz
DC-TM08-A2B	62.7	19.2	18.2	lhz
DC-TM08-B1	48.0	34.5	17.5	lhz
DC-TM08-T	74.1	21.6	4.3	harz
RK-TM17-18	67.1	24.2	8.8	lhz
RK-TM17-19	77.0	20.5	12.5	lhz
RK-TM17-20	46.9	33.4	19.7	lhz
RK-TM17-21	59.3	26.3	14.4	lhz
RK-TM17-22	56.8	24.4	18.9	lhz
RK-TM17-25	71.4	25.8	2.9	harz
RK-TM17-25A	78.8	11.4	9.8	lhz

The peridotites – most of which are lherzolites – from Mt. Timothy display a range of modal mineralogies. Most contain 50-70% modal olivine, 20-30% modal orthopyroxene (enstatite), and 8-20% modal clinopyroxene (diopside), with one relative outlier at over 80% olivine and two more at below 50% olivine. Subordinate harzburgites with between 70% and 80% modal olivine are also found in the Mt. Timothy suite. The vast majority of harzburgites from these localities still contain low percentages (~2-5%) of clinopyroxene: unlike at Summit Lake, "pure" harzburgites – xenoliths comprised entirely of olivine and orthopyroxene with no clinopyroxene present – are extremely rare.

Summit Lake samples have higher modal olivine -(~70-80%), lower modal orthopyroxene (~12-20%), and lower modal clinopyroxene (~7-15%) than lherzolites from Mt. Timothy (Figure 3.1). The range of modal percentages for these minerals are also narrower than those from Mt. Timothy. Harzburgites present in the Summit Lake unit include both clinopyroxene-poor harzburgites like those at Mt. Timothy (1-3% modal clinopyroxene and 18-25% modal orthopyroxene) and entirely clinopyroxene-free harzburgites (~30-45% orthopyroxene).

Wehrlites, extremely uncommon at the Mt. Timothy sites, are moderately common in the Summit Lake unit and generally comprise roughly 15-30% modal clinopyroxene. Rather than the Cr-diopside found in other xenolith types, the clinopyroxene found in these wehrlites is almost exclusively augite. Olivine websterites are rare but present, containing ~25-35% modal orthopyroxene and ~35-55% clinopyroxene, while smaller websterites, orthopyroxenites, and clinopyroxenites are relatively common. Like with the wehrlites, the clinopyroxene in clinopyroxenites and websterites from Summit Lake is predominantly augite rather than Cr-diopside.

4. GEOCHEMISTRY

4.1 ANALYTICAL CONDITIONS AND METHODOLOGY

A total of 34 whole rock samples were analyzed for their bulk composition, including 8 samples of the host lavas plus 26 xenolith samples. The host lava samples included four from different parts of the Summit Lake unit as well as samples from Mt. Timothy, Teapot Mountain, Coffee Lake, and Lightning Peak. The xenolith samples were selected on the basis of volume. Only samples large enough to provide both a thin section and a geochemical sample were chosen. This restriction especially limited the number of Mt. Timothy xenoliths, which have a smaller average size than the Summit Lake xenoliths.

Lava samples were trimmed of contaminated surfaces and reduced to a workable size using a diamond saw, split, and then fed into a jaw crusher to create 1-2 cm chips. These chips were then hand-picked to remove any minor xenolithic material left in the host lava. Xenoliths were trimmed of weathered surfaces using a diamond saw before analysis. All 26 xenolith samples were sent to Activation Laboratories in Ancaster, Ontario for geochemical analyses, where they underwent pulverization via an agate mill.

Analyses of major, trace, and rare earth elements at Activation Laboratories were carried out with their WRA + Trace 4Lithoresearch analysis package. Major elements plus select trace elements (Ba, Be, Sc, Sr, V, Y, and Zr) were analyzed using a sequential Thermo Jarrell-Ash ENVIRO II or a Varian Vista 735 ICP-OES, while the remaining trace elements and all rare earth elements were analyzed with a Perkin Elmer Sciex ELAN [6000, 6100, or 9000] ICP-MS. Additional analyses for quantitative chalcophile elements were also undertaken via dilution and digestion of the samples and analysis on an Agilent 700 Series ICP.

4.1.1 NANOPARTICULATE PRESSED POWDER PELLETS

The residual powders of the 26 xenolith bulk geochemistry samples analyzed by Activation Laboratories were the submitted to Christopher Lawley at the Geological Survey of Canada in Ottawa for additional analysis. An alternate technique, where nanoparticulate powders pulverized using wet milling are pressed into pellets and analyzed directly via LA-ICP-MS, was used here. This technique was utilized due to the much more precise measurements of trace and rare earth elements it yields compared to more traditional methods (Garbe-Schönberg and Müller, 2014; Peters and Pettke, 2016). Grain sizes after milling are typically < 1.5 μm, lending greatly enhanced cohesion and homogeneity in these pellets compared to more traditional methods (Garbe-Schönberg and Müller, 2014). This also makes this method suitable for analyzing much smaller volumes of material than could be reliably analyzed with other methods. A significant number of trace elements that are below detection limits in the original dataset including flux elements Li and B and chalcophile elements As, Sb, Tl, In, and Bi are revealed by this procedure. Measurement trueness using this procedure is equivalent to that for solution ICP-MS or LA-ICP-MS measurements of glasses for most trace and rare earth elements listed (Peters and Pettke, 2016).

The sample powders first pulverized by wet milling at Activation Laboratories were then mixed with a microcrystalline cellulose as a binder and pressed into pellets using a Specac 5 mm evacuable die. The pellets were analyzed using an Agilent 7700x ICP-MS coupled to a Photon Machines Analyte G2 193-nm excimer laser ablation system at the Geological Survey of Canada in Ottawa. Five replicate analyses were performed for each sample, with the reported result representing the median of these standards. A doped synthetic basalt glass standard from the United States Geological Survey, GSD-1G, was utilized as a primary calibration standard

(Guillong et al., 2005). Measurement trueness for the most abundant major and trace element compositions were within <10% of accepted values, and even the more variable measurement trueness of trace to ultratrace elements were largely within <20% of target values. Reproducibility of the results for this method was excellent for most major (<5%) and trace (<10%) elements (Lawley, 2019).

4.2 GEOCHEMISTRY OF HOST LAVAS

Major element contents of the lava samples are listed in Table 4.1. Table 4.2 contains trace and rare earth element compositions for the same samples. The tables include compositions for both the Summit Lake and Mt. Timothy host units as well as several other nearby xenolith-bearing volcanic deposits. The lavas are classified on the basis of alkali versus SiO_2 contents (Figure 4.1). Most are basanites, based on normative mineralogy calculations revealing >10% olivine for all samples.

Of the eight xenolith host basalt samples measured by this study, there is a distinct separation in alkali contents between the silica and alkali contents of the southern units (Mt. Timothy, Lightning Peak, and Coffee Lake) and the Summit Lake units to the north. The Summit Lake samples all contain significantly higher silica concentrations (~46-48% SiO_2) and have K_2O concentrations that are marginally higher than their Na_2O concentrations. The Mt. Timothy, Lightning Peak, and Coffee lake units have lower SiO_2 concentrations (~43-44%) and contain Na_2O:K_2O ratios of at least 2:1. The “talus quarry” sample is from a different exposure relative to the other three samples of the Summit Lake Quarry unit. This sample’s alkali concentration is notably lower than those three samples, and it plots as a basalt (Figure 4.1). This may suggest that the geographically proximal Teapot Mountain plug and the Summit Lake lava units are, if

Table 4.1 - Whole rock major element compositions of the xenolith-hosting lavas collected from around Summit Lake and Mt. Timothy.

Sample	**TP17-05**	**CF17-05**	**LP17-00**	**TM17-25**
Locality	Teapot Mountain	Coffee Lake	Lightning Peak	Timothy Lake
Rock type	Basalt	Basanite (Ol = 13.5 wt.%)	Picro-basalt	Picro-basalt
SiO_2	47.93	43.20	43.52	43.78
TiO_2	1.225	2.363	2.494	2.402
Al_2O_3	15.62	11.62	11.53	10.95
Fe_2O_3(T)	9.89	13.41	13.5	13.51
MnO	0.166	0.213	0.189	0.19
MgO	9.27	11.19	13.19	14.16
CaO	10.09	9.74	9.05	8.9
Na_2O	3.01	4.08	3.24	2.96
K_2O	1.17	2.02	1.72	1.65
P_2O_5	0.68	1.49	0.91	0.87
Total	100.1	99.26	98.81	98.84
LOI	1.09	-0.06	-0.52	-0.52

Sample	**TL17-18**	**SL17-28A**	**SL17-50**	**SL17-77**
Locality	Talus quarry	Summit Lake	Summit Lake	Summit Lake
Rock type	Basalt	Basanite (Ol = 10.4 wt.%)	Basanite (Ol = 12.2 wt.%)	Basanite (Ol = 12.2 wt.%)
SiO_2	45.90	46.50	45.81	46.15
TiO_2	1.608	1.627	1.696	1.716
Al_2O_3	14.86	15.86	15.11	15.85
Fe_2O_3(T)	9.12	9.31	9.61	9.32
MnO	0.151	0.155	0.158	0.154
MgO	10.61	8.72	9.93	9.65
CaO	10.31	9.8	10.10	10.05
Na_2O	2.20	3.06	2.69	2.76
K_2O	2.51	3.18	2.99	2.95
P_2O_5	0.54	0.65	0.63	0.62
Total	98.83	98.97	99.29	99.71
LOI	1.02	0.12	0.56	0.48

Table 4.2 - Whole rock trace and rare earth element compositions of the xenolith-hosting lavas collected from around Summit Lake and Mt. Timothy. Data listed is from the Activation Laboratories LA-ICPMS dataset.

Sample	**TP17-05**	**CF17-05**	**LP17-00**	**TM17-25**	**TL17-18**	**SL17-28A**	**SL17-50**	**SL17-77**
Locality	Teapot Mountain	Coffee Lake	Lightning Peak	Timothy Lake	Teapot Mountain	Coffee Lake	Lightning Peak	Timothy Lake
Rock type	Basalt	Basanite	Picro-basalt	Picro-basalt	Basalt	Basanite	Picro-basalt	Picro-basalt
Sc	27	19	16	16	30	27	30	29
Be	1	3	2	2	1	2	2	2
V	220	186	187	181	228	223	235	230
Cr	450	390	480	570	360	240	280	310
Co	41	54	63	65	45	40	43	42
Ni	220	380	510	550	260	170	220	220
Cu	60	20	40	40	50	50	70	60
Zn	70	140	130	130	70	70	70	70
Ga	15	20	19	18	15	16	16	16
Ge	1.1	1.1	1.1	1.2	1.3	1.1	1.2	1.2
As	< d.l.	< d.l.	< d.l.	< d.l.	< d.l.	< d.l.	< d.l.	< d.l.
Rb	42	49	43	43	81	92	83	86
Sr	993	1730	1112	1017	718	772	707	724
Y	22	31.7	25	24.5	20.4	22	21.8	21.7
Zr	148	324	334	322	146	180	163	165
Nb	46.3	113	84.9	80.9	50.5	63.3	59.1	60.6
Mo	< d.l.	11	7	6	< d.l.	3	3	3
Ag	< d.l.	1	1.1	1	< d.l.	< d.l.	< d.l.	< d.l.
In	< d.l.	< d.l.	< d.l.	< d.l.	< d.l.	< d.l.	< d.l.	< d.l.
Sn	1	2	2	2	1	1	1	1
Sb	< d.l.	0.2	< d.l.	< d.l.	< d.l.	< d.l.	< d.l.	< d.l.
Cs	1.2	0.8	0.6	0.7	1.8	2.1	1.8	2
Ba	1753	849	650	589	1507	1754	1689	1666
Bi	< d.l.	< d.l.	< d.l.	< d.l.	< d.l.	< d.l.	< d.l.	< d.l.
Hf	3.1	6.1	7.1	6.8	3.5	3.8	3.6	3.6
Ta	2.87	7.23	5.63	5.37	3.85	4.54	4.37	4.43
W	< d.l.	4.7	< d.l.	< d.l.	< d.l.	3.5	< d.l.	< d.l.
Tl	< d.l.	< d.l.	< d.l.	< d.l.	0.28	0.14	< 0.05	< 0.05
Pb	< d.l.	7	< d.l.	< d.l.	< d.l.	< d.l.	< d.l.	< d.l.
Th	4.93	12.5	7.39	7.33	3.04	4.04	3.71	3.81
U	1.31	4.06	2.32	2.26	0.88	1.12	1.07	1.1
La	47.5	129	73.3	70.3	33.4	45.8	40.6	38.8
Ce	94.9	239	145	140	68.2	90.3	82.4	79
Pr	10.8	25.7	16.4	15.9	8.03	10.3	9.44	9.1
Nd	40.1	93.8	62.6	61.2	31.2	38.5	37.3	36
Sm	6.62	15.8	11.9	11.3	5.9	6.8	6.65	6.57
Eu	2	4.75	3.7	3.55	1.85	2.05	2	1.91
Gd	5.13	10.9	8.92	8.84	4.72	5.13	5.08	4.98
Tb	0.77	1.43	1.23	1.19	0.69	0.72	0.77	0.71
Dy	4.18	7.2	6.02	5.7	3.97	4.17	4.23	3.92
Ho	0.77	1.19	0.96	0.91	0.73	0.76	0.79	0.76
Er	2.26	2.91	2.26	2.23	2.1	2.22	2.23	2.16
Tm	0.34	0.359	0.282	0.271	0.303	0.322	0.325	0.303
Yb	2.24	2.01	1.54	1.52	1.92	1.96	2.14	2.03
Lu	0.343	0.289	0.203	0.2	0.286	0.301	0.324	0.295

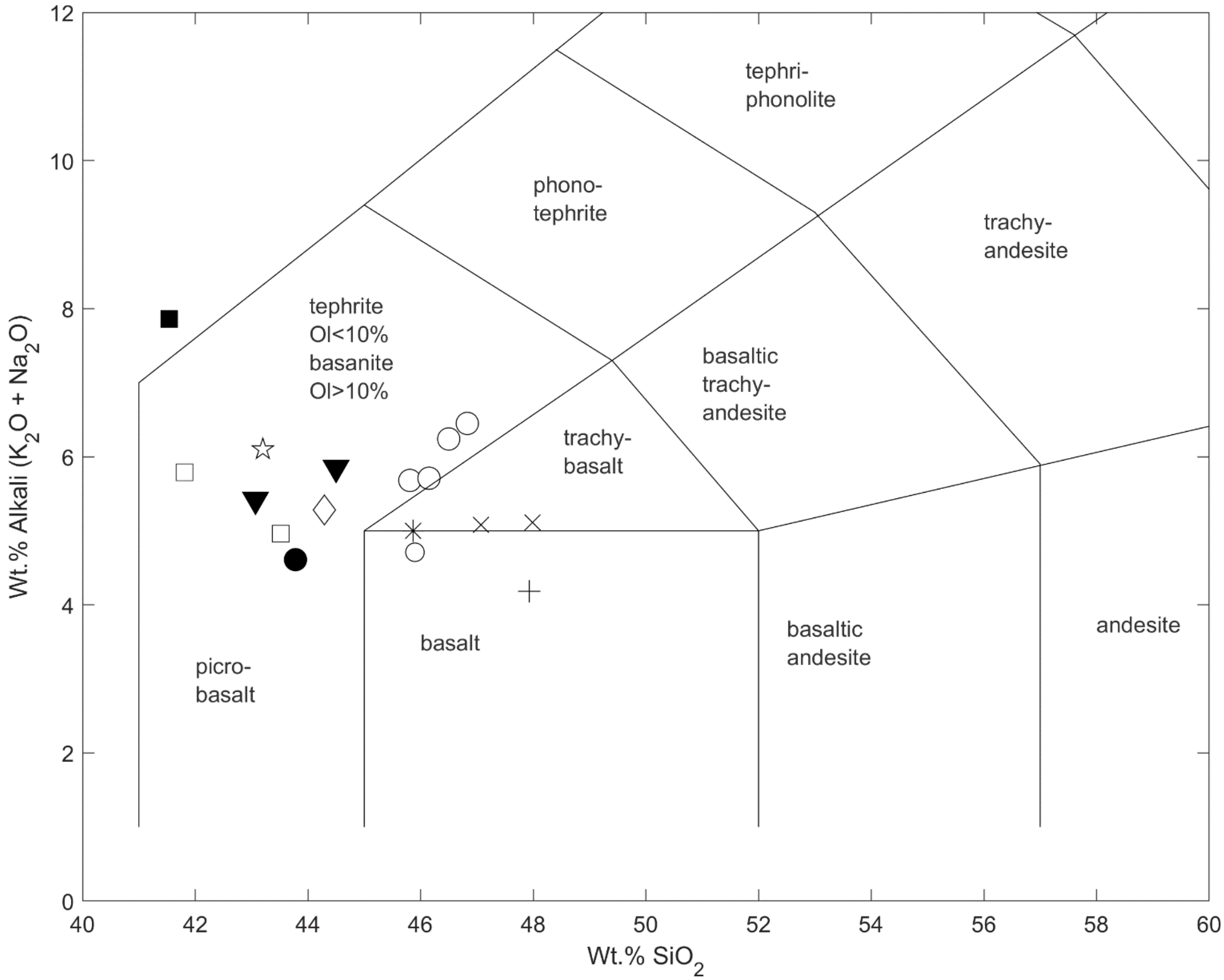

Figure 4.1 – Total alkali silica diagram for xenolith-hosting basalts from south-central British Columbia, both from this study and previous work. Superscripts denote data from previous studies: [1]Peslier et al. (2002); [2]Fujii and Scarfe (1982); [3]Canil et al. (1987). Open circles = Summit Lake[1]; filled circle = Mt. Timothy; open squares = Lightning Peak[1]; star = Coffee Lake; filled triangles = West Kettle River[1,2]; open diamond= Kostal Lake[1]; asterisk = Lassie Lake[1]; plus = Teapot Mountain; filled square = Big Timothy[1]; crosses = Rayfield River[1,3]

not products of the exact same volcanic event, at least contemporaneous and similarly sourced volcanic units.

The Summit Lake and Talus Quarry host units have trace (Figure 4.2) and rare earth element (Figure 4.3) compositions that mostly fall within the reported range of compositions for other xenolith-hosting volcanics in the southern Cordillera. Comparing the two sites to each other, the Summit Lake samples are depleted in most trace elements relative to both Mt. Timothy and other Cordilleran values. The most striking differences in trace element concentrations between the two sites are the sharp spike in Ba concentration and steep dip in Th and U concentrations in the Summit Lake unit compared to the Mt. Timothy unit. The low Th and U concentrations for Summit Lake are also significantly lower than for any other recorded xenolith host unit in the southern Cordillera, while Cs and Rb are more enriched in these basalts than in other recorded xenolith-bearing Cordilleran volcanics. Also present is a slight enrichment in Yb for the Mt. Timothy host unit relative to the Summit Lake unit.

The rare earth element plots of Figure 4.3 display enriched light rare earth element (LREE) concentrations relative to heavy rare earth element (HREE) concentrations in all host lavas. The Mt. Timothy unit falls right in the middle of the range of REE compositions reported for southern Cordilleran host units, while the Summit Lake unit is moderately depleted in all LREEs and MREEs relative to other reported values, particularly for the lightest REES La, Ce, and Pr. The REE patterns of the two sites, however, are very distinct from each other. While the Mt. Timothy unit decreases systematically from the heaviest to the lightest REEs, the Summit Lake unit plateaus at the lightest elements, leading to significantly more enriched Tm, Yb, and Lu concentrations relative to Mt. Timothy.

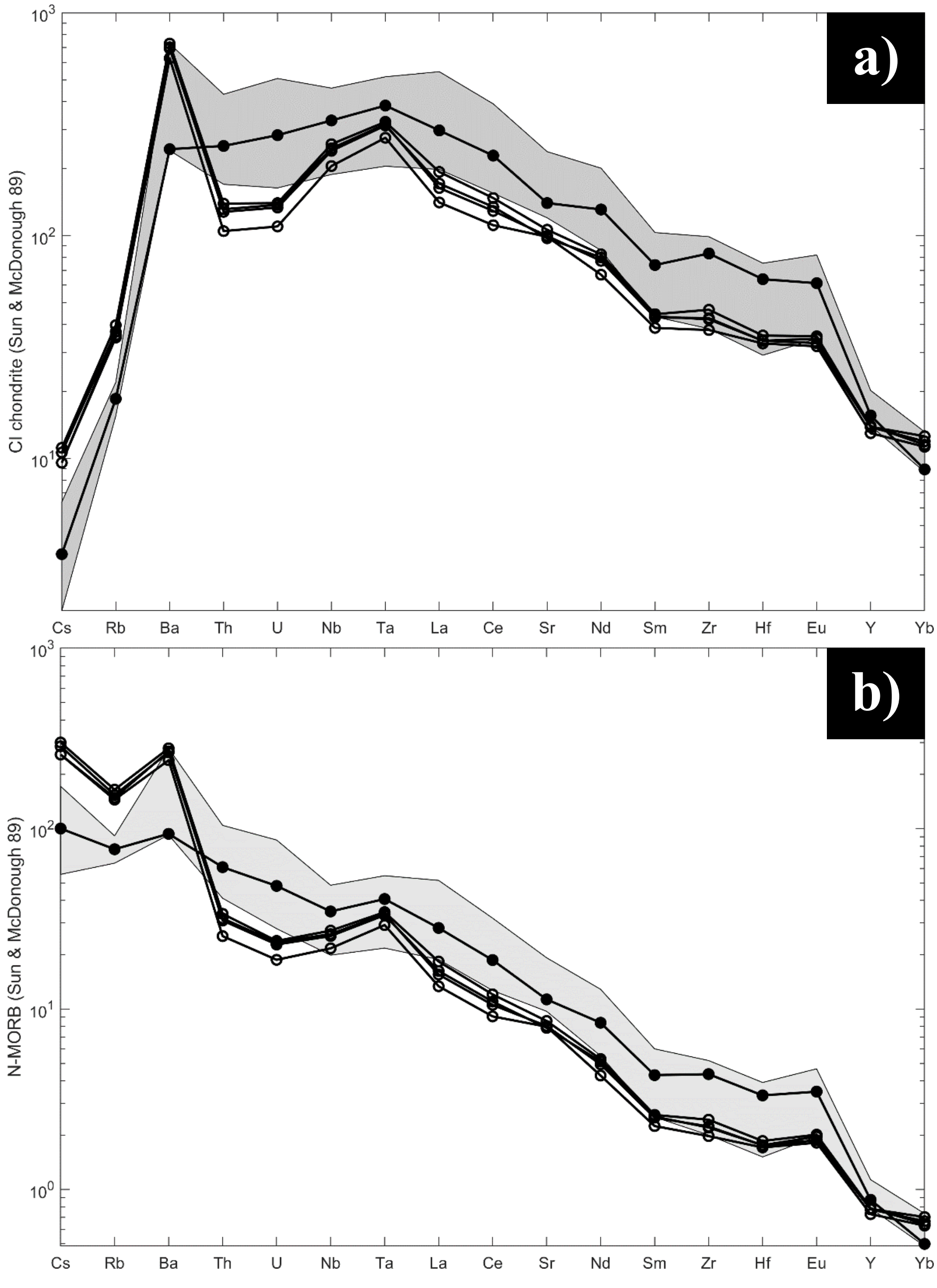

Figure 4.2 – Trace element patterns for host basalts from Summit Lake (open circles) and Mt. Timothy (closed circles), normalized to (a) chondritic and (b) N-MORB values. The gray area represents ranges of elemental concentrations for similar xenolith-hosting alkaline basalts from across the southern Cordillera; includes data from this study for Coffee Lake, Teapot Mountain, and Lightning Peak localities as well as data from the Tasse alkaline basalts collected by Friedman et al. (2016). All normalization values are from Sun and McDonough (1989).

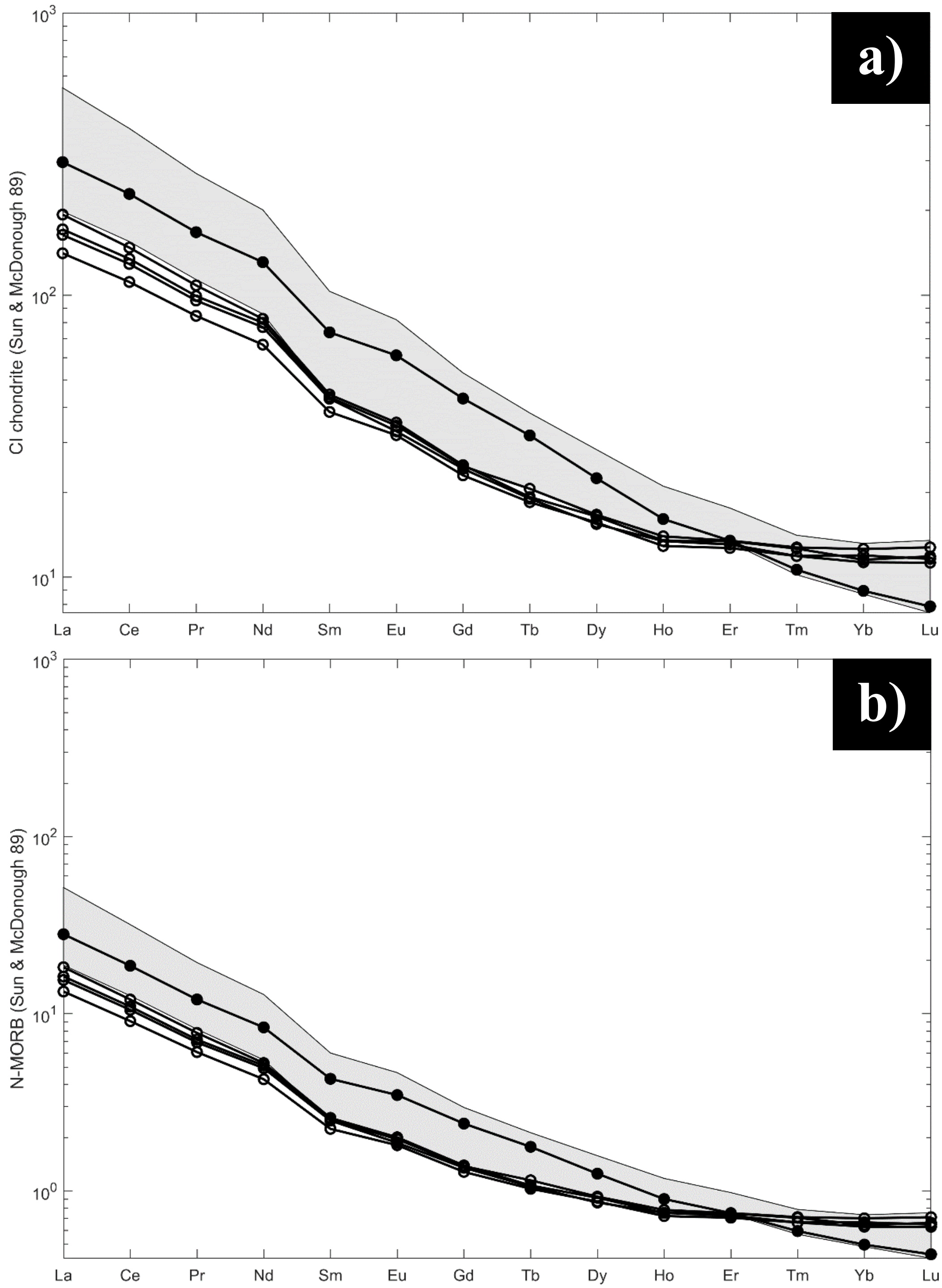

Figure 4.3 – Rare earth element patterns for host basalts from Summit Lake (open circles) and Mt. Timothy (closed circles), normalized to (a) chondritic and (b) N-MORB values. The gray area represents ranges of elemental concentrations for similar xenolith-hosting alkaline basalts from across the southern Cordillera; includes data from this study for Coffee Lake, Teapot Mountain, and Lightning Peak localities as well as data from the Tasse alkaline basalts collected by Friedman et al. (2016). All normalization values are from Sun and McDonough (1989).

The Teapot Mountain and the Summit Lake lavas show distinctly similar trace and rare earth element patterns. When combined with the observation that the Summit Lake quarry unit contains a much higher percentage of xenoliths by volume than the plug-like Teapot Mountain unit and the proximity of the two units to each other, one might hypothesize that the two units represent different stages of volcanic activity from the same magmatic source.

4.3 BULK XENOLITH GEOCHEMISTRY

Table 4.3 summarizes the major element compositions, and Table 4.4 the trace and rare earth element compositions, of the whole rock xenoliths from Summit Lake and Mt. Timothy analyzed in this study. The majority of the samples for which bulk chemistry was taken are lherzolites, although two harzburgites were measured from Mt. Timothy while three were measured from Summit Lake.

The eight Mt. Timothy samples are characterized by 42.6-46.3 wt.% SiO_2, and the Summit Lake peridotites vary from 40.9-46.5 wt.% SiO_2. MgO concentrations range from 36.7-44.5 wt.% for Mt. Timothy and from 35.4-46.4 wt.% for Summit Lake, while Fe_2O_3 contents are from 7.9 wt.% to 10.1 wt.% for Mt. Timothy and from 8.7-11.6 wt.% for Summit Lake. Mg-numbers for both sites fall in very narrow ranges and are slightly higher for Mt. Timothy (89.3-91.1) than they are for Summit Lake (88.3-90.8). Both sites have similar ranges of Al_2O_3

Table 4.3 - Whole rock major element compositions of the xenoliths collected from around Summit Lake and Mt. Timothy. Data listed is from the ActLabs LA-ICPMS dataset. Rock types include lherzolites (lhz), harzburgites (harz), and crustal xenoliths.

Sample	**TM08-00**	**TM08-48**	**TM08-54**	**TM08-63**	**TM08-64**	**TM08-A2A**	**TM17-20**
Rock type	harz	lhz	lhz	lhz	lhz	lhz	lhz
SiO_2	42.63	45.38	44.61	44.33	43.00	46.34	45.62
Al_2O_3	2.31	3.19	3.74	3.67	1.63	2.82	4.47
Fe_2O_3(T)	10.11	8.27	7.94	8.61	8.95	9.15	8.76
MnO	0.136	0.131	0.128	0.13	0.136	0.126	0.132
MgO	43.22	38.49	41.09	39.69	44.46	38.82	36.89
CaO	1.11	3.8	2.53	3.33	1.01	2.59	3.92
Na_2O	0.16	0.34	0.24	0.28	0.12	0.33	0.37
K_2O	0.05	0.03	< 0.01	< 0.01	0.02	0.08	< 0.01
TiO_2	0.12	0.122	0.085	0.091	0.073	0.117	0.138
P_2O_5	0.04	< 0.01	0.01	0.01	0.01	0.03	< 0.01
Total	99.51	99.50	100.10	99.82	99.12	100.20	100.20
LOI	-0.37	-0.26	-0.24	-0.32	-0.29	-0.19	-0.13

Sample	**TM17-25A**	**SL17-02**	**SL17-36**	**SL17-41**	**SL17-43**	**SL17-47**	**SL17-48**
Rock type	lhz	lhz	lhz	lhz	lhz	crustal	lhz
SiO_2	43.53	43.04	45.42	46.51	43.5	48.26	40.87
Al_2O_3	3.19	12.65	3.68	3.50	3.48	18.68	2.57
Fe_2O_3(T)	8.54	10.13	8.73	9.30	9.78	4.51	11.57
MnO	0.127	0.15	0.133	0.133	0.144	0.077	0.165
MgO	40.85	7.15	37.67	35.43	38.67	5.46	38.63
CaO	2.78	22.44	3.65	3.82	3.58	14.49	5.03
Na_2O	0.23	0.67	0.26	0.28	0.25	1.65	0.19
K_2O	< 0.01	0.41	0.16	0.07	0.06	0.72	0.07
TiO_2	0.094	1.04	0.103	0.115	0.151	0.476	0.183
P_2O_5	< 0.01	0.72	0.01	< 0.01	0.01	0.03	0.02
Total	98.92	100.30	100.00	99.36	100.00	100.40	99.82
LOI	-0.43	1.94	0.19	0.19	0.41	6.1	0.53

Sample	**SL17-49**	**SL17-57**	**SL17-74**	**SL17-80**	**SL17-81B**	**SL17-81C**	**SL17-82**
Rock type	lhz	lhz	harz	crustal	lhz	lhz	lhz
SiO_2	44.65	41.59	43.54	49.65	44.4	45.63	44.00
Al_2O_3	3.53	3.10	1.59	16.26	3.23	2.66	3.10
Fe_2O_3(T)	9.11	11.56	9.34	6.94	9.35	9.90	8.66
MnO	0.142	0.171	0.136	0.107	0.145	0.139	0.126
MgO	38.22	38.50	44.23	5.06	37.99	38.28	39.34
CaO	3.40	4.58	0.80	15.81	3.10	2.75	2.88
Na_2O	0.24	0.26	0.06	1.45	0.27	0.23	0.16
K_2O	0.06	0.02	0.02	0.74	0.20	0.13	0.02
TiO_2	0.118	0.177	0.023	0.641	0.127	0.101	0.086
P_2O_5	0.03	< 0.01	< 0.01	0.09	< 0.01	< 0.01	< 0.01
Total	99.85	100.00	99.78	99.94	99.15	100.20	98.45
LOI	0.35	0.06	0.06	3.19	0.34	0.39	0.08

Sample	**SL17-84**	**SL17-85**	**SL17-97**	**TL17-01**	**TL17-12**
Rock type	lhz	lhz	harz	harz	lhz
SiO_2	46.3	43.62	43.06	42.54	41.46
Al_2O_3	3.43	2.66	1.37	0.76	0.94
Fe_2O_3(T)	8.77	8.94	10.43	9.31	10.42
MnO	0.127	0.125	0.146	0.127	0.141
MgO	37.49	41.04	44.02	46.43	45.88
CaO	3.21	2.02	0.97	0.54	0.65
Na_2O	0.24	0.16	0.05	0.05	0.08
K_2O	0.13	0.05	0.01	0.03	0.07
TiO_2	0.118	0.059	0.021	0.021	0.036
P_2O_5	< 0.01	< 0.01	0.01	0.01	< 0.01
Total	100.30	99.03	99.81	99.82	99.61
LOI	0.48	0.35	-0.28	0.02	-0.08

Table 4.4 - Whole rock trace and rare earth element compositions for the xenoliths collected from Summit Lake and Mt. Timothy. Listed data is taken from the nanoparticulate pressed powder pellet dataset collected by Chris Lawley.

Sample	**TM08-00**	**TM08-48**	**TM08-54**	**TM08-63**	**TM08-64**	**TM08-A2A**	**TM17-20**	**TM17-25A**	**SL17-02**
Rock type	harz	lhz	lhz	lhz	lhz	lhz	lhz	lhz	crustal
Sc	9.2	16.8	15.5	18.1	8.3	13.7	18.7	14.5	25.3
V	48.2	75.6	74.2	83.7	37.1	63.6	98.3	73.2	179.0
Cr	1656	2674	3822	2830	1076	2221	3022	2934	140
Co	124	107	108	109	130	107	102	114	26
Ni	22487	2101	2022	2015	2406	1994	1800	2178	69
Cu	3.6	14.7	3.1	5.3	3.9	15.7	6.1	18.7	79.9
Zn	55.3	49.2	47.8	49.4	51.4	47.0	53.9	55.8	100.9
Ga	2.4	2.6	3.1	3.1	1.5	2.9	4.1	2.9	17.5
Ge	0.86	0.91	0.97	0.98	0.81	0.88	0.94	0.96	2.44
As	0.11	0.21	0.21	0.14	0.11	1.57	0.12	0.15	0.93
Rb	1.18	0.39	0.22	0.24	0.44	1.18	0.21	0.18	2.18
Sr	19.82	14.32	6.82	2.58	6.99	31.21	7.53	5.63	560.44
Y	1.46	3.69	2.75	3.23	1.21	2.92	4.13	2.61	19.88
Zr	7.7	6.2	4.1	2.1	3.2	9.8	4.2	3.2	230.9
Nb	1.64	0.54	0.37	0.17	0.58	1.95	0.37	0.07	24.69
Mo	2.50	0.08	0.06	2.45	1.12	0.16	1.88	1.58	0.26
Ag	0.01	0.01	0.00	0.02	0.01	0.01	0.01	0.02	0.04
In	0.01	0.01	0.01	0.02	0.01	0.01	0.02	0.01	0.09
Sn	0.33	0.13	0.18	0.69	0.40	0.15	0.23	0.41	2.50
Sb	0.03	0.02	0.04	0.02	0.05	0.03	0.03	0.02	0.03
Cs	0.04	0.02	0.02	0.02	0.01	0.03	0.01	0.01	0.02
Ba	16.8	6.7	5.4	4.0	6.4	28.3	2.7	2.0	127.4
Bi	0.00	0.00	0.00	0.01	0.00	0.06	0.00	0.01	0.02
Hf	0.20	0.18	0.13	0.10	0.08	0.26	0.18	0.11	4.95
Ta	0.09	0.03	0.02	0.01	0.03	0.09	0.01	0.00	2.82
W	0.04	0.02	0.01	0.02	0.02	0.10	0.02	0.03	0.14
Tl	0.00	0.00	0.00	0.00	0.00	0.00	0.00	0.00	0.01
Pb	0.75	0.23	0.13	2.51	1.35	0.72	0.80	0.52	2.49
Th	0.15	0.05	0.04	0.03	0.07	0.19	0.03	0.02	11.43
U	0.05	0.03	0.02	0.02	0.04	0.06	0.02	0.03	0.93
La	1.18	0.53	0.38	0.11	0.52	1.70	0.28	0.13	45.04
Ce	2.5	1.1	0.8	0.6	1.1	3.6	0.6	0.4	103.2
Pr	0.29	0.18	0.11	0.05	0.13	0.40	0.10	0.08	12.88
Nd	1.19	0.91	0.55	0.32	0.55	1.66	0.61	0.46	50.17
Sm	0.27	0.31	0.19	0.18	0.13	0.43	0.28	0.19	8.48
Eu	0.09	0.13	0.08	0.08	0.05	0.14	0.12	0.07	1.84
Gd	0.28	0.51	0.34	0.35	0.18	0.50	0.47	0.32	5.96
Tb	0.04	0.08	0.06	0.07	0.03	0.07	0.09	0.06	0.73
Dy	0.26	0.62	0.44	0.51	0.19	0.52	0.68	0.43	4.17
Ho	0.05	0.13	0.10	0.12	0.04	0.11	0.15	0.10	0.74
Er	0.17	0.43	0.32	0.40	0.15	0.34	0.47	0.30	2.11
Tm	0.02	0.06	0.04	0.06	0.02	0.05	0.07	0.04	0.28
Yb	0.18	0.38	0.34	0.38	0.15	0.31	0.48	0.29	1.86
Lu	0.03	0.06	0.05	0.06	0.03	0.05	0.07	0.05	0.27

Sample	**SL17-36**	**SL17-41**	**SL17-43**	**SL17-47**	**SL17-48**	**SL17-49**	**SL17-57**	**SL17-74**	**SL17-80**
Rock type		lhz	lhz	crustal		lhz		harz	crustal
Sc	18.1	16.2	15.4	8.1	17.8	16.4	17.3	8.6	14.4
V	85.9	79.3	80.3	50.7	83.9	80.5	94.1	36.0	95.2
Cr	2390	2164	2588	53	2010	2383	3094	2018	113
Co	103	100	113	12	120	107	117	122	20
Ni	1861	1842	2121	37	1638	2040	1959	2361	61
Cu	17.1	33.5	41.3	89.9	10.3	33.0	17.5	2.3	212.1
Zn	40.3	45.9	52.8	44.9	55.9	54.9	64.6	54.0	71.8
Ga	3.2	3.1	3.5	17.9	3.3	3.0	4.1	1.5	21.2
Ge	0.98	0.91	0.93	1.69	0.88	0.94	0.89	0.78	2.15
As	0.40	0.18	1.12	0.86	0.72	0.53	0.39	1.66	1.39
Rb	2.33	0.93	0.90	1.97	1.47	0.83	0.34	0.26	2.94
Sr	16.64	12.05	12.64	1256.44	24.02	9.81	23.11	2.60	974.48
Y	3.99	3.77	3.74	9.41	5.47	3.53	4.86	0.48	13.05
Zr	5.5	5.1	6.1	116.0	16.5	4.0	8.0	0.8	134.6
Nb	0.17	0.57	1.26	68.92	1.76	0.42	0.32	0.11	21.85
Mo	2.81	0.18	0.37	1.10	2.03	0.10	0.11	0.16	0.16
Ag	0.02	0.01	0.02	0.06	0.01	0.01	0.00	0.00	0.05
In	0.01	0.01	0.01	0.03	0.02	0.01	0.02	0.01	0.06
Sn	0.50	0.14	0.10	0.95	0.25	0.11	0.12	0.05	1.53
Sb	0.16	0.02	0.02	0.03	0.07	0.02	0.03	0.02	0.04
Cs	0.045	0.02	0.04	0.01	0.05	0.02	0.01	0.02	0.06
Ba	14.5	18.6	23.8	418.2	16.0	9.4	1.0	1.6	262.5
Bi	0.013	0.00	0.00	0.01	0.01	0.01	0.00	0.00	0.02
Hf	0.17	0.17	0.21	2.56	0.47	0.15	0.28	0.02	3.14
Ta	0.01	0.04	0.08	3.61	0.12	0.03	0.04	0.01	1.63
W	0.06	0.03	0.03	0.39	0.06	0.02	0.02	0.03	0.06
Tl	0.21	0.02	0.02	0.01	0.01	0.02	0.06	0.00	0.01
Pb	3.83	1.52	0.76	1.87	2.97	0.97	0.27	0.57	3.49
Th	0.07	0.07	0.10	8.37	0.23	0.04	0.03	0.03	3.88
U	0.03	0.02	0.04	1.21	0.08	0.02	0.01	0.02	0.64
La	0.64	0.55	0.93	43.43	1.71	0.40	1.19	0.14	51.27
Ce	1.8	1.4	2.4	77.5	5.1	1.0	4.2	0.3	94.9
Pr	0.27	0.20	0.32	8.28	0.76	0.13	0.67	0.04	10.12
Nd	1.37	0.95	1.59	28.98	3.82	0.68	3.40	0.18	35.94
Sm	0.37	0.31	0.44	4.20	0.96	0.26	0.84	0.04	5.43
Eu	0.13	0.12	0.15	1.06	0.28	0.10	0.26	0.01	1.27
Gd	0.52	0.48	0.56	2.78	1.04	0.43	0.91	0.06	3.71
Tb	0.09	0.08	0.09	0.34	0.15	0.08	0.14	0.01	0.45
Dy	0.66	0.62	0.64	1.90	0.99	0.58	0.88	0.07	2.58
Ho	0.15	0.14	0.14	0.35	0.21	0.13	0.18	0.02	0.49
Er	0.46	0.43	0.43	1.01	0.64	0.43	0.55	0.06	1.36
Tm	0.07	0.06	0.06	0.14	0.09	0.06	0.08	0.01	0.19
Yb	0.47	0.45	0.39	0.98	0.58	0.42	0.52	0.08	1.38
Lu	0.07	0.07	0.06	0.15	0.08	0.06	0.08	0.01	0.21

Sample	**SL17-81B**	**SL17-81C**	**SL17-82**	**SL17-84**	**SL17-85**	**SL17-97**	**TL17-018**	**TL17-12**
Rock type	lhz	lhz	lhz	lhz	lhz	harz	lava	lhz
Sc	15.2	14.4	14.1	15.7	12.3	8.7	34.8	6.5
V	75.2	64.9	69.0	76.8	58.8	39.3	235.9	29.0
Cr	2464	2015	2548	2781	2616	2357	365	3845
Co	108	109	110	106	114	124	47	140
Ni	1988	1968	2150	1982	2201	2308	252	2549
Cu	29.8	23.0	25.9	24.1	20.6	3.2	43.1	3.4
Zn	53.8	48.7	54.4	52.6	53.5	62.0	64.1	59.7
Ga	3.0	2.5	2.7	3.3	2.4	1.5	14.4	1.2
Ge	0.89	0.82	0.88	0.86	0.83	0.80	1.77	0.79
As	0.29	1.13	0.18	0.62	0.34	0.12	0.47	0.49
Rb	3.16	1.85	0.49	1.42	0.64	0.23	75.19	2.23
Sr	11.58	15.49	5.24	10.30	4.78	7.39	724.03	11.82
Y	3.45	3.06	2.72	3.72	1.87	0.58	19.86	0.64
Zr	5.1	5.1	3.2	12.2	4.0	0.9	145.9	3.5
Nb	0.25	0.33	0.05	0.26	0.07	0.17	52.60	0.87
Mo	0.10	0.07	1.74	0.07	0.06	1.18	1.86	0.08
Ag	0.02	0.01	0.01	0.01	0.01	0.01	0.04	0.00
In	0.01	0.01	0.01	0.01	0.01	0.01	0.06	0.01
Sn	0.11	0.07	0.14	0.20	0.07	0.12	0.89	0.09
Sb	0.02	0.02	0.04	0.02	0.02	0.04	0.05	0.02
Cs	0.04	0.02	0.01	0.03	0.01	0.01	1.88	0.07
Ba	15.8	9.8	2.7	19.0	4.0	3.6	1385.1	23.0
Bi	0.00	0.00	0.00	0.01	0.01	0.00	0.01	0.00
Hf	0.18	0.15	0.11	0.30	0.10	0.02	3.69	0.08
Ta	0.02	0.03	0.00	0.02	0.00	0.01	3.37	0.05
W	0.02	0.01	0.04	0.01	0.01	0.01	0.27	0.02
Tl	0.03	0.03	0.06	0.13	0.02	0.00	0.40	0.01
Pb	2.24	0.90	0.99	0.79	0.40	0.60	3.33	0.31
Th	0.02	0.04	0.02	0.11	0.03	0.02	3.25	0.06
U	0.01	0.02	0.01	0.03	0.02	0.01	0.85	0.03
La	0.43	0.60	0.10	0.42	0.15	0.19	31.19	0.58
Ce	1.3	1.5	0.3	1.1	0.4	0.5	66.3	1.4
Pr	0.21	0.21	0.06	0.15	0.06	0.07	7.73	0.16
Nd	1.14	0.96	0.39	0.74	0.30	0.33	31.20	0.64
Sm	0.35	0.28	0.18	0.27	0.11	0.07	5.77	0.12
Eu	0.12	0.10	0.07	0.10	0.04	0.02	1.75	0.04
Gd	0.48	0.42	0.33	0.44	0.21	0.07	4.91	0.11
Tb	0.08	0.07	0.06	0.08	0.04	0.01	0.64	0.02
Dy	0.58	0.52	0.44	0.59	0.29	0.09	3.92	0.10
Ho	0.13	0.12	0.10	0.13	0.07	0.02	0.76	0.02
Er	0.40	0.36	0.32	0.43	0.23	0.07	2.17	0.08
Tm	0.06	0.05	0.05	0.06	0.03	0.01	0.29	0.01
Yb	0.40	0.37	0.32	0.42	0.23	0.09	1.90	0.08
Lu	0.06	0.06	0.05	0.07	0.04	0.02	0.28	0.01

concentrations, although it is generally found in higher concentrations in the Mt. Timothy xenoliths (1.6-4.5 wt.%) than it is in the Summit Lake xenoliths (0.8-3.7 wt.%).

The bulk of the samples from Summit Lake display flat to moderately enriched LREE patterns, with a select few displaying more LREE-depleted patterns (Figure 4.4). Most Mt. Timothy samples have slightly concave-up LREE patterns, where the lightest LREEs (La, Ce) are enriched and the lowest abundances are found in Pr, Nd, and Sm, followed by relatively flat MREE and HREE distributions. Two Mt. Timothy samples – both harzburgites – are very strongly enriched in LREEs, which is curiously not the case with any of the three Summit Lake harzburgite samples for which bulk geochemistry was collected. The enrichment in the LREEs displayed by some of these samples may be indicative of slight enrichments by metasomatic processes.

Trace and rare earth element contents for peridotites from both suites largely fall well within the range of values reported for peridotite xenoliths from other Cordilleran suites (Figures 4.4 and 4.5). The only elements whose values fall outside of the range of compositions reported elsewhere are Ba, Ta, and P for two Summit Lake samples and K and Ta for two Mt. Timothy samples, all lower than the reported Cordilleran range. These samples include both lherzolites and harzburgites. Most rare earth element compositions fall very slightly on the higher end of Cordilleran values, while the handful of harzburgites measured here are more depleted than most (Figure 4.4). This reflects the lack of clinopyroxene, more compatible with REEs than olivine or orthopyroxene, in these samples.

Tb/Yb ratios from these samples can be used to interpret aspects of their source and evolution (Figure 4.6). Yb strongly partitions into garnet as a melt evolves, yielding distinct garnet and spinel stability fields for these peridotites: as expected, all ratios for these upper mantle spinel peridotites fall within or above the spinel stability field (Bodinier et al., 1988). Many of the Summit Lake and Mt. Timothy samples have relatively high Tb/Yb ratios, with a few even displaying Tb enrichment relative to chondritic values. Peslier et al. (2002) suggest that strong enough metasomatism affecting similar peridotites can disturb their MREEs and result in Tb enrichment, and these data may then indicate that these peridotites did experience minor metasomatism.

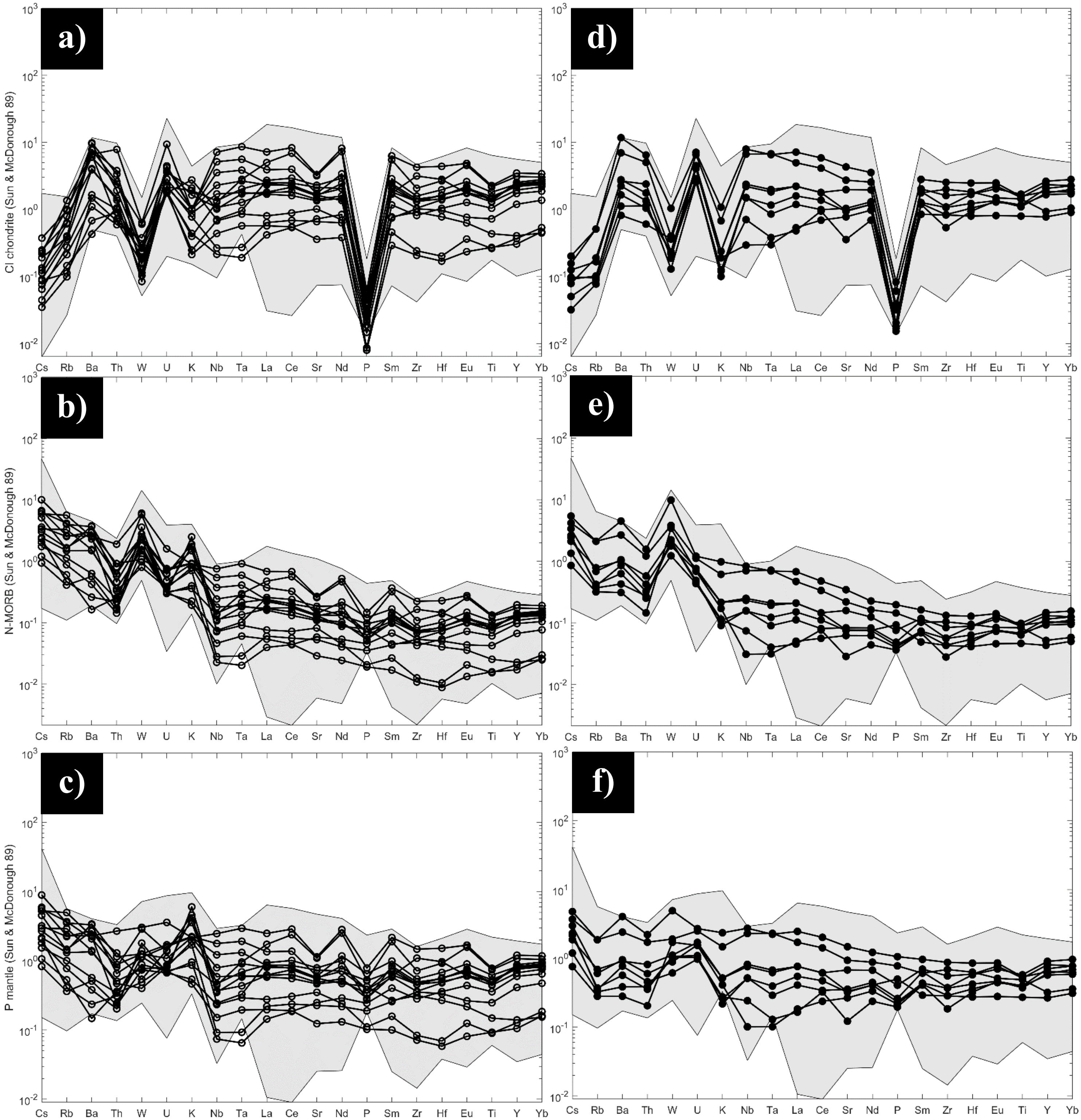

Figure 4.4 – Trace element patterns for peridotite xenoliths from Summit Lake (a-c) and Mt. Timothy (d-f), normalized to Cl-chondrite (a, d), N-MORB (b, e), and primitive mantle (c, f) values. The gray area represents ranges of trace element concentrations from ultramafic xenoliths from other localities across the southern Cordillera (data from Peslier et al., 2002; Friedman et al., 2016). All normalization values from Sun and McDonough (1989). Data from the nanoparticulate pressed powder pellet dataset.

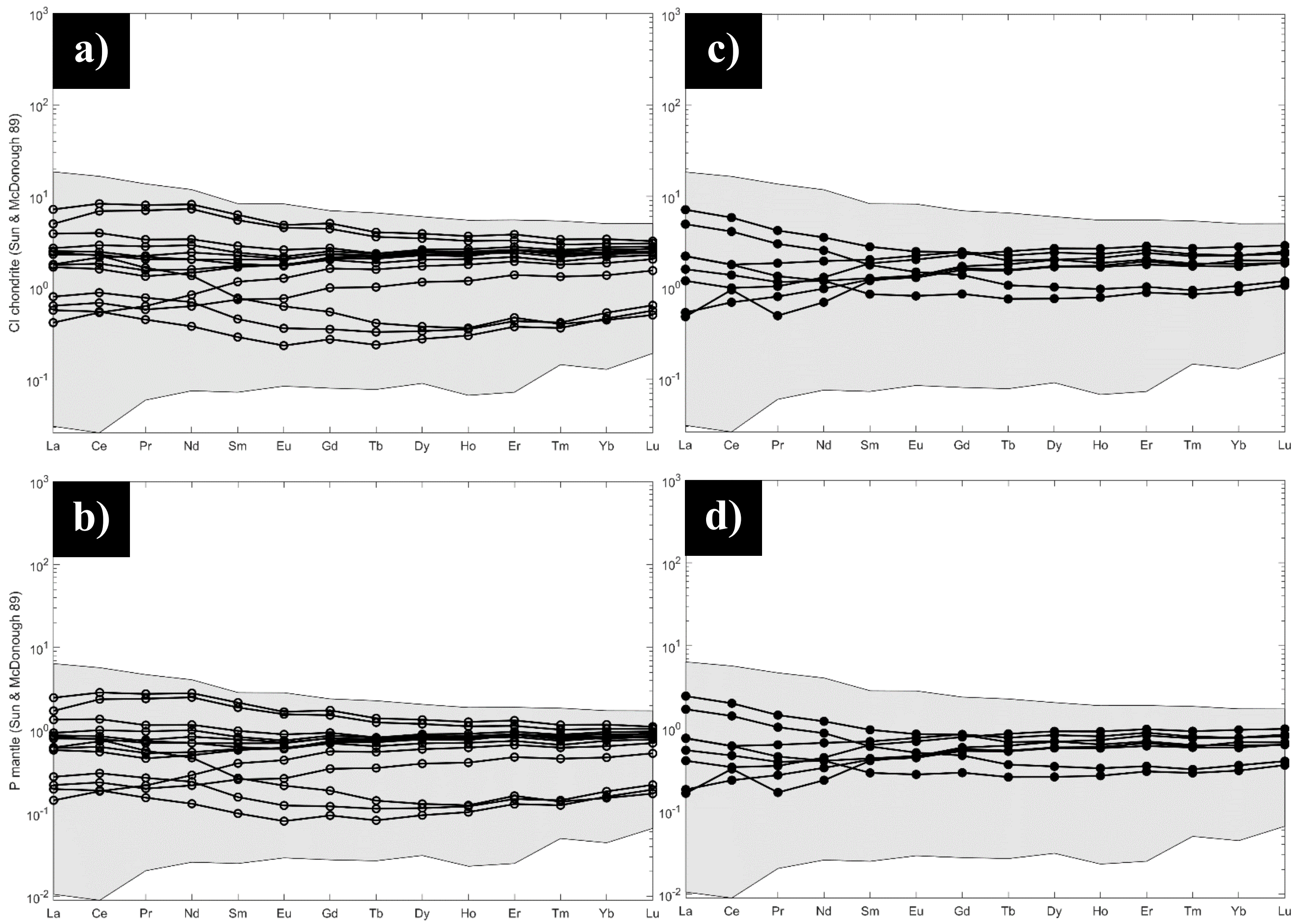

Figure 4.5 – Rare earth element patterns for peridotite xenoliths from Summit Lake (a and b) and Mt. Timothy (c and d), normalized to Cl-chondrite (a and c) and primitive mantle (b and d) values. The gray area represents ranges of rare earth element concentrations from ultramafic xenoliths from other localities across the southern Cordillera (data from Peslier et al., 2002; Friedman et al., 2016). All normalization values from Sun and McDonough (1989). Data from the nanoparticulate pressed powder pellet dataset.

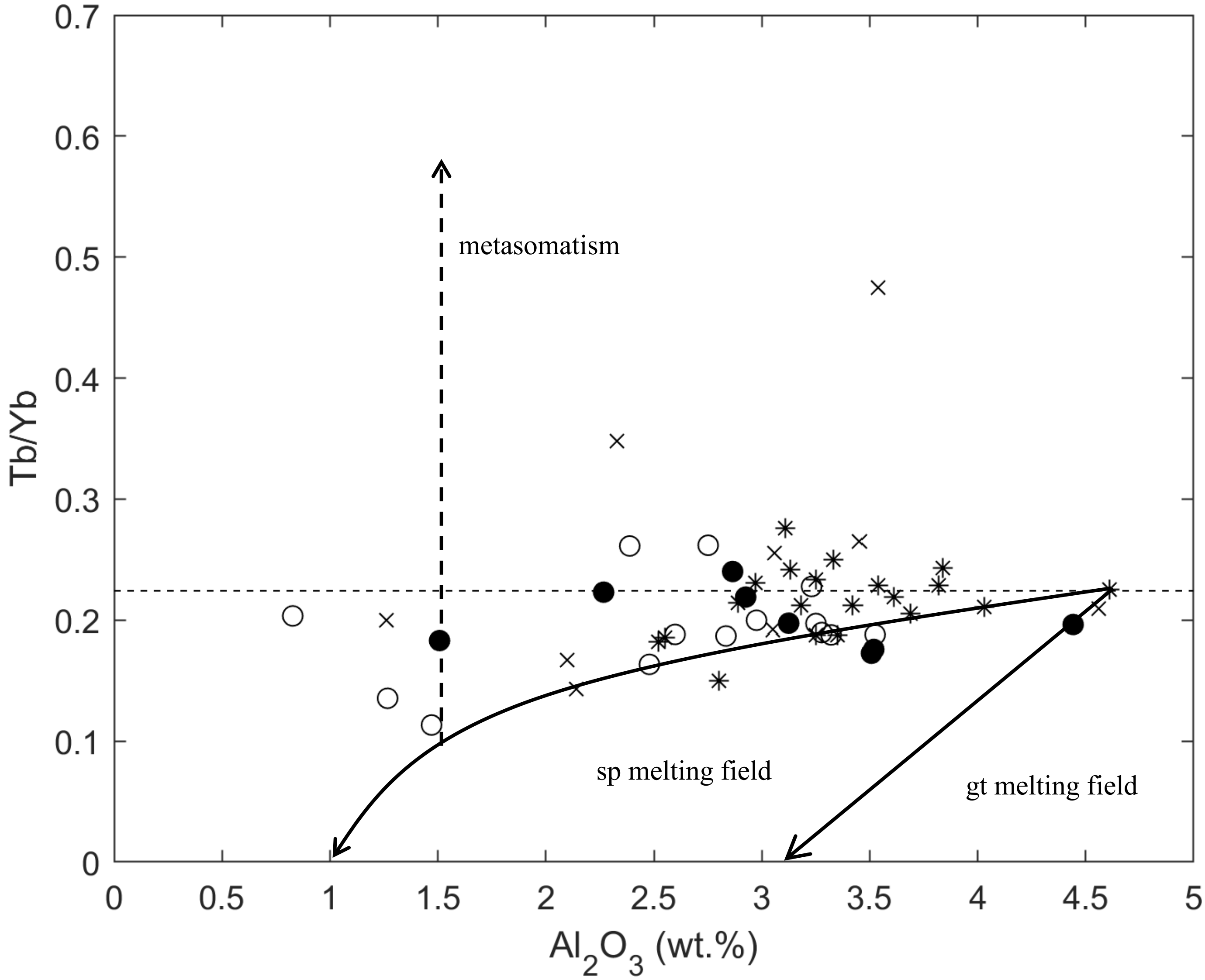

Figure 4.6 – Tb/Yb vs. Al_2O_3 for peridotite xenoliths from Summit lake (open circles), Mt. Timothy (filled circles), and Tasse alkaline basalts (asterisks; data from Friedman et al., 2016). Solid lines are melting trends for spinel stable and garnet stable assemblages (Bodinier et al., 1988; McDonough and Frey, 1990), and the dashed horizontal line indicates chondritic Tb/Yb (McDonough and Sun, 1995). Figure modeled after Peterson (2005). Data from the nanoparticulate pressed powder pellet dataset.

5. GEOTHERM-CONSTRAINED 2-PYROXENE GEOTHERMOMETRY

5.1 EMP ANALYTICAL CONDITIONS AND METHODOLOGY

A total of 53 peridotite samples – 26 from Summit Lake and 27 from Mt. Timothy – were analyzed for the compositions of their constituent orthopyroxenes and clinopyroxenes using the University of British Columbia's electron microprobe. A minimum of four orthopyroxene-clinopyroxene mineral pairs were measured in each sample. Within each mineral pair, a minimum of three measurements were taken along the boundary between the two grains, with four to six measurements preferred when allowed by the length and quality of the grain boundary. Each point was taken a minimum of 15-20 μm from the boundary itself in an attempt to avoid contamination. A total of seven wehrlite (SL17-48, SL17-57, TL17-15, TL17-16A), dunite (SL17-87, SL17-55B), and harzburgite (TL17-16B) samples from the Summit Lake area lacked any pyroxene pairs, while one additional lherzolite sample (SL17-83) lacked any adjacent orthopyroxene and clinopyroxene grains. These samples were thus precluded from these analyses.

Microprobe analyses of all orthopyroxenes and clinopyroxenes were collected on the fully automated CAMECA SX-50 instrument housed in the Electron Microbeam and X-Ray Diffraction Facility in UBC's Department of Earth, Ocean, and Atmospheric Sciences. The instrument was operated in the wavelength-dispersion mode with an excitation voltage of 15 kV, a beam current of 20 nA, a peak count time of 20 s, a background count-time of 10 s, and a spot diameter of 5 μm. Data reduction was done using the 'PAP' $\phi(\rho Z)$ method for all minerals (Pouchou & Pichoir, 1985). Mg standards differed between the two pyroxenes, with clinopyroxene data processed using a diopside standard and orthopyroxene data processed using an olivine standard. All other elements considered used the same standards, X-ray lines, and crystals for both pyroxenes: albite, Na$K\alpha$, TAP; kyanite, Al$K\alpha$, TAP; diopside, Si$K\alpha$, TAP; orthoclase, K$K\alpha$, PET; diopside, Ca$K\alpha$, PET; rutile, Ti$K\alpha$, PET; synthetic magnesiochromite, Cr$K\alpha$, LIF; synthetic rhodonite, Mn$K\alpha$, LIF; and synthetic fayalite, Fe$K\alpha$, LIF.

5.2 PYROXENE COMPOSITIONS

Electron microprobe analyses of orthopyroxene and clinopyroxene compositions (Table 5.1) for the Summit Lake and Mt. Timothy xenoliths are broadly similar to those reported from other spinel-bearing peridotites elsewhere in the Canadian Cordillera (Peslier et al., 2002; Harder and Russell, 2006; Greenfield et al., 2013). Clinopyroxenes from the Summit Lake suite range in Mg# (100*Mg/(Mg + Fe)) from 87.1 to 92.1 (average 89.5), while those from the Mt. Timothy xenoliths range from 89.1 to 94.1 (average 91.3). Orthopyroxenes from Summit Lake xenoliths range from 87.4 to 91.4 (average 89.7), while those from Mt. Timothy range from 89.6 to 92.0 (average 90.5). There is significantly more variability in clinopyroxene Mg# from both suites than there is for orthopyroxene. The former has variations of 1.07 and 1.22, respectively, for Summit Lake and Mt. Timothy, while Mg# standard deviations for orthopyroxenes from both suites are 0.91 and 0.69. Mg# for both pyroxenes are systemically higher in Mt. Timothy xenoliths than they are in Summit Lake xenoliths, as can be seen in Figure 5.1.

5.3 GEOTHERM-CONSTRAINED GEOTHERMOMETRY

Geothermobarometry for these peridotite xenoliths has been conducted using the Brey & Köhler (1990) geothermometer. This model is based on the exchange of Ca and Fe-Mg between coexisting orthopyroxene and clinopyroxene grains. The BK90 model applies a series of

Table 5.1 – Clinopyroxene and orthopyroxene compositions in selected SL and TM peridotite xenoliths as measured with UBC's electron microprobe. All Wt. % are averages of *n* measurements, with ± standard deviations included. An expanded version of this table with all measured xenoliths can be found in Appendix A.

	SL08-29		**SL17-33**		**SL17-53**		**SL17-76**		**SL17-84**	
Cpx:	**n = 4**		**n = 8**		**n = 6**		**n = 6**		**n = 5**	
SiO_2	50.66	± 0.33	50.09	± 0.37	52.13	± 0.37	49.52	± 0.42	50.25	± 0.24
TiO_2	0.46	± 0.02	0.42	± 0.02	0.19	± 0.05	0.70	± 0.04	0.49	± 0.01
Al_2O_3	6.75	± 0.16	7.16	± 0.06	4.22	± 0.10	7.44	± 0.09	6.72	± 0.05
Cr_2O_3	0.84	± 0.04	0.30	± 0.04	1.25	± 0.07	0.35	± 0.02	0.69	± 0.04
FeO_T	3.47	± 0.07	3.50	± 0.11	2.97	± 0.09	3.98	± 0.05	3.46	± 0.09
MnO	0.11	± 0.01	0.10	± 0.02	0.08	± 0.02	0.11	± 0.01	0.09	± 0.02
MgO	16.62	± 0.24	16.49	± 0.05	17.68	± 0.15	16.30	± 0.06	16.58	± 0.20
CaO	19.49	± 0.26	20.34	± 0.09	20.55	± 0.06	20.08	± 0.06	19.95	± 0.10
Na_2O	1.08	± 0.07	0.96	± 0.03	0.87	± 0.03	0.94	± 0.03	0.97	± 0.07
Total	99.49	± 1.22	99.39	± 0.31	99.96	± 0.29	99.41	± 0.53	99.21	± 0.31
Mg#	89.51	± 0.07	89.36	± 0.33	91.38	± 0.27	87.96	± 0.11	89.52	± 0.24
Opx:										
SiO_2			53.14	± 0.40	55.23	± 0.23	52.74	± 0.23	53.68	± 0.08
TiO_2	53.68	± 0.34	0.12	± 0.01	0.07	± 0.02	0.21	± 0.01	0.15	± 0.01
Al_2O_3	0.13	± 0.01	5.75	± 0.05	3.24	± 0.06	5.85	± 0.04	5.21	± 0.11
Cr_2O_3	5.28	± 0.02	0.20	± 0.02	0.65	± 0.01	0.23	± 0.03	0.44	± 0.02
FeO_T	0.47	± 0.02	6.64	± 0.14	5.99	± 0.11	7.46	± 0.08	6.55	± 0.11
MnO	6.42	± 0.06	0.14	± 0.01	0.13	± 0.01	0.15	± 0.02	0.14	± 0.01
MgO	0.12	± 0.01	32.69	± 0.17	33.55	± 0.10	31.71	± 0.04	32.41	± 0.17
CaO	32.26	± 0.09	1.04	± 0.02	1.12	± 0.02	1.16	± 0.01	1.11	± 0.06
Na_2O	1.12	± 0.02	0.01	± 0.01	0.02	± 0.01	0.05	± 0.02	0.00	± 0.01
Total	0.03	± 0.01	99.75	± 0.48	100.02	± 0.30	99.56	± 0.22	99.71	± 0.35
Mg#	99.51	± 0.58	89.77	± 0.22	90.90	± 0.16	88.34	± 0.11	89.82	± 0.11

	TM08-38		**TM08-41**		**TM08-T**		**TM17-19**		**TM17-25**	
Cpx:	**n = 5**		**n = 4**		**n = 6**		**n = 5**		**n = 4**	
SiO_2	53.02	± 0.40	50.79	± 0.47	51.45	± 0.18	50.39	± 0.51	52.10	± 0.17
TiO_2	0.03	± 0.01	0.39	± 0.01	0.53	± 0.02	0.51	± 0.01	0.02	± 0.01
Al_2O_3	2.89	± 0.17	7.00	± 0.04	6.81	± 0.03	6.86	± 0.09	2.66	± 0.09
Cr_2O_3	1.07	± 0.09	0.71	± 0.02	0.74	± 0.03	0.75	± 0.04	1.05	± 0.06
FeO_T	2.17	± 0.06	3.55	± 0.03	3.27	± 0.06	3.02	± 0.10	2.03	± 0.05
MnO	0.08	± 0.01	0.09	± 0.00	0.10	± 0.02	0.09	± 0.02	0.07	± 0.01
MgO	17.83	± 0.16	16.28	± 0.04	15.98	± 0.15	16.01	± 0.10	17.98	± 0.03
CaO	22.52	± 0.20	19.60	± 0.11	19.29	± 0.16	19.83	± 0.13	23.05	± 0.11
Na_2O	0.51	± 0.02	1.27	± 0.04	1.50	± 0.05	1.53	± 0.02	0.54	± 0.05
Total	100.12	± 0.51	99.69	± 0.54	99.67	± 0.30	99.03	± 0.47	99.51	± 0.31
Mg#	93.62	± 0.18	89.09	± 0.06	89.72	± 0.09	90.42	± 0.35	94.05	± 0.13
Opx:										
SiO_2	55.95	± 0.43	54.56	± 0.33	54.34	± 0.21	52.94	± 0.60	55.33	± 0.26
TiO_2	0.01	± 0.01	0.12	± 0.01	0.15	± 0.01	0.13	± 0.02	0.01	± 0.01
Al_2O_3	2.60	± 0.16	5.34	± 0.03	5.01	± 0.05	5.04	± 0.09	2.47	± 0.06
Cr_2O_3	0.58	± 0.03	0.38	± 0.01	0.42	± 0.03	0.40	± 0.03	0.62	± 0.03
FeO_T	5.52	± 0.08	6.70	± 0.07	6.58	± 0.05	6.35	± 0.11	5.40	± 0.13
MnO	0.14	± 0.03	0.15	± 0.00	0.14	± 0.01	0.15	± 0.01	0.13	± 0.02
MgO	34.48	± 0.18	32.20	± 0.13	32.25	± 0.11	32.83	± 0.14	34.72	± 0.10
CaO	0.67	± 0.06	1.10	± 0.02	0.97	± 0.05	0.84	± 0.01	0.66	± 0.01
Na_2O	0.00	± 0.00	0.06	± 0.01	0.06	± 0.01	0.04	± 0.02	0.00	± 0.00
Total	99.97	± 0.50	100.61	± 0.23	99.92	± 0.35	98.73	± 0.73	99.37	± 0.40
Mg#	91.76	± 0.10	89.55	± 0.09	89.74	± 0.06	90.21	± 0.13	91.97	± 0.17

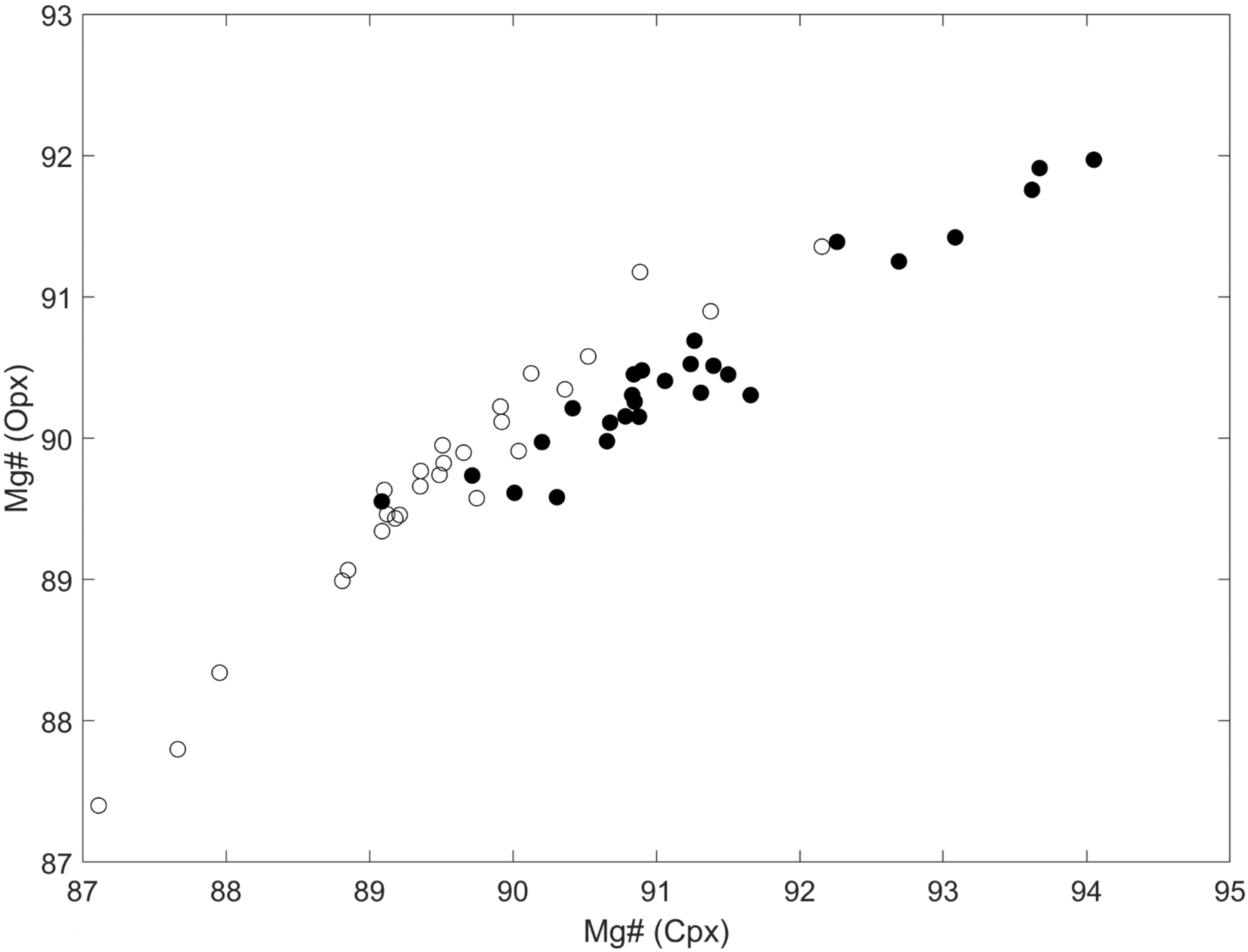

Figure 5.1 – Mg# for clinopyroxenes plotted against those for orthopyroxenes. Open circles are Summit Lake xenoliths; filled circles are Mt. Timothy xenoliths.

corrections to the Wells model, and places emphasis on Mg-Fe exchange (Wells, 1977). The BK90 geothermometer reproduces experimental data to an accuracy of ±15°C, and displays no systematic dependence on temperature, pressure, or compositional parameters (Brey and Köhler, 1990; see Appendix C for more details).

The Brey and Köhler thermometer is one of a group of similar empirical models suitable for spinel peridotites such as those found at xenolith-bearing volcanic centers across the Canadian Cordillera. However, there are presently few, if any, reliable geobarometers that can be applied to these same rocks. The majority of peridotite geobarometers rely on the presence of garnet. For example, a barometer put forward in the same paper by Brey and Köhler that is used in conjunction with the BK90 geothermometer is built around the exchange of Al between garnet and orthopyroxene (Brey and Köhler, 1990). However, garnet-bearing peridotites are entirely absent in mantle xenoliths derived from the Quaternary volcanics of the Intermontane Belt. As a result, conventional geobarometers are generally ineffective when applies to these samples (Francis et al., 2010).

The BK90 thermometer calculates temperature as a function of pressure, and thus it is generally solved simultaneously with a barometer that calculates pressure as a function of temperature. In lieu of a proper barometer, this study opts to follow the example of Harder and Russell (2006) and Greenfield et al. (2013) by substituting a model geotherm as a proxy for depth and pressure. This model geotherm (Equation 2) is calculated from local heat flow data, assumes conductive heat flow in a two-layer lithosphere, and incorporates a number of geophysical parameters for two separate layers in the crustal and mantle lithosphere that have been calculated by previous researchers for the southern Cordillera. These include a constant crustal thickness (Z_{Moho}) of 33 km and a surface temperature (T_0) of 10 °C (Hyndman, 2010).

Crustal and mantle densities are set at, respectively, 2800 and 3300 kg m^{-3}, and crustal and mantle thermal conductivities (K_1 and K_2) at 2.5 and 3.2 W m^{-1} K^{-1} (Greenfield et al., 2013). The crustal heat production (A_0) in the Intermontane Belt of approximately 1.3 µW m^{-3} is taken from Lewis et al. (1992). The mantle lithosphere is assumed to have no significant heat production.

This two-layer lithosphere is modelled by Harder and Russell (2006) and Greenfield et al. (2013) using the following three equations. Equations 1 and 2, respectively, model temperature as a function of depth for the crustal and mantle portions of the lithosphere, incorporating all the geophysical parameters described above to create geotherms for the lithosphere underling a specific region. Equation 3 uses these same parameters to model surface heat flow q_0 (mW m^{-2}).

$$(1) \quad T(z) = T_0 + \frac{q_0 z}{K_1} + \frac{A_0 {Z_{Moho}}^2}{K_1}\left(1 - \frac{z}{Z_{Moho}} - e^{\frac{-z}{Z_{Moho}}}\right), \qquad 0 < z < Z_{Moho}$$

$$(2) \quad T(z) = T_{Moho} + \frac{(q_0 - 0.6321 A_0 Z_{Moho})}{K_2}(z - Z_{Moho}), \qquad Z_{Moho} < z < Z_{asthenosphere}$$

$$(3) \quad q_0 = 0.3679 Z_{Moho} A_0 + \frac{(T_{Moho} - T_0)K_1}{Z_{Moho}}$$

Greenfield et al. (2013) and Harder and Russell (2006) used the lowest temperature xenoliths to approximate the Moho temperature (T_{Moho}). For example, the lowest temperature xenolith (RK-TM17-25) at Mt. Timothy would be taken as being close to the depth of the Moho and its Brey and Köhler temperature would be computed for that depth (i.e. pressure). Running all Mt. Timothy xenoliths through the Brey and Köhler (1990) geothermometry model using an arbitrary pressure value of 12 kbar reveals the lowest temperature sample in this collection to be TM17-25. With this sample assumed to record the conditions at the Moho beneath this region, we again run this individual sample through the BK90 model using the Moho depth for the southern Cordillera suggested by Lewis et al. (1992) and Hyndman (2010) of 33 km, which equates to a pressure of 9.05 kbar. This results in a temperature of 813.4 °C for this sample – ±

15 °C based on the uncertainties prescribed by Brey and Köhler (1990) – which is then used as the value for Moho temperature (T_M) in the calculations for all subsequent xenoliths. It is also used in the calculation for surface heat flow (q_0) using Equation 3 (see above) from Greenfield et al. (2013), which comes out at 76.7 mW m^{-2}. This value reproduces results from nearby xenolith suites slightly more accurately than the value of 73 mW m^{-2} given by Lewis et al. (1992) as an average for the Cordillera south of 59°.

5.4 GEOTHERMOMETRY RESULTS

Temperature, pressure, and depth results for the peridotites from Summit Lake and Mt. Timothy are presented in Table 5.2 and Figures 5.2 and 5.3. Averages are all calculated assuming an average Moho temperature of 813 °C, with a minimum of 788 °C and a maximum of 838 °C, and a uniform Moho depth of 33 km. All three geotherms are displayed in Figure 5.2. The model geotherm described above is assumed to be the same for both field sites given the uniform thickness of the lithosphere in the Intermontane Belt and the heat flow values reported by Lewis et al. (1992). The standard deviations listed in Table 5.2 for temperature, depth, and pressure were propagated from the variability between multiple electron microprobe measurements for each individual xenolith (see section 5.1).

5.4.1 SUMMIT LAKE RESULTS

A total of 26 peridotite xenolith samples from the Summit Lake suite were analyzed with these methods. The equilibrium conditions recorded from these samples are uniformly hot and deep, averaging 1088 °C, 14.67 kbar, and 50.7 km, with no noticeable outliers either high or low.

Table 5.2 – Depth, pressure, and temperatures, plus standard deviations, calculated for peridotite xenoliths from Summit Lake (SL) and Mt. Timothy (TM). Samples labeled with the 'TL' prefix are from "talus quarry,' a separate exposure of the same Summit Lake unit. Samples labeled with a 17 (e.g. SL17-#) were collected in the summer of 2017, while those labeled with an 08 (e.g. SL08-#) were collected by Dante Canil in the summer of 2008. Lhz = lherzolite; harz = harzburgite; ol-webs = olivine websterite.

ID	Type	T (°C)	± σ	P (kbar)	± σ	Depth (km)	± σ
SL08-02	lhz	1084	7	14.60	0.14	50.5	0.5
SL08-15	lhz	1082	8	14.56	0.17	50.4	0.5
SL08-29	lhz	1119	17	15.31	0.34	52.7	1.1
SL08-44	lhz	1092	9	14.76	0.19	51.0	0.6
SL17-10	lhz	1099	8	14.90	0.16	51.4	0.5
SL17-33	ol-webs	1061	9	14.12	0.19	49.0	0.6
SL17-36	lhz	1094	11	14.81	0.22	51.2	0.7
SL17-41	lhz	1070	11	14.31	0.23	49.6	0.7
SL17-43	lhz	1086	8	14.64	0.16	50.6	0.5
SL17-49	lhz	1090	11	14.73	0.22	50.9	0.7
SL17-53	harz	1076	11	14.44	0.23	50.0	0.7
SL17-55A	lhz	1099	3	14.90	0.07	51.5	0.2
SL17-68	lhz	1081	6	14.53	0.12	50.3	0.4
SL17-70	lhz	1072	4	14.35	0.09	49.7	0.3
SL17-70-2	lhz	1078	8	14.47	0.17	50.1	0.5
SL17-74	harz	1099	13	14.90	0.26	51.4	0.8
SL17-76	ol-webs	1071	6	14.34	0.13	49.7	0.4
SL17-81A	lhz	1092	3	14.76	0.06	51.0	0.2
SL17-81B	lhz	1101	11	14.95	0.23	51.6	0.7
SL17-82	lhz	1066	6	14.23	0.13	49.3	0.4
SL17-84	lhz	1090	18	14.72	0.37	50.9	1.2
SL17-85	lhz	1092	12	14.75	0.24	51.0	0.8
SL17-91	lhz	1112	11	15.17	0.22	52.3	0.7
SL17-97	harz	1100	8	14.92	0.17	51.5	0.5
TL17-01	harz	1073	6	14.36	0.12	49.7	0.4
TL17-11	lhz	1101	9	14.95	0.18	51.6	0.6
TM08-17	lhz	951	8	11.88	0.16	41.9	0.5
TM08-22	harz	869	16	10.18	0.33	36.6	1.0
TM08-25B	lhz	851	24	9.83	0.48	35.4	1.5
TM08-25C	lhz	1065	9	14.21	0.18	49.3	0.6
TM08-30	lhz	901	20	10.84	0.42	38.6	1.3
TM08-34	harz	988	49	12.63	1.00	44.3	3.2
TM08-38	harz	936	22	11.57	0.45	40.9	1.4

TM08-41	lhz	1090	15	14.71	0.32	50.8	1.0
TM08-43	lhz	936	11	11.56	0.23	40.9	0.7
TM08-48	lhz	1012	8	13.11	0.17	45.8	0.5
TM08-49	lhz	1005	4	12.98	0.09	45.4	0.3
TM08-52	lhz	980	19	12.46	0.40	43.7	1.3
TM08-54	lhz	939	13	11.62	0.27	41.1	0.8
TM08-63	lhz	871	5	10.24	0.10	36.7	0.3
TM08-64	lhz	1008	11	13.04	0.23	45.6	0.7
TM08-A1	harz	870	26	10.22	0.54	36.7	1.7
TM08-A2A(1)	lhz	942	10	11.68	0.20	41.3	0.6
TM08-A2A(2)	lhz	956	16	11.97	0.32	42.2	1.0
TM08-A2B	lhz	965	13	12.15	0.27	42.8	0.9
TM08-B1	lhz	964	21	12.15	0.43	42.8	1.3
TM08-T	harz	1091	14	14.73	0.29	50.9	0.9
TM17-18	lhz	838	12	9.55	0.24	34.6	0.8
TM17-19	lhz	1020	25	13.29	0.51	46.4	1.6
TM17-20	lhz	968	22	12.23	0.44	43.0	1.4
TM17-21	lhz	867	14	10.15	0.29	36.5	0.9
TM17-22	lhz	952	14	11.88	0.29	41.9	0.9
TM17-25	lhz	813	6	9.06	0.12	33.0	0.4

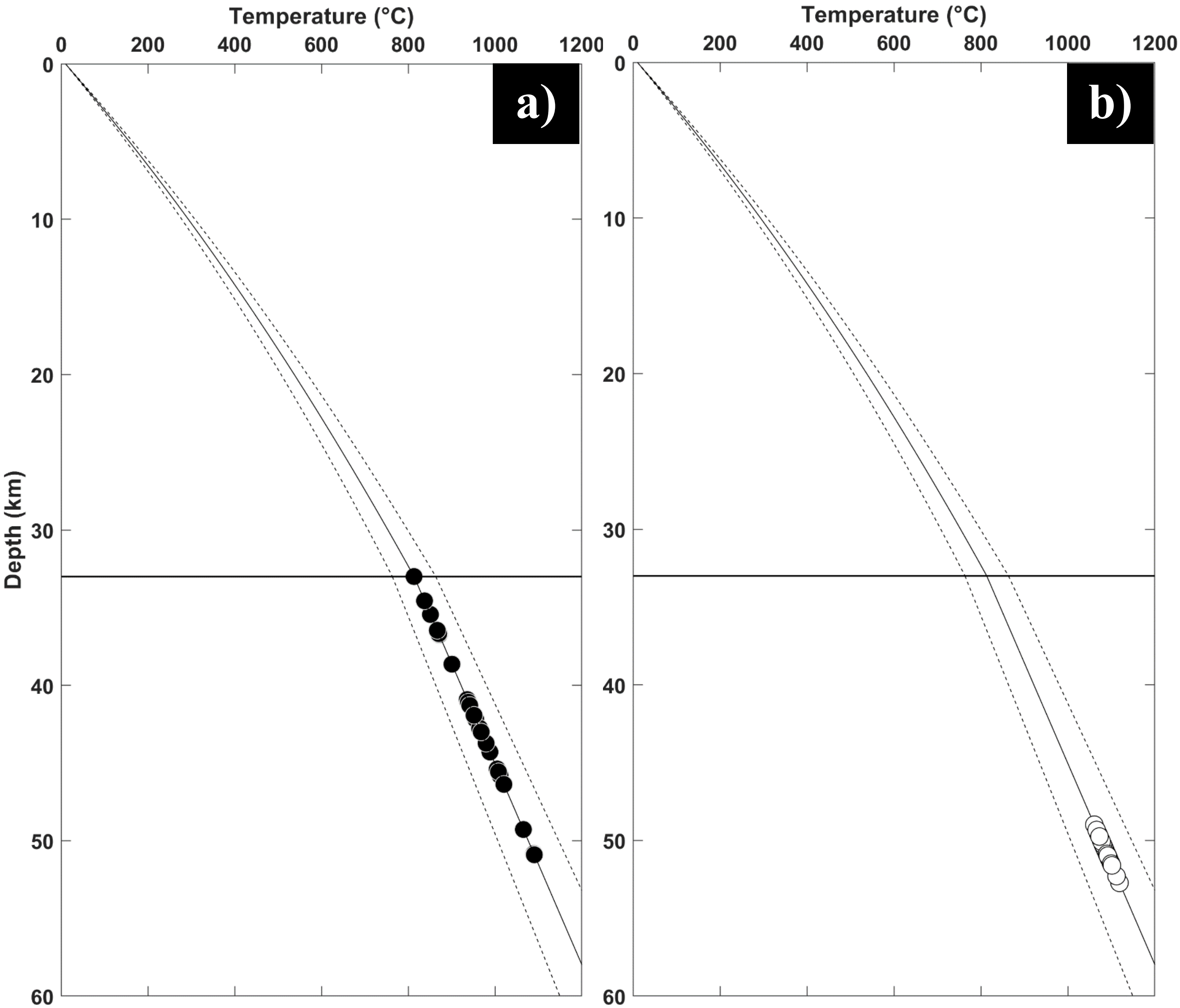

Figure 5.2 – Estimated equilibrium temperature vs. depth for all Mt. Timothy (A) and Summit Lake (B) xenoliths, assuming a Moho temperature of 813.4°C and a Moho depth – indicated by the horizontal line – of 33 km (Greenfield et al., 2013), with full lithospheric geotherm plotted from depth to the crust (Equations 1 and 2). Dashed lines with smaller icons plot hypothetical geotherms with Moho temperatures decreased by 50 °C (the steeper geotherm) and increased by 50 °C (the shallower geotherm).

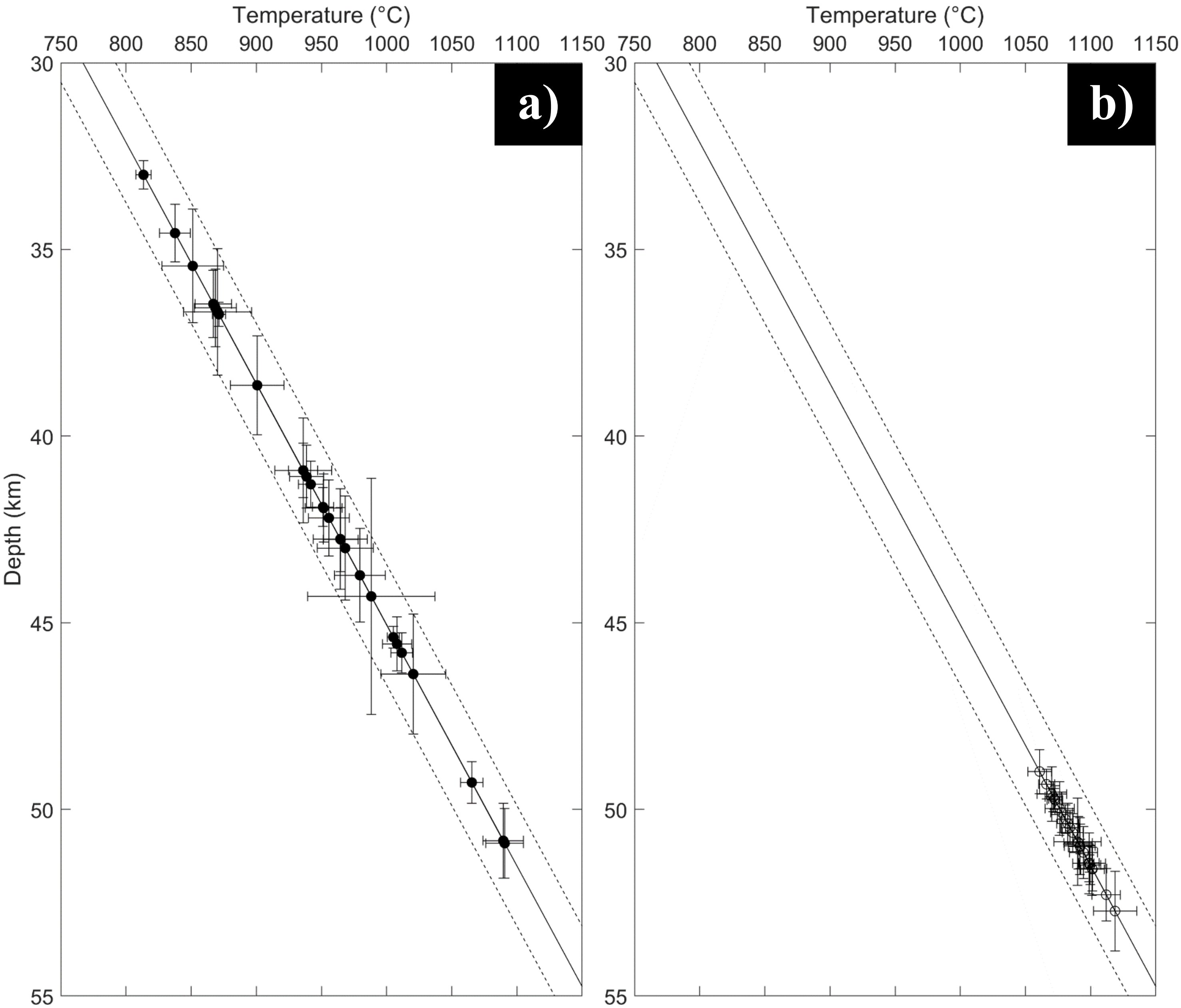

Figure 5.3 – Estimated temperature vs. depth, with errors, for all xenoliths from Mt. Timothy (A) and Summit Lake (B), assuming a geotherm at 814°C. Dashed lines above and below represent a range of Moho temperatures of ±25°C.

The lowest recorded temperature from this suite is 1061 ± 9 °C, equating to a pressure of 14.12 ± 0.19 kbar and a depth of 49.0 ± 0.6 km. This sample (SL17-33) is one of only two olivine websterites in the Summit Lake suite analyzed with the microprobe, and it may be notable that the other olivine websterite (SL17-76) has an equilibration temperature of 1071 ± 6 °C (a pressure of 14.34 ± 0.13 kbar and a depth of 49.7 ± 0.4 km). The highest temperature and most deeply-sourced sample from this collection is SL08-29, which records a temperature of 1119 ± 17 °C, a pressure of 15.31 ± 0.34 kbar, and a depth of 52.7 ± 1.1 km. The uncertainties for temperature, pressure, and depth for this sample are somewhat higher than most other Summit Lake samples, which might be attributed in turn to above average variability in the calcium and magnesium contents of its clinopyroxenes (see the list of mineral compositions in Appendix C).

The comparatively high depths and temperatures recorded by the Summit Lake xenoliths preclude the creation of an independent geotherm for this region. It is reasonable to assume that the Mt. Timothy xenoliths, with their wide range of equilibration conditions, might sample at or near the Moho. The shallowest Summit Lake xenolith (49.0 ± 0.6 km), however, is still far deeper than any published values given for Moho depth in the Intermontane Belt, and thus cannot be used to calculate an independent geotherm for the Summit Lake region. As such the geotherm calculated from the Mt. Timothy samples is used for both xenolith suites.

5.4.2 MT. TIMOTHY RESULTS

` The 27 peridotite xenolith samples from the Mt. Timothy suite that were analyzed with these methods reveal a very different lithospheric column than that outlined by the Summit Lake samples. The lowest temperature – and shallowest – of the Mt. Timothy samples records an equilibrium temperature of 813 ± 6 °C, a pressure of 9.06 ± 0.12 kbar, and a depth of 33.0 ± 0.4

km. The next lowest-temperature Mt. Timothy sample (TM17-18), at 838 ± 12 °C, is only 24 °C hotter on average than TM17-25 – not an insignificant gap, but not one so wide as to deem TM17-25 an outlier with any degree of certainty.

The highest temperature recorded by a Mt. Timothy sample belongs to TM08-T, which is modeled to have equilibrated at a temperature of 1091 ± 14 °C, a pressure of 14.73 ± 0.29 kbar, and a depth of 50.9 ± 0.9 km. Another sample, TM08-41, records nearly identical equilibration conditions (1090 ± 15 °C, 14.71 ± 0.32 kbar, and 50.8 ± 1.0 km), and an additional five xenoliths from the Mt. Timothy suite also record equilibration temperatures of over 1000 °C. This highlights the significant range of the lithospheric column sampled by the Mt. Timothy xenolith suite. While majority of these 27 samples are calculated to have equilibrated between 900 °C and 1000 °C (or 38.6 km to 45.5 km), there are enough samples above 1000 °C and below 900 °C to present a moderately even spread of equilibration depths and temperatures from this data set.

The great breadth of equilibrium conditions recorded by the Mt. Timothy mantle xenoliths stands in sharp contrast to the Summit Lake suite. The Summit Lake xenoliths record a slightly deeper, higher temperature, and significantly smaller section of the Cordilleran lithosphere, with the lowest- and highest-temperature xenoliths only separated by 58 °C and 3.73 km. The significantly larger section of the lithospheric mantle sampled by the Mt. Timothy xenoliths stretches from near or at the Moho all the way down to overlap with the depth of the Summit Lake section (49.0 km to 52.7 km), with the hottest and coolest Mt. Timothy samples separated by 277 °C and 17.91 km. This difference in variability between the suites extends even to variability within individual xenolith samples: the average standard deviation associated with equilibration temperatures for Summit Lake xenoliths is ± 9 °C (minimum ± 3 °C, maximum ±

18 °C), while the Mt. Timothy xenoliths average ± 16 °C with a minimum of ± 4 °C and a maximum of ± 49 °C.

This discrepancy between the two suites in terms of depths and temperatures sampled is made especially interesting by the fact that the Summit Lake lavas host a much wider variety of rock types than the Mt. Timothy volcanics. While both suites are dominated by spinel lherzolites with subordinate harzburgite, the Summit Lake unit also contains significant numbers of pyroxenites, websterites, olivine websterites, wehrlites, and totally clinopyroxene-free harzburgites. Additionally, as discussed in Chapter 3, Summit Lake also hosts a diverse suite of crustal xenoliths, while the crustal xenoliths present at Mt. Timothy are sparse, small, and homogenous. However, despite the homogeneity of rock types present at Mt. Timothy relative to the Summit Lake xenoliths, the former still samples a significantly broader portion of the mantle lithosphere than the latter based on these models.

These data display no systematic relationship between equilibrium temperature and rock type, with harzburgites plotting at both shallower and deeper locations within both the Summit Lake and the Mt. Timothy columns (Figure 5.4). As mentioned previously, the two measured olivine websterites from Summit Lake are both moderately high-temperature, but the sample size is much too small to draw any conclusions. This could be remedied by a larger number of samples being analyzed to more thoroughly evaluate the relationship between rock type and equilibration conditions in both suites.

One effect of the narrowness of the Summit Lake sampling window on a study such as this is that the method used by Harder and Russell (2006) and by Greenfield et al. (2013) for creating a similar lithospheric column, where the lowest-temperature xenoliths in a suite are used

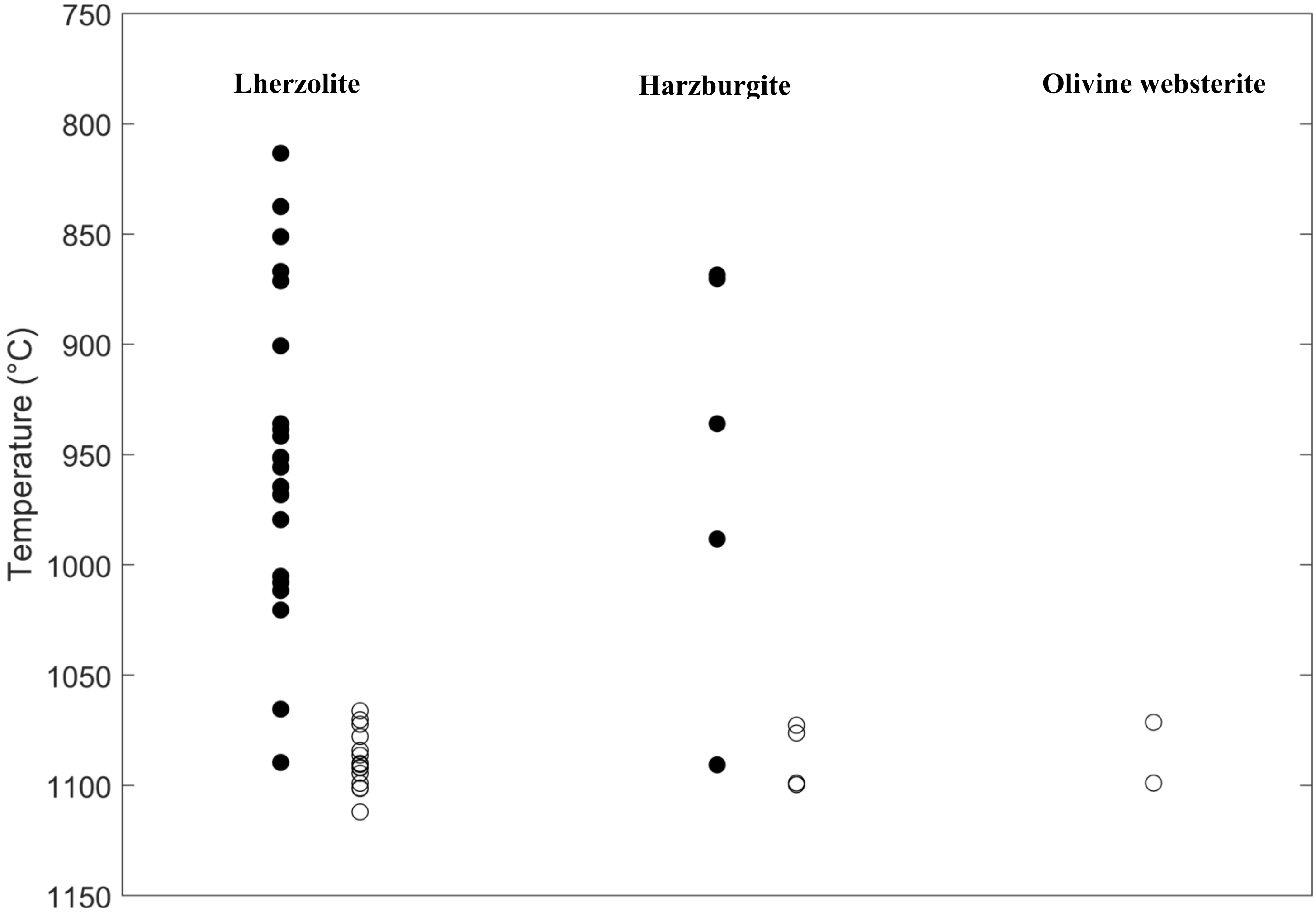

Figure 5.4 – Mantle xenolith rock types versus equilibration temperature. Rock types determined using the point counting code described in Appendix E. Filled circles = Mt. Timothy; open circles = Summit Lake.

to approximate the depth of the Moho, is of very little use. This method assumes a relatively thorough and even sampling of the lithospheric mantle by the xenolith-hosting magmas, and while this could apply to the Mt. Timothy xenolith suite, the Summit Lake volcanics sample much too narrow a window of the mantle lithosphere to be used to directly estimate the depth of the Moho in this region.

There appear to be few significant relationships between pyroxene composition and depth in either suite (Figure 5.5). Variations in both orthopyroxene and clinopyroxene Mg# with depth are almost entirely random for the Summit Lake xenoliths, and display ranges of Mg# values over their small temperature window that are equal to or greater than the Mg# ranges for Mt. Timothy. There is, however, a noticeable trend of decreasing Mg# with temperature and depth for the Mt. Timothy xenoliths that is especially pronounced in the orthopyroxene compositions.

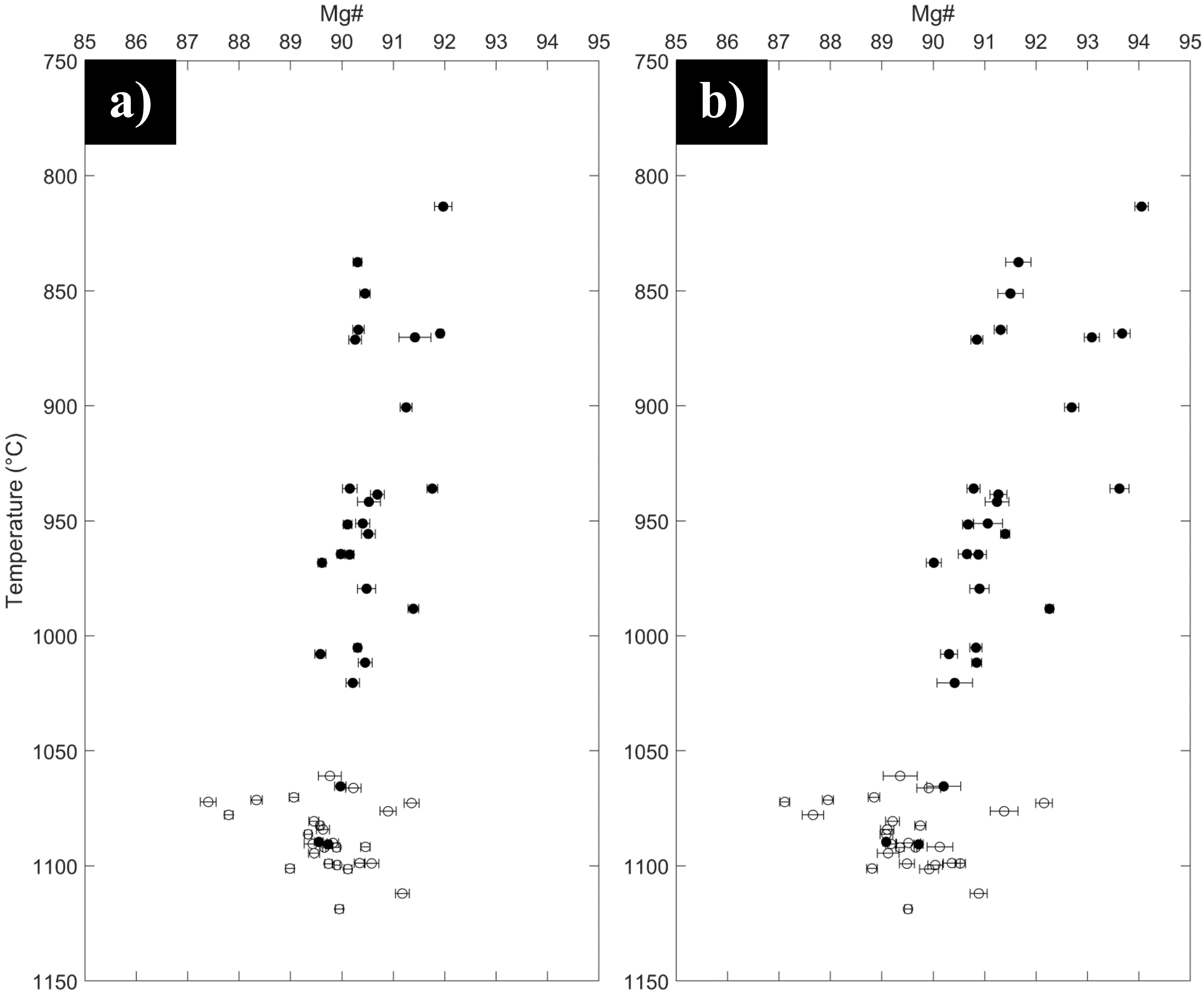

Figure 5.5 – Mg# for (A) orthopyroxenes (enstatite) and (B) clinopyroxenes (diopside) versus BK90 equilibration temperatures for peridotite xenoliths from Summit Lake (open circles) and Mt. Timothy (filled circles).

6. DISCUSSION

6.1 MANTLE SOURCES AND EVOLUTION

Peridotite xenolith suites from Mt. Timothy and Summit Lake that have been sampled and analyzed in this study, in general, are not radically different from other sites in this part of the Cordillera. However, they add to our understanding of the mantle lithosphere in the Canadian Cordillera by nature of their significantly different geographic and tectonostratigraphic locations.

6.1.1 ROCK TYPES

Both the Summit Lake and the Mt. Timothy xenolith suites are broadly similar in their distribution of rock types to most other suites in the southern Cordillera. They are both unimodal, with the majority of peridotites classified as lherzolites – while the Summit Lake suite is more diverse in its distribution of peridotite types, it does not have a high enough proportion of harzburgites to be classified as bimodal, as are a number of xenolith suites in the Northern Cordilleran Volcanic Province (Shi et al., 1998). The peridotites from both are spinel-bearing, reflecting the relatively shallow mantle depths recorded by these and other southern Cordilleran peridotite xenoliths. Plagioclase-bearing peridotites, which can be found at a very small handful of other Cordilleran xenolith suites (most notably a xenolith-rich dike at Mt. Preston), were not observed among the samples collected from either locality (Peterson, 2005). Neither amphiboles, present in the Lightning Peak xenolith suite in the Okanagan, nor phlogopite, found in xenoliths near Kostal Lake in the Wells Gray-Clearwater volcanic field, are found in the samples from Summit Lake or Mt. Timothy (Brearley and Scarfe, 1984; Canil and Scarfe, 1989).

The distribution of rock types at Mt. Timothy is especially similar to other xenolith-bearing units in the southern Cordillera. 21 of the 27 samples from this region that were studied in detail are spinel-bearing lherzolites, while the remaining six are harzburgites. Coupled with the occasional occurrence of dunites and websterites observed at the xenolith-bearing units, this distribution of rock types and modal mineralogies is similar to the relatively proximal xenolith suites at Big Timothy and Quesnel Lake (Canil et al., 1987; Greenfield et al., 2013; Friedman et al., 2016). While there are minor differences between these and other sites in the southern Cordillera, the similarities – corroborated by the xenolith collection at Mt. Timothy – indicate that these sites all sampled a relatively mineralogically homogenous mantle lithosphere.

The Summit Lake xenoliths, while still a unimodal collection dominated by spinel-bearing lherzolites, seem to sample a more mineralogically diverse mantle lithosphere than Mt. Timothy and most other xenolith-bearing suites in the southern Canadian Cordillera. The prevalence of augite-bearing wehrlites in particular is rare among southern Cordilleran xenolith suites, with the suite at Kostal Lake being the only other recorded to contain a larger proportion (Canil and Scarfe, 1989; Peslier et al., 2002). The Rayfield River suite does contain similar augite-bearing xenoliths, albeit in a smaller proportion than at Summit Lake or Kostal Lake. These two suites are notably the closest suites in the southern Cordillera to the North American craton. Peslier et al. (2002) suggest that the abundance of augite-bearing xenoliths in these suites is the product of reactions between the predominant Cr-diopside lherzolite source and alkaline melts, and that circulation of these melts might be facilitated by conditions in the transition zone between the Cordilleran orogen and the North American craton occupied by these suites.

6.1.2 TEXTURES

The bulk of the xenoliths sampled from both suites lack any particularly notable textural features. Most peridotites display protogranular textures, and the xenoliths from Summit Lake are generally finer-grained than those from Mt. Timothy (Mercier and Nicolas, 1975). As with most other Cordilleran suites, hydrous phases are not present (Peslier et al., 2002). There are rare occurrences of elongated spinel fabrics in a few Summit Lake lherzolites, but there is no apparent correlation between these fabrics and chemistry or depth. The lack of striking fabrics or textural features in xenoliths from both sites is consistent with other peridotite xenolith suites in the southern Canadian Cordillera (Littlejohn and Greenwood, 1974).

6.1.3 XENOLITH GEOCHEMISTRY

Major element compositions from both sites are largely in line with data sets from other xenolith collections in the Canadian Cordillera (Figure 6.1), albeit very marginally more enriched in Al_2O_3, TiO_2, and CaO on average relative to MgO. These data sets do not reveal any significant differences in major element compositions between xenoliths suites from the northern and southern Cordillera. Additionally, xenolith major element compositions between Summit Lake and Mt. Timothy display no major differences, although samples from Mt. Timothy do trend toward marginally higher TiO_2 and Al_2O_3 concentrations than those from Summit Lake. These similarities between regions reflect the broadly homogeneous composition of the lithospheric mantle beneath the Canadian Cordillera.

These shared trends in major element compositions versus MgO displayed in Figure 6.1 are interpreted to reflect degrees of melt extraction from a fertile peridotite source, where the primitive, low MgO peridotite source has its CaO, Al_2O_3, and TiO_2 contents decreased and its MgO content increased as it undergoes this basaltic melt extraction. Both the Summit Lake and Mt. Timothy xenolith suites thereby sample a range of depleted lithospheric material. Although the ranges of MgO values for the two localities are largely similar, the Summit Lake results do

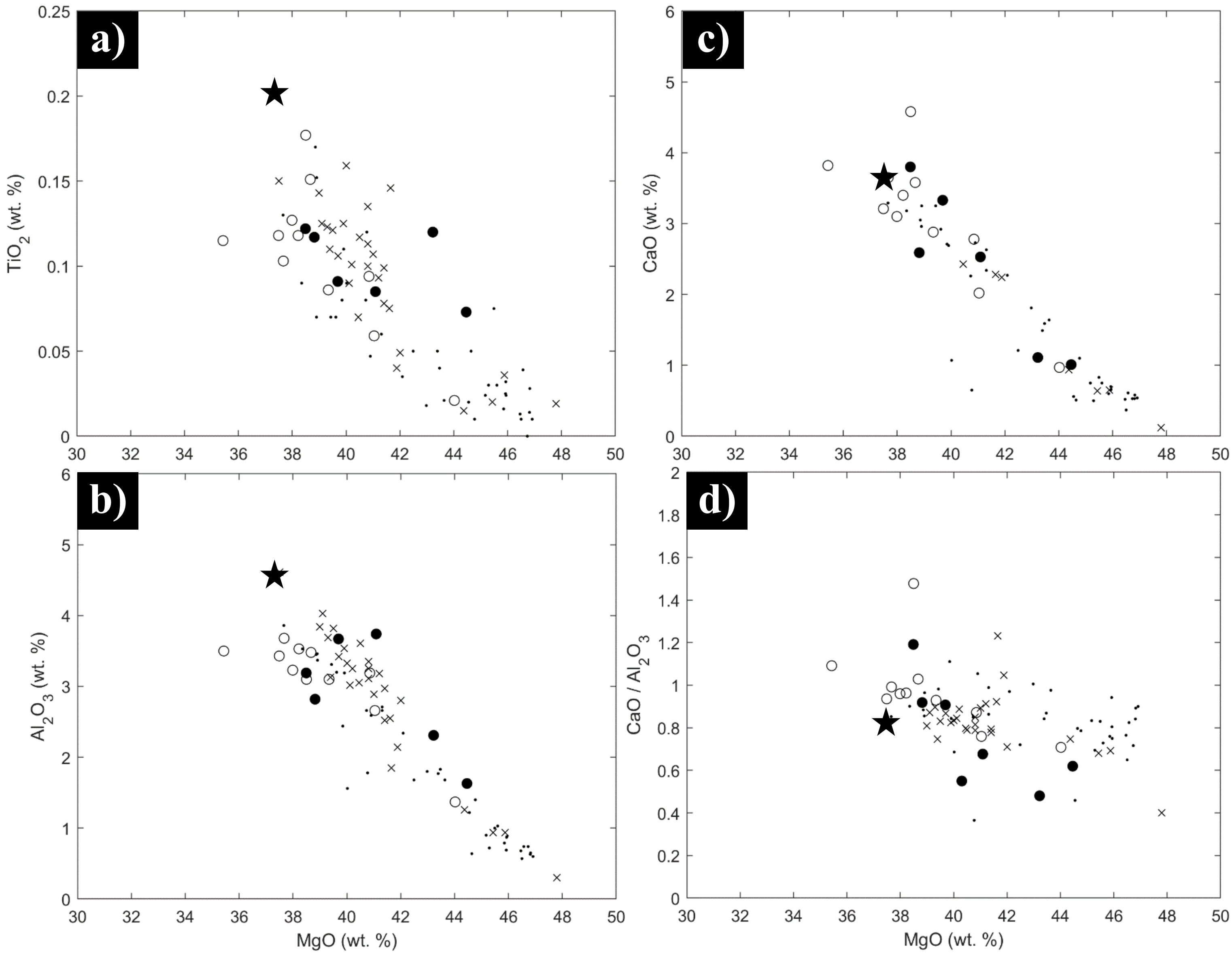

Figure 6.1 – MgO wt. % for bulk xenolith compositions plotted against TiO_2, CaO, Al_2O_3, and CaO/Al_2O_3. Summit Lake = open circles; Mt. Timothy = filled circles; other southeastern Cordilleran xenoliths (from Peslier et al., 2002) = crosses; xenoliths from Northern Cordilleran Volcanic Province (from Harder and Russell, 2006) = points. Primitive mantle values (stars) are taken from McDonough and Rudnick (1998).

contain both the most depleted (higher MgO) and least depleted (lower MgO) samples analyzed for this study. The marginally higher TiO_2, CaO, and Al_2O_3 contents of the Mt. Timothy xenoliths relative to their MgO concentrations may reflect minor differences in the compositions of the lithospheric mantle source material between the two localities, although the overall similarity between the ranges of MgO values between the two sites indicates that they underwent similar degrees of basaltic melt extraction.

The trace and rare earth element patterns of the Summit Lake and Mt. Timothy xenoliths are largely in line with compositions from other Cordilleran xenolith suites (Figures 4.5 and 4.6). The slight enrichment of the lightest LREEs displayed by some Mt. Timothy samples may be a product of small degrees of metasomatism enriching the peridotites in these elements. This suggestion of minor metasomatism is corroborated by the fairly high Tb/Yb ratios present in a number of samples from both suites (Figure 4.7), where Tb becomes slightly enriched by sufficient metasomatism (Peslier et al., 2002).

Moderately enriched LILEs (Rb, Ba, and K) and depleted HFSEs (Nb, Ta, Ti, and Y) compared to a MORB source for most peridotites from both sites (Figure 4.6b/e) are also found in peridotite xenoliths from other Cordilleran suites. Slab dehydration processes tend to mobilize LILEs and keep HFSEs immobile: therefore, these trace element compositions – along with those from other southern Cordilleran peridotite xenoliths – indicate a sub-continental lithospheric mantle source formed above a subducted oceanic slab (Friedman et al., 2016).

6.1.4 PYROXENE COMPOSITION

The major element compositions of clinopyroxenes and orthopyroxenes in the Summit Lake and Mt. Timothy xenoliths are broadly similar to others from the Canadian Cordillera.

Plotting these data with results from previous studies of other southern Cordilleran xenoliths reveals similar geochemical signatures, albeit with higher absolute values for major element concentrations (Peslier et al., 2002; Greenfield et al., 2013).). When plotted against pyroxene compositions from cratonic peridotites from the Canadian Shield, pyroxenes from both sites display orogenic geochemical signatures distinct from the cratonic signatures of the deeper-sourced peridotites (Figures 6.2 and 6.3). The high concentrations of Al_2O_3 in both clinopyroxene and orthopyroxene are particularly distinct from the cratonic peridotites. The handful of xenoliths that display geochemical signatures similar to the cratonic samples are clinopyroxene-poor harzburgites.

The clear divide between orogenic and cratonic geochemical signatures for these xenoliths suggests an autochthonous interpretation of the Cordilleran lithospheric mantle, where the lithosphere sampled by these xenoliths is associated with the overlying crustal material rather than with the cratonic lithosphere to the east. In this scenario the mantle and crustal lithosphere would be brought onboard during accretion as a single package. This could cast doubt upon the likelihood of the lithospheric delamination processes suggested by some sources to have occurred during accretion, which would result in a cratonic mantle lithosphere overlain by an accreted crustal lithosphere.

6.1.5 SUMMARY

The mineralogical and geochemical properties of the peridotite xenoliths from Summit Lake and Mt. Timothy both are largely similar to other xenolith suites from the southern Canadian Cordillera, corroborating previous conclusions of a broadly homogenous mantle lithosphere beneath southern and central British Columbia. The augite-bearing xenoliths present at Summit Lake may be related to this unit’s location at the margin of the North American craton. Minor LREE and MREE signatures in a handful of xenoliths may indicate that these xenoliths underwent a small degree of metasomatism. Slightly depleted HFSEs and slightly enriched LILEs are a product of slab dehydration processes. Orthopyroxene and clinopyroxene compositions display strong orogenic signatures, lending support to the idea of the Cordilleran lithosphere as autochthonous rather than allochthonous.

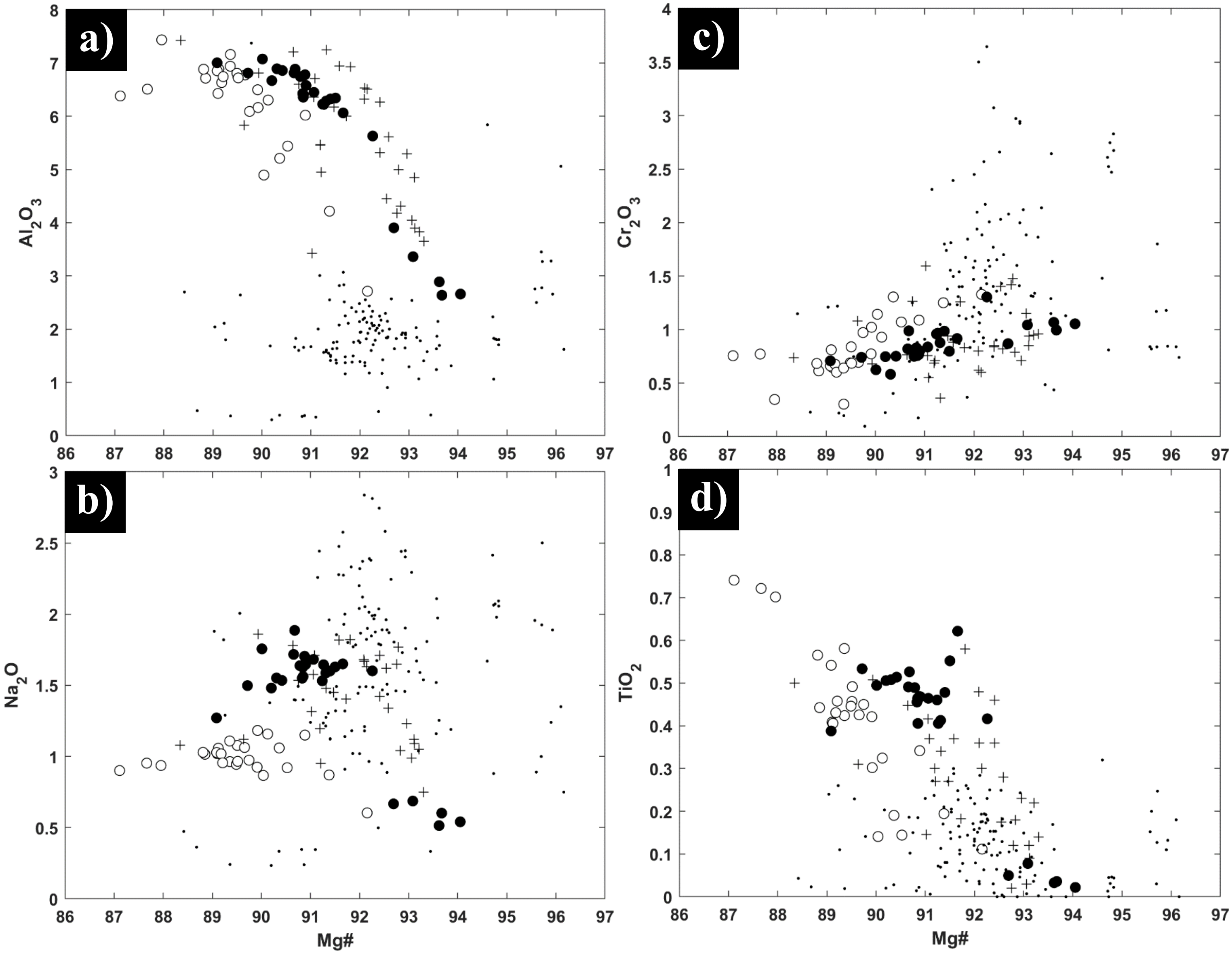

Figure 6.2 – Major elements of clinopyroxenes in Cordilleran (from this study) and cratonic (from previous studies) xenoliths plotted against Mg# (Mg/(Mg + Fe)). Filled circles = Mt. Timothy; open circles = Summit Lake; asterisks = Jericho kimberlite, Nunavut (Kopylova et al., 1999); crosses = Torrie kimberlite, Northwest Teritories (MacKenzie and Canil, 1999); points = Ekati Diamond Mine, Northwest Territories (Menzies et al., 2004).

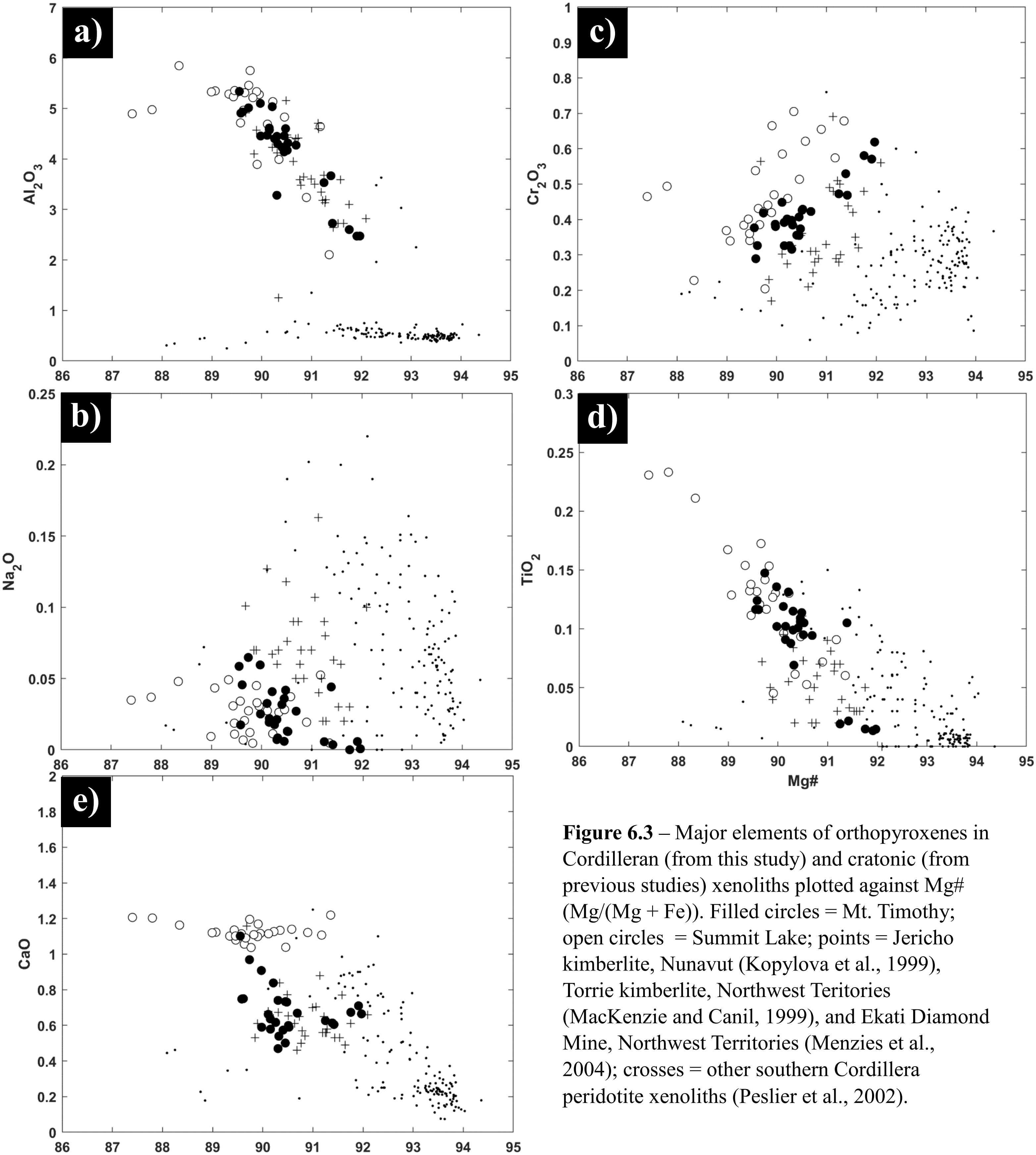

Figure 6.3 – Major elements of orthopyroxenes in Cordilleran (from this study) and cratonic (from previous studies) xenoliths plotted against Mg# (Mg/(Mg + Fe)). Filled circles = Mt. Timothy; open circles = Summit Lake; points = Jericho kimberlite, Nunavut (Kopylova et al., 1999), Torrie kimberlite, Northwest Teritories (MacKenzie and Canil, 1999), and Ekati Diamond Mine, Northwest Territories (Menzies et al., 2004); crosses = other southern Cordillera peridotite xenoliths (Peslier et al., 2002).

6.2 VERTICAL ORGANIZATION OF THE MANTLE LITHOSPHERE

The peridotite xenoliths from Mt. Timothy and Summit Lake are distinct in the ranges of lithospheric depths and temperatures that they sample, and these depths can be linked to systematic changes in mineralogy and geochemistry.

6.2.1 GEOCHEMISTRY AND LITHOSPHERIC CONDITIONS

Plotting calculated depths of equilibrium against various bulk trace and rare earth element compositions for selected peridotite xenoliths does not reveal any clear internal correlations between the two for either site. For example, attempting to discern a relationship between depth and the concentrations of various porphyry metals found in these xenoliths (Figure 6.4) reveals a certain amount of apparent randomness to these concentrations with depth of equilibration. Metal compositions here are either unchanging with depth, as in the Cu and Zn concentrations for Mt. Timothy xenoliths (Figures 6.4a and 6.4f), or they are indiscriminately scattered across all levels in the mantle lithosphere, as can be observed in the Ag and Mo concentrations for Mt. Timothy xenoliths (Figures 6.4b and 6.4c). There are some outliers within these data, such as the exceptionally high-W Mt. Timothy peridotite in Figure 6.5e, that likely indicate individual samples that have been subjected to higher degrees of metasomatic enrichment than others. Additionally, while the tectonostratigraphic environments occupied by the two sites are vastly different, and while the proximity of Mt. Timothy to a number of porphyry deposits contrasts sharply with the relative isolation of the Summit Lake unit, there are no apparent trends in metal concentrations between the Mt. Timothy and Summit Lake datasets. The small sample size renders this inconclusive, however, as some relationship should be expected between proximity to metallogenic porphyry deposits and mantle fertility (Begg et al., 2010).

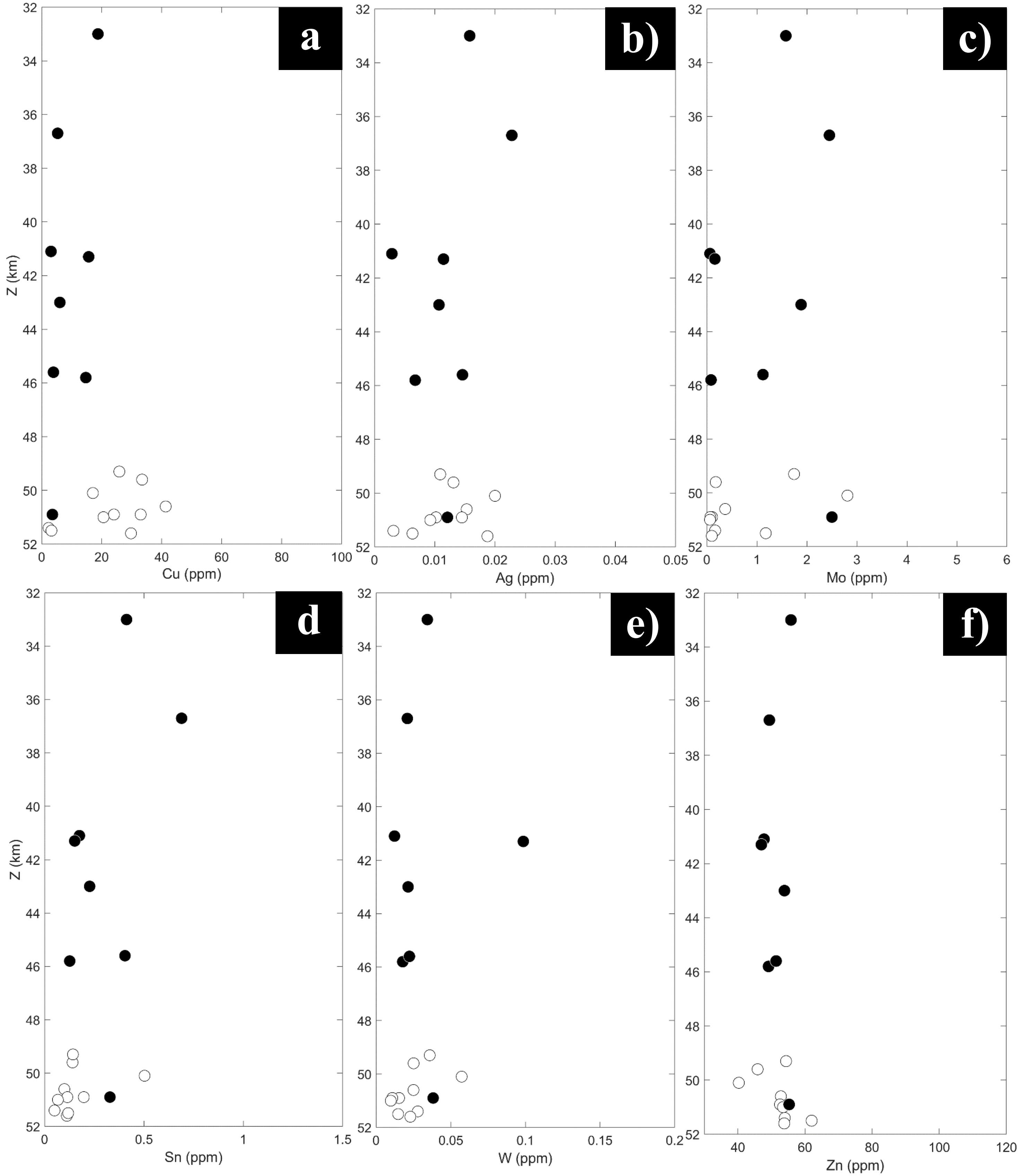

Figure 6.4 – Various bulk siderophile and chalcophile metal contents for peridotite xenoliths from Summit Lake (open circles) and Mt. Timothy (filled circles) plotted against the depths calculated for these xenoliths in Chapter 5. All data is from the pressed nanoparticulate powder pellet dataset.

6.2.2 THERMAL PROPERTIES AND DEPTH

The Mt. Timothy peridotites sample a broad range of temperatures and depths (813-1091 °C; 33.0-50.9 km) that is somewhat similar to a number of other xenolith suites in the southern Cordillera (Figure 6.5). With an assumed Moho depth of 33 km and a lithosphere-asthenosphere transition depth of 55-60 km, Mt. Timothy's total sampling range of 17.9 km and 278 °C covers at least two thirds of the total thickness of the mantle lithosphere beneath southern British Columbia (Hyndman, 2010). A minimum thickness for the mantle lithosphere of 17.9 km, equating to a minimum total lithospheric thickness of 50.9 km, corroborates what similar xenolith geothermobarometry studies have estimated for the southern Canadian Cordillera (Greenfield et al., 2013).

Conversely, the Summit Lake suite represents sampling of a significantly narrower and deeper window of mantle lithosphere than Mt. Timothy (at 1061-1119 °C and 49.0-52.7 km). While the range sampled by the Mt. Timothy peridotites allows us to use them to estimate Moho temperature and minimum lithospheric thickness and facilitates calculation of a petrology-based local geotherm, the same cannot be done with a sampling window as narrow as that from Summit Lake. This is for obvious reasons, since neither a mantle lithosphere thickness of 3.7 km nor a Moho temperature of 1061 °C is a remotely reasonable estimate. This narrow window also means that no conclusions can be drawn about the handful of samples with distinct mineral fabrics regarding their temperature or depth: while fabrics in xenoliths from directly at the Moho or the lithosphere-asthenosphere boundary might be linked to geophysical stresses experienced at that point in the lithospheric column, none of the Summit Lake xenoliths come from anywhere close to either transition zone.

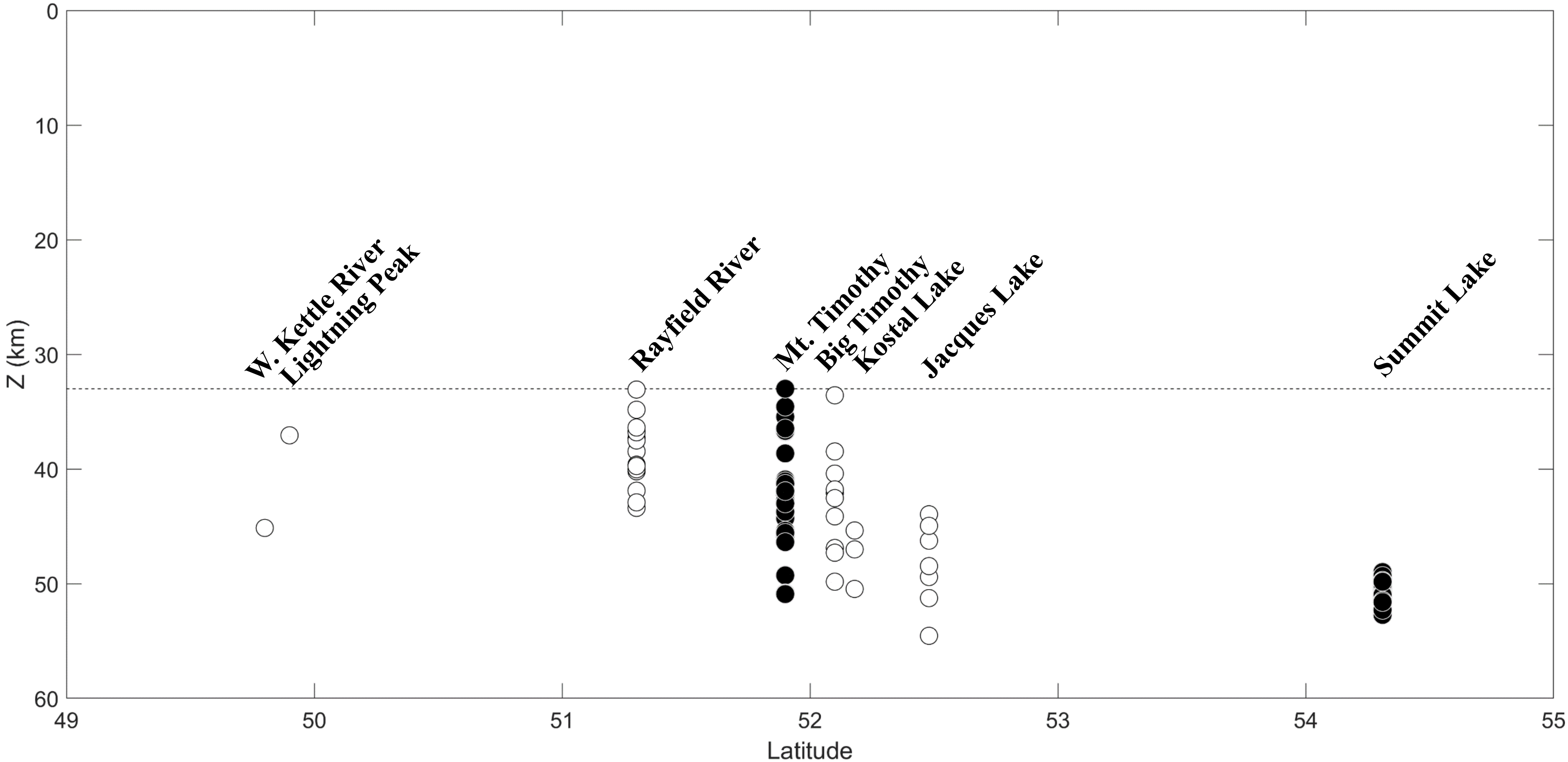

Figure 6.5 – Apparent source depths recorded by lithospheric xenoliths from suites across the southern Cordillera, plotted against latitude (from south to north). Summit Lake and Mt. Timothy data are from this study; additional data for other suites are from Peslier et al. (2002), Prescott (1983), and Greenfield et al. (2013). The dashed line marks a flat Cordilleran Moho at 33 km (Hyndman, 2010).

6.2.3 THERMAL STATE OF THE SOUTHERN CORDILLERAN LITHOSPHERIC MANTLE

The near-uniformly thin and hot nature of the lithosphere in the Canadian Cordillera has been thoroughly documented by a multitude of studies (Lewis et al., 1992; Clowes et al., 1995; Harder and Russell, 2006; Hyndman, 2010). The geothermobarometry done in this study, especially for the previously understudied xenolith suite at Mt. Timothy, corroborates this notion, with the lithospheric column calculated from a petrologically-constrained local geotherm supporting a Moho depth of around 33 km.

Figure 6.5 plots the new data from Mt. Timothy and Summit Lake alongside seven other xenolith suites in the southern Cordillera, whose pyroxene data has all been run through the geotherm-constrained code used for this study to ensure consistency when comparing these data sets (Prescott, 1983; Peslier et al., 2002; Greenfield et al., 2013). Holding all calculations to a Moho depth of 33 km (along with all the other geophysical constraints listed in Chapter 5.3), it illustrates all the different depths and ranges sampled by xenolith suites similar to those in this study. The sparseness of the columns at West Kettle River and Kostal Lake is not by design: other, earlier studies of the xenoliths at these localities have yielded more extensive data sets, but the bulk of xenolith pyroxene data from studies between 1970 and 1990 yields incongruous results when run through the code used in this study. This may be due to differences in data collection methodologies or microprobe standards between those studies and more recent studies.

The trio of xenolith suites situated in the approximate center of this transect along the strike of the Cordillera of Mt. Timothy, Big Timothy, and Rayfield River are similar both in the range and depth of mantle lithosphere sampled, albeit with fewer high-temperature samples from Rayfield River. Aside from being geographically proximal, these three suites occupy similar tectonic environments in that all three exist directly in the center of the Quesnel terrane (see

Figure 2.2; Colpron and Nelson, 2011). The Mt. Timothy and Big Timothy xenolith suites in particular sample extremely similar windows of mantle lithosphere. While no bulk geochemical data is readily available for the Big Timothy peridotites, mineralogical and textural descriptions of these xenoliths from previous literature are also very similar to what has been recorded in this study for the nearby Mt. Timothy xenoliths (Soregaroli, 1968; Littlejohn and Greenwood, 1974; Ross, 1983; Sun et al., 1991; Greenfield et al., 2013). The host lavas at each have also been dated, and the age of 0.465 ± 0.0226 ma (Russell, 2008; unpublished) given for the Mt. Timothy lavas is extremely close to the Rb/Sr date published by Sun et al. (1991) of 0.4 ± 0.04 ma for the Big Timothy unit. Combined with their geographical proximity, this all strongly suggests that the Mt. Timothy and Big Timothy xenolith suites record essentially identical compositions and depths of mantle lithosphere. The material at Rayfield River is somewhat older at 6-10 ma (based on field relationships and levels of preservation), but at the very least it corroborates the Moho depths and geotherms recorded by Mt. Timothy and Big Timothy (Bevier, 1983; Greenfield et al. 2013).

The xenolith suites at Kostal Lake and Jacques Lake, while closer geographically to the trio of Quesnellian localities discussed above, occupy tectonic environments much more similar to the Summit Lake unit. These sites either straddle the boundary between the Intermontane Belt (specifically, the Quesnel terrane) and the North American craton or, in the case of the Kostal Lake unit, are expressed completely within cratonic material. All three record windows of mantle lithosphere that are deeper and narrower in scope than those from the xenolith suites to the south. However, unlike the southern suites, these suites all display significant disparities in mineralogy and ages. At 0.174 ± 0.007 ma (from $^{40}Ar/^{39}Ar$ geochronology), the Jacques Lake unit is significantly younger than the Summit Lake unit, estimated at roughly 26 ma (Bevier, 1983;

Friedman et al., 2016). In fact, the only xenolith-hosting unit in the southern Cordillera known to be younger than at Jacques Lake is the unit at Kostal Lake, which erupted as recently as 7750 BP (Metcalfe, 1987). The phlogopite-bearing Kostal Lake suite is one of only two known Cordilleran xenolith suites that contain a hydrous phase (the other, the Okanagan Peninsula's Lightning Peak, has been reported to contain amphibole), and is also unique for its rock type distribution being comprised by ~60% augite-bearing wehrlites with the usually dominant diopside-bearing lherzolites existing as a secondary rock type (Brearley and Scarfe, 1984; Canil and Scarfe, 1989).

7. CONCLUSION

The units at Summit Lake and Mt. Timothy are two well-preserved and well-exposed examples of the peridotite xenolith-bearing volcanic suites that dot the Intermontane Belt in the southern and northern Canadian Cordillera. The Summit Lake unit, which has been the subject of similar studies in the past, is exposed as a single very thick unit in an inactive quarry. The xenoliths therein are predominantly spinel lherzolites and other ultramafic rock types, but a moderately significant collection of various crustal rock types is also present. The Mt. Timothy xenoliths are found in various smaller exposures on and around the mountain and are almost entirely comprised by spinel lherzolites. These xenoliths had not been subject to any study up to this point. Neither site contains any garnet-bearing peridotites.

A total of 53 xenolith samples – 26 from Summit Lake and 27 from Mt. Timothy – were studied in depth. The majority from both sites were spinel-bearing lherzolites, while a handful of harzburgites from each site and two olivine websterites from Summit Lake were also examined. This distribution of rock types is similar to other sites from the southern Cordillera, and while the Summit Lake unit does contain a higher proportion of harzburgites than the Mt. Timothy unit, it’s not enough to qualify as a bimodal suite like those found in the northern Canadian Cordillera. Mt. Timothy lherzolites were predominantly very fresh and coarse-grained, while those from Summit Lake were finer-grained and somewhat more altered. Point counts done using a MatLab script revealed a range of modal mineralogies for these samples, with higher olivine concentrations generally found in the Summit Lake samples. Mineral textures were almost entirely protogranular. Mineral fabrics were rare, with the only obvious examples being two Summit Lake lherzolites that displayed elongated spinel fabrics.

34 samples, including 8 xenolith-hosting basalts, 8 Mt. Timothy peridotite xenoliths, 16 Summit Lake peridotite xenoliths, and 2 Summit Lake crustal xenoliths, were submitted for bulk geochemical analyses. The Summit Lake host basalts are all more silicic that the host lavas from Mt. Timothy and other southern xenolith-bearing units. The Mt. Timothy host basalt is generally more enriched than the Summit Lake lavas, with the exception of a pronounced depletion in the heaviest rare earth elements.

Major element compositions in peridotite xenoliths from both sites are similar to other Cordilleran data sets, and do not reveal any significant differences between the two sites or between the northern and southern Cordillera. Like with other Cordilleran xenoliths, the major element chemistry of these samples indicates varying degrees of extraction from a fertile peridotite source.

The peridotites were subject to a second round of geochemical analyses using a new method, involving analysis of pressed nanoparticulate powder pellets, chosen for its increased effectiveness in measuring the extremely small abundances of trace and rare earth elements in rocks such as these peridotite xenoliths. Trace and rare earth element concentrations in peridotite xenoliths from both sites largely fall well within the range of reported values for other Cordillera xenoliths. A slight enrichment in MREEs present in many samples may suggest that these rocks were subject to minor metasomatism. This is corroborated by a slight enrichment of the lightest LREEs shown by some Mt. Timothy xenoliths. Additionally, the enrichment in LILEs and depletion in HFSEs displayed by these samples, along with peridotite xenoliths from other Cordilleran suites, indicate the presence of a sub-continental lithospheric mantle source formed above an oceanic slab.

Clinopyroxene and orthopyroxene mineral compositions measured using an electron microprobe reveal orogenic geochemical signature distinct from the cratonic signatures of more deeply sourced mantle xenoliths from the North American craton. These signatures fall in line with those displayed by other Cordilleran lithospheric mantle xenoliths, and lend support to the idea of an autochthonous mantle lithosphere brought onboard with its overlying crustal lithosphere during the accretion of these arc terranes onto the North American craton.

Depths, pressures, and temperatures of equilibration for all 53 peridotite xenoliths were determined by pairing a two-pyroxene geothermometer (Brey and Köhler, 1990) with a localized geotherm based on a number of set geophysical quantities. This geotherm is constructed, with a calculated heat flow of 76.7 mW m^{-2}, by taking the lowest-temperature xenolith (813 °C; 33.0 km; 9.05 kbar) to represent the Moho temperature in this part of the Cordillera. Samples from Summit Lake record a very narrow range of high-temperature conditions (1061 °C to 1119 °C; 49.0 km to 52.7 km) within the deeper mantle lithosphere. Conversely, those from Mt. Timothy record a range of lithospheric conditions reaching from the Moho (813 °C; 33.0 km) to the deep lithosphere (1091 °C; 50.9 km).

This broader range of recorded lithospheric conditions stands in contrast to the mineralogically homogenous nature of the xenoliths at Mt. Timothy. No relationships between rock type and depth are apparent, although this may well be a function of sample size. Additionally, neither site displays any clear correlations between trace element concentrations and depth of equilibration, although this may be attributed to small sample sizes.

The geothermobarometry from both xenolith suites generally corroborates previous interpretations of the nature of the flat, thin, and hot mantle lithosphere underlying the Canadian Cordillera. Comparing these data to datasets from previous studies reveals that the Mt. Timothy xenoliths sample a window of mantle lithosphere very similar to several other sites in this region of the southern Cordillera. Based on geochemistry, geothermometry, and the age of the host units, it may even sample nearly the exact same mantle lithosphere as the nearby Big Timothy xenolith suite. The very narrow and deep window sampled by the Summit Lake unit, on the other hand, is fairly unique among xenolith suites in the southern Cordillera. The presence of relatively abundant augite-bearing wehrlites at this site, a characteristic shared by only two other suites in the southern Cordillera – both located in a similar tectonostratigraphic setting of proximity to Summit Lake – may reflect the proximity of Summit Lake to the boundary between the Cordillera and the North American craton.

REFERENCES

Abraham, A., Francis, D., and Polve, M., 2001. Recent alkaline basalts as probes of the lithospheric mantle roots of the Northern Canadian Cordillera. Chemical Geology, v. 175, p. 361-386.

Begg, G.C., Hronsky, J.A.M., Arndt, N.T., Griffin, W.L., O'Reilly, S.Y, and Hayward, N., 2010. Lithospheric, cratonic, and geodynamic setting of Ni-Cu-PGE sulfide deposits. Economic Geology, v. 105, no. 6, p. 1057-1070.

Bevier, M.L., 1983. Regional stratigraphy and age of Chilcotin Group basalts, south-central British Columbia. Canadian Journal of Earth Sciences, v. 20, p. 515-524.

Bierlein, F.P., Groves, D.I., and Cawood, P.A., 2009. Metallogeny of accretionary orogens – The connection between lithospheric processes and metal endowment. Ore Geology Reviews, v. 36, . 282-292.

Bodinier, J.L., Dupuy, C., and Dostal, J., 1988. Geochemistry and petrogenesis of Eastern Pyrenean peridotites. Geochimica et Cosmochimica Acta, v. 52, p. 2893-2907.

Brearley, M., Scarfe, C., and Fujii, T., 1984. The petrology of ultramafic xenoliths from Summit Lake, near Prince George, British Columbia. Contributions to Mineralogy and Petrology, v. 88, p. 53-63.

Brearley, M. and Scarfe, C.M., 1984. Amphibole in a spinel lherzolite xenolith: evidence for volatiles and partial melting in the upper mantle beneath southern British Columbia. Canadian Journal of Earth Sciences, v. 21, p. 1067-1072.

Brey, G.P. and Köhler, T., 1990. Geothermobarometry in four-phase lherzolites II: new thermobarometers, and practical assessment of existing thermobarometers; Journal of Petrology, v. 31, no. 6, p. 1353-1378.

Canil, D., Brearley, M., and Scarfe, C.M., 1987. Petrology of ultramafic xenoliths from Rayfield River, south-central British Columbia. Canadian Journal of Earth Sciences, v. 24, p. 1679-1687.

Canil, D. and Scarfe, C.M., 1989. Origin of phlogopite in mantle xenoliths from Kostal Lake, Wells Gray Park, British Columbia. Journal of Petrology, v. 30, no. 5, p. 1159-1179.

Christopher, P.A., 1978. East Okanagan uranium area (Kelowna to Beaverdell), south-central British Columbia (NTS 82E/10, 11, 14, 15). British Columbia Ministry of Mines and Petroleum Resources, Preliminary Map 29.

Clowes, R.M., Zelt, C.A., Amor, J.R., and Ellis, R.M., 1995. Lithospheric structure in the southern Canadian Cordillera from a network of seismic refraction lines. Canadian Journal of Earth Sciences, v. 32, p. 1485-1513.

Clowes, R.M., Cook, F.A., and Ludden, J.N., 1998. Lithoprobe leads to new perspectives on continental evolution. GSA Today, v. 8, no. 10, p. 1-7.

Cook, F.A., Clowes, R.M., Snyder, D.B., van der Velden, A.J., Hall, K.W., Erdmer, P., and Evenchick, C.A., 2004. Precambrian crust beneath the Mesozoic northern Canadian Cordillera discovered by Lithoprobe seismic reflection profiling. Tectonics, v. 23, p. 1-28.

Francis, D., Minarik, W., Proenza, Y., and Shi, L., 2010. An overview of the Canadian Cordilleran lithospheric mantle. Canadian Journal of Earth Sciences, v. 47, p. 353-368.

Friedman, E., Polat, A., Thorkelson, D.J., & Frei, R., 2016. Lithospheric mantle xenoliths sampled by melts from upwelling asthenosphere: The Quaternary Tasse alkaline basalts of southeastern British Columbia, Canada. Gondwana Research, v. 33, p. 209-230.

Fujii, T. and Scarfe, C.M., 1982. Petrology of ultramafic nodules from West Kettle River, near Kelowna, southern British Columbia. Contributions to Mineralogy and Petrology, v. 80, p. 297-306.

Garbe-Schönberg, D. and Müller, S., 2014. Nano-particulate pressed powder tablets for LA-ICPMS. Journal of Analytical Atomic Spectrometry, v. 29, p. 990-1000.

Greenfield, A.M.R., Ghent, E.D., and Russell, J.K., 2013. Geothermobarometry of spinel peridotites from southern British Columbia: implications for the thermal conditions in the upper mantle. Canadian Journal of Earth Sciences, v. 50, no. 10, p. 1019-1032.

Guillong, M., Hametner, K., Reusser, E., Wilson, S.A., and Günter, D., 2005. Preliminary characterization of new glass reference materials (GSA-1G, GSC-1G, GSD-1G, and GSE-1G) by laser ablation-inductively coupled plasma-mass spectrometry using 193 nm, 213nm, and 266 nm wavelengths. Geostandards and Geoanalytical Research, v. 29, no. 3, p. 315-331.

Harder, M. and Russell, J.K., 2006. Thermal state of the upper mantle beneath the Northern Cordilleran Volcanic Province (NCVP), British Columbia, Canada. Lithos, v. 87, p. 1-22.

Hyndman, R.D., 2010. The consequences of Canadian Cordillera thermal regime in recent tectonics and elevation: a review. Canadian Journal of Earth Sciences, v. 47, p. 621-632.

Kopylova, M.G., O'Reilly, S.Y., and Genshaft, Yu.S., 1995. Thermal state of the lithosphere beneath Central Mongolia: evidence from deep-seated xenoliths from the Shavaryn-Saram volcanic center in the Tariat depression, Hangai, Mongolia. Lithos, v. 36, p. 243-255.

Kopylova, M.G., Russell, J.K., and Cookenboo, H., 1999. Petrology of peridotite and pyroxenite xenoliths from the Jericho Kimberlite: implications for the thermal state of the mantle beneath the Slave Craton, Northern Canada. Journal of Petrology, v. 40, no. 1, p. 79-104.

Lewis, T.J., Bentkowski, W.H., and Hyndman, R.D., 1992. Crustal temperatures near the Lithoprobe Southern Canadian Cordillera transect. Canadian Journal of Earth Sciences, v. 29, p. 1197-1214.

Little, H.W., 1957. Kettle River (East Half); Similkameen, Kootenay, and Osoyoos Districts, British Columbia (82E). Geological Survey of Canada, Map 6-1957, scale 1:253,440.

Little, H.W., 1961. Kettle River (west half). Geological Survey of Canada, Map 15-1961, scale 1:253,440.

Littlejohn, A.L. and Greenwood, H.J., 1974. Lherzolite nodules in basalts from British Columbia, Canada. Canadian Journal of Earth Sciences, v. 11, p. 1288-1308.

Logan, J.M., Schiarizza, P., Struik, L.C.; Barnett, C., Nelson, J.L., Kowalczyk, P., Ferri, F., Mihalynuk, M.G., Thomas, M.D., Gammon, P., Lett, R., Jackaman, W., and Ferbey, T., 2010. Bedrock geology of the QUEST map area, central British Columbia. Geological Survey of Canada, Open File 6476, 1:500,000 scale.

Logan, J.M. and Schiarizza, P., 2014. The Rayfield River pluton, south-central British Columbia (NTS 92P/6): Geologic setting and copper mineralization. In: Geological Fieldwork 2013, British Columbia Ministry of Energy and Mines, British Columbia Geological Survey Paper 2014-1, p. 15-27.

MacKenzie, J.M. and Canil, D., 1999. Composition and thermal evolution of cratonic mantle beneath the central Archean Slave Province, NWT, Canada. Contributions to Mineralogy and Petrology, v. 134, p. 313-324.

McDonough, W.F., 1990. Constraints on the composition of the continental lithospheric mantle. Earth and Planetary Science Letters, v. 101, p. 1-18.

McDonough, W.F. and Frey, F.A., 1990. Rare earth elements in upper mantle rocks. In: Geochemistry and mineralogy of rare earth elements (eds. B.R. Lipin and G.A. McKlay). Reviews in Mineralogy, Mineralogical Society of America, v. 21, p. 100-145.

McDonough, W.F. and Sun, S.S., 1995. The composition of the Earth. Chemical Geology, v. 120, p. 223-253.

McDonough, W.F. and Rudnick, R.L., 1998. Mineralogy and composition of the upper mantle. Reviews in Mineralogy and Geochemistry, v. 37, p. 139-164.

Menzies, A., Westerlund, K., Grütter, H., Gurney, J.J., Carlson, J., Fung, A., and Nowicki, T., 2004. Peridotitic mantle xenoliths from kimberlites on the Ekati Diamond Mine property, N.W.T., Canada: major element compositions and implications for the lithosphere beneath the central Slave craton. Lithos, v. 77, no. 1, p. 395-412.

Mercier, J.C.C. and Nicolas, A., 1975. Textures and fabrics of upper-mantle peridotites as illustrated by xenoliths from basalts. Journal of Petrology, v. 16, no. 2, p. 454-487.

Metcalfe, P.M., 1987. Petrogenesis of alkaline lavas from Wells Gray Provincial Park and constraints on the sub-Cordillera upper mantle. Pd.D. thesis, University of Alberta, Edmonton, Canada.

Monger, J. and Price, R., 2002. The Canadian Cordillera: geology and tectonic evolution. CGES Recorder, v. 27, no. 2, p. 17-36.

Nelson, J. and Colpron, M., 2007. Tectonics and metallogeny of the British Columbia, Yukon, and Alaskan Cordillera, 1.8 Ga to the present. *In:* Goodfellow, W.D., ed., Mineral Deposits of Canada: A Synthesis of Major Deposit-Types, District Metallogeny, the Evolution of Geological Provinces, and Exploration Methods. Geological Association of Canada, Mineral Deposits Division, Special Publication No. 5, p. 755-791.

Peslier, A.H., Reisberg, L., Ludden, J., & Francis, D., 2000a. Re-Os constraints on harzburgite and lherzolite formation in the lithospheric mantle: A study of Northern Canadian Cordillera xenoliths. Geochimica et Cosmochimica Acta, v. 64, no. 17, p. 3061-3071.

Peslier, A.H., Reisberg, L., Ludden, J., and Francis, D., 2000b. Os isotopic systematics in mantle xenoliths: age constraints on the Canadian Cordillera lithosphere. Chemical Geology, v. 166, p. 85-101.

Peslier, A.H., Francis, D., & Ludden, J., 2002. The lithospheric mantle beneath continental margins: Melting and melt-rock reaction in Canadian Cordillera xenoliths. Journal of Petrology, v. 43, no. 11, p. 2013-2047.

Peters, D. and Pettke, T., 2016. Evaluation of major to ultra-trace element bulk rock chemical analysis of nanoparticulate pressed powder pellets by LA-ICP-MS. Geostandards and Geoanalytical Research, v. 41, no. 1, p. 5-28.

Peterson, N.D. Carbonated mantle lithosphere in the Western Canadian Cordillera. M.Sc. thesis, University of British Columbia, 2010.

Pouchou, J.L. and Pichoir, R.F., 1985. PAP $\phi(\rho Z)$ procedure for improved quantitative microanalysis. Microbeam Analysis 1985, p. 104-106.

Prescott, J.W. Petrogenesis of ultramafic xenoliths from the Canadian Cordillera and Alaska. M.Sc. thesis, McGill University, 1983.

Resnick, J., Anderson, R.G., Russell, J.K., Edwards, B.R., and Grainger, N.C., 1999. Neogene basaltic flow rocks, xenoliths, and related diabase, northern Nechako River map area, central British Columbia. In: Current Research 1999-A, Geological Survey of Canada, p. 157-167.

Richards, J.P., 2009. Postsubduction porphyry Cu-Au and epithermal Au deposits: products of remelting of subduction-modified lithosphere. Geology, v. 37, no. 3, p. 247-250.

Ross, J.V., 1983. The nature and rheology of the Cordilleran upper mantle of British Columbia: inferences from peridotite xenoliths. Tectonophysics, v. 100, p. 321-357.

Schiarizza, P. and Macauley, J., 2007. Geology of the Hendrix Lake area, NTS 93A/02. British Columbia Ministry of Energy, Mines, and Petroleum Resources, British Columbia Geological Survey Open File 2007-3, 1:50,000 scale.

Schiarizza, P., Bligh, J.S., Bluemel, B., and Tait, D., 2008. Geology of the Timothy Lake area, NTS 92P/14. British Columbia Ministry of Energy, Mines, and Petroleum Resources, British Columbia Geological Survey Open File 2008-5, 1:50,000 scale.

Schiarizza, P., Israel, S., Heffernan, S., Boulton, A., Bligh, J., Bell, K., Bayliss, S., Macauley, J., Bluemel, B., Zuber, J., Friedman, R.M., Orchard, M.J., and Poulton, T.P., 2013. Bedrock geology between Thuya and Woodjam creeks, south-central British Columbia, NTS 92P/7, 8, 9, 10, 14, 15, 16; 93A/2, 3, 6. British Columbia Ministry of Energy, Mines, and Natural Gas, British Columbia Geological Survey Open File 2013-05, 4 sheets, 1:100,000 scale.

Soregaroli, A.E., 1968. Geology of the Boss Mountain Mine, British Columbia: Ph.D thesis. University of British Columbia.

Struik, L.C., 1994. Geology of the McLeod Lake map area (93J), British Columbia. Geological Survey of Canada, Open File 2439, 1:250,000 scale.

Sun, S.S. and McDonough, W.F., 1989. Chemical and isotopic systematics of oceanic basalts: implications for mantle composition and processes. In: Saunders, A.D. and Norry, M.J. (Eds.), Magmatism in the Ocean Basins. Society of London, Special Publications 42, p. 313-345.

Sun, M., Armstrong, R.L., and Maxwell, R.J., 1991. Proterozoic mantle under Quesnellia: variably reset Rb-Sr mineral isochrons in ultramafic nodules carried up in Cenozoic volcanic cents of the southern Omineca Belt. Canadian Journal of Earth Sciences, v. 28, p. 1239-1253.

Sun, M. and Kerrich, R., 1995. Rare earth element and high field strength element characteristics of whole rocks and mineral separates of ultramafic nodules in Cenozoic volcanic vents of southeastern British Columbia, Canada. Geochimica et Cosmochimica Acta, v. 59, no. 23, p. 4863-4879.

Wells, P.R.A., 1977. Pyroxene thermometry in simple and complex systems. Contributions to Mineralogy and Petrology, v. 62, p. 129-139.

APPENDIX A – PYROXENE GEOCHEMISTRY

Table A.1 – Clinopyroxene and orthopyroxene compositions in peridotite xenoliths as measured with UBC's electron microprobe. All Wt. % are averages of *n* measurements, with ± standard deviations included.

	SL08-02		**SL08-15**		**SL08-29**		**SL08-44**		**SL17-10**	
Cpx:	**n = 4**		**n = 3**		**n = 4**		**n = 4**		**n = 4**	
SiO_2	50.84	± 0.37	50.96	± 0.12	50.66	± 0.33	50.70	± 0.44	51.74	± 0.35
TiO_2	0.41	± 0.01	0.45	± 0.02	0.46	± 0.02	0.43	± 0.02	0.19	± 0.03
Al_2O_3	6.43	± 0.10	6.09	± 0.04	6.75	± 0.16	6.77	± 0.04	5.21	± 0.08
Cr_2O_3	0.81	± 0.03	0.97	± 0.01	0.84	± 0.04	0.69	± 0.02	1.31	± 0.06
FeO_T	3.61	± 0.05	3.45	± 0.04	3.47	± 0.07	3.39	± 0.02	3.23	± 0.06
MnO	0.10	± 0.01	0.09	± 0.01	0.11	± 0.01	0.09	± 0.01	0.08	± 0.01
MgO	16.54	± 0.07	16.94	± 0.02	16.62	± 0.24	16.50	± 0.08	16.97	± 0.06
CaO	20.05	± 0.07	20.19	± 0.08	19.49	± 0.26	19.89	± 0.11	19.88	± 0.07
Na_2O	1.02	± 0.03	0.97	± 0.04	1.08	± 0.07	1.06	± 0.03	1.06	± 0.04
Total	99.82	± 0.46	100.13	± 0.40	99.49	± 1.22	99.55	± 0.79	99.67	± 0.76
Mg#	89.10	± 0.13	89.75	± 0.11	89.51	± 0.07	89.66	± 0.03	90.36	± 0.16
Opx:										
SiO_2	53.85	± 0.44	54.78	± 0.26	53.68	± 0.34	53.52	± 0.66	54.87	± 0.26
TiO_2	0.12	± 0.01	0.13	± 0.02	0.13	± 0.01	0.13	± 0.01	0.06	± 0.01
Al_2O_3	4.97	± 0.04	4.71	± 0.01	5.28	± 0.02	5.33	± 0.08	3.99	± 0.07
Cr_2O_3	0.43	± 0.02	0.54	± 0.04	0.47	± 0.02	0.42	± 0.03	0.71	± 0.02
FeO_T	6.77	± 0.07	6.70	± 0.03	6.42	± 0.06	6.45	± 0.06	6.25	± 0.08
MnO	0.13	± 0.02	0.15	± 0.02	0.12	± 0.01	0.14	± 0.01	0.14	± 0.02
MgO	32.85	± 0.12	32.31	± 0.07	32.26	± 0.09	32.21	± 0.13	32.83	± 0.05
CaO	1.06	± 0.02	1.11	± 0.03	1.12	± 0.02	1.10	± 0.01	1.13	± 0.01
Na_2O	0.01	± 0.01	0.03	± 0.01	0.03	± 0.01	0.05	± 0.02	0.03	± 0.01
Total	100.18	± 0.40	100.48	± 0.48	99.51	± 0.58	99.36	± 1.02	100.01	± 0.52
Mg#	89.63	± 0.13	89.58	± 0.06	89.95	± 0.08	89.90	± 0.07	90.35	± 0.10

	SL17-33		SL17-36		SL17-41		SL17-43		SL17-49	
Cpx:	**n = 8**		**n = 5**		**n = 5**		**n = 5**		**n = 8**	
SiO_2	50.09	± 0.37	50.99	0.40	50.60	± 0.30	50.55	± 0.14	50.73	± 0.44
TiO_2	0.42	± 0.02	0.41	0.01	0.44	± 0.01	0.54	± 0.01	0.43	± 0.02
Al_2O_3	7.16	± 0.06	6.88	0.08	6.72	± 0.05	6.85	± 0.03	6.63	± 0.06
Cr_2O_3	0.30	± 0.04	0.65	0.02	0.61	± 0.03	0.66	± 0.03	0.68	± 0.05
FeO_T	3.50	± 0.11	3.54	0.07	3.71	± 0.03	3.64	± 0.05	3.55	± 0.04
MnO	0.10	± 0.02	0.10	0.02	0.10	± 0.02	0.11	± 0.00	0.10	± 0.01
MgO	16.49	± 0.05	16.28	0.06	16.57	± 0.13	16.65	± 0.02	16.43	± 0.07
CaO	20.34	± 0.09	19.87	0.05	20.19	± 0.08	20.03	± 0.12	19.91	± 0.13
Na_2O	0.96	± 0.03	1.06	0.10	1.02	± 0.02	1.03	± 0.03	1.02	± 0.03
Total	99.39	± 0.31	99.78	0.41	99.97	± 0.45	100.07	± 0.17	99.49	± 0.52
Mg#	89.36	± 0.33	89.12	0.21	88.85	± 0.11	89.09	± 0.12	89.18	± 0.11
Opx:										
SiO_2	53.14	± 0.40	54.28	± 0.31	53.99	± 0.26	53.70	± 0.37	53.74	± 0.35
TiO_2	0.12	± 0.01	0.11	± 0.01	0.13	± 0.01	0.15	± 0.01	0.13	± 0.02
Al_2O_3	5.75	± 0.05	5.29	± 0.04	5.35	± 0.02	5.28	± 0.03	5.23	± 0.06
Cr_2O_3	0.20	± 0.02	0.34	± 0.05	0.34	± 0.01	0.38	± 0.03	0.40	± 0.02
FeO_T	6.64	± 0.14	6.79	± 0.05	7.03	± 0.08	6.86	± 0.04	6.73	± 0.10
MnO	0.14	± 0.01	0.15	± 0.01	0.16	± 0.02	0.15	± 0.01	0.14	± 0.02
MgO	32.69	± 0.17	32.32	± 0.28	32.14	± 0.09	32.28	± 0.06	31.97	± 0.13
CaO	1.04	± 0.02	1.08	± 0.02	1.12	± 0.02	1.10	± 0.00	1.14	± 0.02
Na_2O	0.01	± 0.01	0.01	± 0.01	0.04	± 0.01	0.05	± 0.01	0.03	± 0.02
Total	99.75	± 0.48	100.37	± 0.62	100.31	± 0.40	99.97	± 0.32	99.52	± 0.40
Mg#	89.77	± 0.22	89.46	± 0.11	89.07	± 0.09	89.34	± 0.07	89.43	± 0.17

	SL17-53		SL17-55A		SL17-68		SL17-70		SL17-70-2	
Cpx:	**n = 6**		**n = 7**		**n = 5**		**n = 5**		**n = 3**	
SiO_2	52.13	± 0.37	49.92	± 0.28	50.40	± 0.19	49.93	± 0.28	49.77	± 0.33
TiO_2	0.19	± 0.05	0.45	± 0.02	0.46	± 0.01	0.74	± 0.01	0.72	± 0.03
Al_2O_3	4.22	± 0.10	6.81	± 0.05	6.74	± 0.06	6.38	± 0.05	6.51	± 0.06
Cr_2O_3	1.25	± 0.07	0.69	± 0.03	0.60	± 0.05	0.76	± 0.02	0.77	± 0.02
FeO_T	2.97	± 0.09	3.52	± 0.06	3.59	± 0.05	4.31	± 0.03	4.07	± 0.09
MnO	0.08	± 0.02	0.09	± 0.02	0.11	± 0.01	0.12	± 0.01	0.14	± 0.01
MgO	17.68	± 0.15	16.82	± 0.05	16.66	± 0.07	16.34	± 0.05	16.21	± 0.08
CaO	20.55	± 0.06	19.83	± 0.10	20.14	± 0.08	19.99	± 0.06	19.79	± 0.11
Na_2O	0.87	± 0.03	0.94	± 0.01	0.96	± 0.02	0.90	± 0.03	0.95	± 0.03
Total	99.96	± 0.29	99.08	± 0.44	99.67	± 0.20	99.47	± 0.30	98.93	± 0.76
Mg#	91.38	± 0.27	89.49	± 0.15	89.21	± 0.14	87.11	± 0.10	87.66	± 0.21
Opx:										
SiO_2	55.23	± 0.23	52.94	± 0.58	53.66	± 0.23	53.61	± 0.16	52.98	± 0.35
TiO_2	0.07	± 0.02	0.14	± 0.01	0.14	± 0.01	0.23	± 0.01	0.23	± 0.00
Al_2O_3	3.24	± 0.06	5.46	± 0.04	5.35	± 0.02	4.89	± 0.06	4.98	± 0.06
Cr_2O_3	0.65	± 0.01	0.42	± 0.02	0.36	± 0.01	0.46	± 0.02	0.49	± 0.01
FeO_T	5.99	± 0.11	6.59	± 0.06	6.79	± 0.07	8.05	± 0.13	7.70	± 0.07
MnO	0.13	± 0.01	0.14	± 0.02	0.15	± 0.01	0.19	± 0.01	0.19	± 0.00
MgO	33.55	± 0.10	32.35	± 0.10	32.32	± 0.09	31.31	± 0.08	31.08	± 0.06
CaO	1.12	± 0.02	1.20	± 0.01	1.10	± 0.01	1.21	± 0.01	1.20	± 0.01
Na_2O	0.02	± 0.01	0.03	± 0.02	0.02	± 0.01	0.03	± 0.03	0.04	± 0.01
Total	100.02	± 0.30	99.28	± 0.66	99.90	± 0.26	99.99	± 0.33	98.89	± 0.57
Mg#	90.90	± 0.16	89.74	± 0.07	89.46	± 0.09	87.40	± 0.15	87.80	± 0.17

	SL17-74		SL17-76		SL17-81A		SL17-81B		SL17-82	
Cpx:	**n = 6**		**n = 6**		**n = 5**		**n = 4**		**n = 4**	
SiO_2	52.00	± 0.19	49.52	± 0.42	50.61	± 0.27	50.99	± 0.44	50.48	± 0.72
TiO_2	0.14	± 0.02	0.70	± 0.04	0.58	± 0.01	0.57	± 0.03	0.42	± 0.02
Al_2O_3	5.44	± 0.03	7.44	± 0.09	6.94	± 0.05	6.88	± 0.03	6.50	± 0.09
Cr_2O_3	1.07	± 0.04	0.35	± 0.02	0.64	± 0.03	0.68	± 0.03	0.77	± 0.05
FeO_T	3.20	± 0.03	3.98	± 0.05	3.51	± 0.03	3.73	± 0.05	3.34	± 0.10
MnO	0.09	± 0.02	0.11	± 0.01	0.11	± 0.02	0.10	± 0.01	0.09	± 0.01
MgO	17.17	± 0.09	16.30	± 0.06	16.53	± 0.06	16.60	± 0.12	16.71	± 0.18
CaO	20.27	± 0.11	20.08	± 0.06	19.85	± 0.12	19.89	± 0.03	20.45	± 0.14
Na_2O	0.92	± 0.05	0.94	± 0.03	1.11	± 0.03	1.03	± 0.05	0.93	± 0.10
Total	100.31	± 0.22	99.41	± 0.53	99.90	± 0.35	100.47	± 0.49	99.69	± 0.76
Mg#	90.53	± 0.10	87.96	± 0.11	89.35	± 0.08	88.81	± 0.11	89.91	± 0.23
Opx:										
SiO_2	54.76	± 0.30	52.74	± 0.23	53.85	± 0.39	53.72	± 0.44	53.84	± 0.46
TiO_2	0.05	± 0.01	0.21	± 0.01	0.17	± 0.01	0.17	± 0.01	0.13	± 0.01
Al_2O_3	4.35	± 0.04	5.85	± 0.04	5.31	± 0.04	5.33	± 0.04	5.13	± 0.04
Cr_2O_3	0.62	± 0.03	0.23	± 0.03	0.39	± 0.02	0.37	± 0.03	0.46	± 0.03
FeO_T	6.11	± 0.10	7.46	± 0.08	6.66	± 0.03	7.07	± 0.05	6.31	± 0.10
MnO	0.13	± 0.01	0.15	± 0.02	0.15	± 0.01	0.15	± 0.02	0.13	± 0.03
MgO	32.94	± 0.07	31.71	± 0.04	32.40	± 0.11	32.08	± 0.26	32.67	± 0.07
CaO	1.14	± 0.02	1.16	± 0.01	1.09	± 0.02	1.12	± 0.02	1.13	± 0.01
Na_2O	0.04	± 0.02	0.05	± 0.02	0.02	± 0.01	0.01	± 0.01	0.01	± 0.01
Total	100.14	± 0.36	99.56	± 0.22	100.05	± 0.34	100.03	± 0.57	99.82	± 0.44
Mg#	90.58	± 0.14	88.34	± 0.11	89.66	± 0.03	88.99	± 0.08	90.22	± 0.15

	SL17-84		SL17-85		SL17-91		SL17-97		TL17-01	
Cpx:	**n = 5**		**n = 4**		**n = 5**		**n = 5**		**n = 5**	
SiO_2	50.25	± 0.24	51.06	± 0.59	51.94	± 0.10	52.24	± 0.19	53.04	± 0.17
TiO_2	0.49	± 0.01	0.32	± 0.00	0.34	± 0.01	0.14	± 0.03	0.11	± 0.05
Al_2O_3	6.72	± 0.05	6.30	± 0.07	6.02	± 0.05	4.90	± 0.10	2.71	± 0.04
Cr_2O_3	0.69	± 0.04	0.93	± 0.04	1.09	± 0.03	1.14	± 0.07	1.33	± 0.01
FeO_T	3.46	± 0.09	3.24	± 0.10	3.02	± 0.05	3.45	± 0.05	2.81	± 0.06
MnO	0.09	± 0.02	0.11	± 0.01	0.09	± 0.01	0.08	± 0.01	0.09	± 0.02
MgO	16.58	± 0.20	16.60	± 0.08	16.88	± 0.14	17.48	± 0.07	18.50	± 0.09
CaO	19.95	± 0.10	19.81	± 0.18	19.87	± 0.13	20.30	± 0.15	21.14	± 0.10
Na_2O	0.97	± 0.07	1.16	± 0.04	1.15	± 0.01	0.87	± 0.03	0.60	± 0.02
Total	99.21	± 0.31	99.54	± 0.91	100.41	± 0.31	100.60	± 0.36	100.34	± 0.20
Mg#	89.52	± 0.24	90.13	± 0.25	90.89	± 0.17	90.04	± 0.14	92.15	± 0.16
Opx:										
SiO_2	53.68	± 0.08	53.90	± 0.39	54.56	± 0.20	54.93	± 0.14	56.43	± 0.28
TiO_2	0.15	± 0.01	0.09	± 0.01	0.09	± 0.01	0.05	± 0.01	0.06	± 0.02
Al_2O_3	5.21	± 0.11	4.83	± 0.04	4.64	± 0.04	3.89	± 0.13	2.10	± 0.05
Cr_2O_3	0.44	± 0.02	0.51	± 0.01	0.57	± 0.02	0.66	± 0.03	0.68	± 0.02
FeO_T	6.55	± 0.11	6.19	± 0.08	5.70	± 0.09	6.58	± 0.03	5.72	± 0.11
MnO	0.14	± 0.01	0.14	± 0.01	0.12	± 0.01	0.15	± 0.01	0.12	± 0.01
MgO	32.41	± 0.17	32.93	± 0.15	33.06	± 0.06	32.90	± 0.09	33.91	± 0.06
CaO	1.11	± 0.06	1.04	± 0.02	1.11	± 0.01	1.17	± 0.02	1.22	± 0.03
Na_2O	0.00	± 0.01	0.03	± 0.02	0.05	± 0.01	0.03	± 0.01	0.00	± 0.01
Total	99.71	± 0.35	99.67	± 0.55	99.92	± 0.21	100.38	± 0.20	100.27	± 0.38
Mg#	89.82	± 0.11	90.46	± 0.09	91.18	± 0.13	89.91	± 0.06	91.36	± 0.15

	TL17-11		TM08-17		TM08-22		TM08-25B		TM08-25C	
Cpx:	**n = 6**		**n = 5**		**n = 3**		**n = 5**		**n = 5**	
SiO_2	51.20	± 0.17	51.51	± 0.62	52.64	± 0.38	51.40	± 0.34	51.34	± 0.30
TiO_2	0.30	± 0.02	0.46	± 0.02	0.04	± 0.03	0.55	± 0.03	0.51	± 0.03
Al_2O_3	6.16	± 0.07	6.45	± 0.12	2.64	± 0.11	6.34	± 0.10	6.67	± 0.57
Cr_2O_3	1.02	± 0.03	0.84	± 0.04	1.00	± 0.08	0.80	± 0.04	0.75	± 0.05
FeO_T	3.32	± 0.06	2.70	± 0.11	2.14	± 0.06	2.52	± 0.07	3.12	± 0.06
MnO	0.10	± 0.02	0.08	± 0.01	0.07	± 0.03	0.08	± 0.02	0.09	± 0.01
MgO	16.62	± 0.09	15.42	± 0.17	17.78	± 0.03	15.23	± 0.10	16.11	± 0.33
CaO	19.62	± 0.10	20.33	± 0.18	22.69	± 0.16	21.07	± 0.17	19.63	± 0.28
Na_2O	1.18	± 0.04	1.68	± 0.02	0.60	± 0.05	1.63	± 0.08	1.48	± 0.16
Total	99.54	± 0.20	99.48	± 0.84	99.60	± 0.42	99.63	± 0.49	99.70	± 0.38
Mg#	89.92	± 0.18	91.06	± 0.28	93.67	± 0.16	91.50	± 0.24	90.20	± 0.33
Opx:										
SiO_2	54.18	± 0.16	54.31	± 0.34	55.45	± 0.38	54.73	± 0.26	53.97	± 0.24
TiO_2	0.10	± 0.01	0.10	± 0.00	0.01	± 0.02	0.11	± 0.02	0.14	± 0.01
Al_2O_3	4.69	± 0.03	4.23	± 0.31	2.47	± 0.12	4.14	± 0.21	5.10	± 0.02
Cr_2O_3	0.58	± 0.03	0.36	± 0.07	0.57	± 0.01	0.36	± 0.03	0.39	± 0.03
FeO_T	6.36	± 0.05	6.31	± 0.09	5.47	± 0.05	6.36	± 0.08	6.52	± 0.07
MnO	0.15	± 0.02	0.16	± 0.00	0.11	± 0.01	0.14	± 0.02	0.14	± 0.03
MgO	32.55	± 0.17	33.37	± 0.16	34.85	± 0.06	33.81	± 0.12	32.81	± 0.07
CaO	1.11	± 0.01	0.57	± 0.02	0.71	± 0.05	0.50	± 0.01	0.91	± 0.02
Na_2O	0.03	± 0.02	0.03	± 0.02	0.01	± 0.01	0.01	± 0.00	0.06	± 0.03
Total	99.77	± 0.28	99.45	± 0.45	99.66	± 0.32	100.16	± 0.29	100.03	± 0.28
Mg#	90.12	± 0.08	90.41	± 0.14	91.91	± 0.06	90.45	± 0.10	89.97	± 0.11

	TM08-30		TM08-34		TM08-38		TM08-41		TM08-43	
Cpx:	**n = 6**		**n = 5**		**n = 5**		**n = 4**		**n = 6**	
SiO_2	51.89	± 0.61	52.44	± 0.45	53.02	± 0.40	50.79	± 0.47	51.43	± 0.38
TiO_2	0.05	± 0.01	0.42	± 0.02	0.03	± 0.01	0.39	± 0.01	0.49	± 0.03
Al_2O_3	3.90	± 0.15	5.63	± 0.51	2.89	± 0.17	7.00	± 0.04	6.75	± 0.14
Cr_2O_3	0.87	± 0.05	1.31	± 0.08	1.07	± 0.09	0.71	± 0.02	0.75	± 0.03
FeO_T	2.40	± 0.03	2.36	± 0.09	2.17	± 0.06	3.55	± 0.03	2.76	± 0.03
MnO	0.08	± 0.01	0.08	± 0.02	0.08	± 0.01	0.09	± 0.00	0.09	± 0.02
MgO	17.08	± 0.18	15.79	± 0.60	17.83	± 0.16	16.28	± 0.04	15.28	± 0.10
CaO	22.25	± 0.14	20.34	± 0.59	22.52	± 0.20	19.60	± 0.11	20.55	± 0.20
Na_2O	0.67	± 0.02	1.60	± 0.33	0.51	± 0.02	1.27	± 0.04	1.64	± 0.05
Total	99.19	± 0.87	100.01	± 0.28	100.12	± 0.51	99.69	± 0.54	99.74	± 0.68
Mg#	92.69	± 0.14	92.26	± 0.08	93.62	± 0.18	89.09	± 0.06	90.78	± 0.12
Opx:										
SiO_2	55.45	± 0.32	55.70	± 0.11	55.95	± 0.43	54.56	± 0.33	54.52	± 0.69
TiO_2	0.02	± 0.01	0.11	± 0.01	0.01	± 0.01	0.12	± 0.01	0.10	± 0.01
Al_2O_3	3.53	± 0.16	3.67	± 0.11	2.60	± 0.16	5.34	± 0.03	4.57	± 0.22
Cr_2O_3	0.47	± 0.04	0.53	± 0.06	0.58	± 0.03	0.38	± 0.01	0.33	± 0.03
FeO_T	5.84	± 0.06	5.68	± 0.08	5.52	± 0.08	6.70	± 0.07	6.51	± 0.10
MnO	0.14	± 0.01	0.14	± 0.01	0.14	± 0.03	0.15	± 0.00	0.16	± 0.01
MgO	34.15	± 0.17	33.83	± 0.14	34.48	± 0.18	32.20	± 0.13	33.45	± 0.13
CaO	0.63	± 0.01	0.61	± 0.01	0.67	± 0.06	1.10	± 0.02	0.58	± 0.02
Na_2O	0.01	± 0.01	0.04	± 0.01	0.00	± 0.00	0.06	± 0.01	0.02	± 0.01
Total	100.23	± 0.36	100.32	± 0.26	99.97	± 0.50	100.61	± 0.23	100.26	± 0.59
Mg#	91.25	± 0.12	91.39	± 0.10	91.76	± 0.10	89.55	± 0.09	90.15	± 0.14

	TM08-48		TM08-49		TM08-52		TM08-54		TM08-63	
Cpx:	**n = 6**		**n = 5**		**n = 7**		**n = 6**		**n = 4**	
SiO_2	52.14	± 0.15	51.93	± 0.25	51.27	± 0.44	51.00	± 0.39	51.07	± 0.23
TiO_2	0.46	± 0.02	0.46	± 0.01	0.47	± 0.01	0.41	± 0.02	0.41	± 0.02
Al_2O_3	6.36	± 0.03	6.43	± 0.07	6.58	± 0.05	6.22	± 0.09	6.40	± 0.13
Cr_2O_3	0.82	± 0.03	0.83	± 0.02	0.80	± 0.04	0.97	± 0.03	0.76	± 0.04
FeO_T	2.87	± 0.04	2.85	± 0.03	2.83	± 0.05	2.69	± 0.05	2.79	± 0.04
MnO	0.10	± 0.01	0.08	± 0.01	0.07	± 0.02	0.08	± 0.01	0.08	± 0.01
MgO	15.96	± 0.10	15.83	± 0.08	15.85	± 0.09	15.78	± 0.13	15.53	± 0.04
CaO	20.17	± 0.09	20.28	± 0.10	20.21	± 0.05	20.40	± 0.08	21.03	± 0.11
Na_2O	1.63	± 0.03	1.55	± 0.03	1.65	± 0.02	1.64	± 0.03	1.56	± 0.06
Total	100.51	± 0.25	100.23	± 0.34	99.74	± 0.46	99.20	± 0.46	99.63	± 0.15
Mg#	90.84	± 0.10	90.83	± 0.12	90.90	± 0.19	91.27	± 0.16	90.85	± 0.12
Opx:										
SiO_2	54.50	± 0.46	54.59	± 0.19	54.62	± 0.38	53.80	± 0.43	54.37	± 0.57
TiO_2	0.11	± 0.01	0.11	± 0.01	0.11	± 0.02	0.09	± 0.02	0.09	± 0.02
Al_2O_3	4.46	± 0.09	4.45	± 0.08	4.60	± 0.08	4.27	± 0.06	4.40	± 0.15
Cr_2O_3	0.41	± 0.02	0.40	± 0.03	0.37	± 0.03	0.42	± 0.04	0.33	± 0.03
FeO_T	6.22	± 0.10	6.26	± 0.06	6.24	± 0.12	6.14	± 0.08	6.42	± 0.07
MnO	0.13	± 0.02	0.13	± 0.02	0.14	± 0.02	0.13	± 0.02	0.14	± 0.02
MgO	33.05	± 0.09	32.72	± 0.18	33.26	± 0.09	33.55	± 0.11	33.35	± 0.10
CaO	0.73	± 0.01	0.74	± 0.01	0.73	± 0.02	0.67	± 0.01	0.62	± 0.02
Na_2O	0.04	± 0.02	0.02	± 0.02	0.04	± 0.02	0.03	± 0.02	0.02	± 0.01
Total	99.64	± 0.57	99.43	± 0.32	100.12	± 0.41	99.12	± 0.51	99.73	± 0.62
Mg#	90.45	± 0.13	90.31	± 0.07	90.48	± 0.18	90.69	± 0.13	90.26	± 0.12

	TM08-64		TM08-A1		TM08-A2A1		TM08-A2A2		TM08-A2B	
Cpx:	**n = 6**		**n = 3**		**n = 5**		**n = 4**		**n = 4**	
SiO_2	51.44	± 0.21	52.48	± 0.30	51.32	± 0.32	52.10	± 0.21	51.67	± 0.43
TiO_2	0.51	± 0.02	0.08	± 0.01	0.46	± 0.03	0.48	± 0.02	0.47	± 0.03
Al_2O_3	6.89	± 0.06	3.36	± 0.11	6.23	± 0.26	6.32	± 0.26	6.78	± 0.15
Cr_2O_3	0.58	± 0.04	1.04	± 0.10	0.96	± 0.06	0.99	± 0.04	0.77	± 0.05
FeO_T	3.00	± 0.05	2.28	± 0.07	2.67	± 0.07	2.63	± 0.02	2.76	± 0.05
MnO	0.10	± 0.01	0.06	± 0.01	0.09	± 0.02	0.09	± 0.00	0.11	± 0.01
MgO	15.70	± 0.09	17.21	± 0.11	15.62	± 0.17	15.68	± 0.10	15.41	± 0.07
CaO	20.12	± 0.11	22.55	± 0.02	20.63	± 0.14	20.68	± 0.11	20.30	± 0.13
Na_2O	1.55	± 0.05	0.69	± 0.04	1.53	± 0.03	1.60	± 0.03	1.70	± 0.03
Total	99.90	± 0.22	99.76	± 0.24	99.52	± 0.24	100.59	± 0.14	99.97	± 0.50
Mg#	90.31	± 0.16	93.08	± 0.15	91.24	± 0.23	91.40	± 0.09	90.88	± 0.16
Opx:										
SiO_2	54.38	± 0.22	55.95	± 0.33	54.36	± 0.41	54.34	± 0.21	55.13	± 0.08
TiO_2	0.12	± 0.01	0.02	± 0.01	0.11	± 0.01	0.09	± 0.01	0.09	± 0.01
Al_2O_3	4.91	± 0.09	2.73	± 0.11	4.31	± 0.36	4.17	± 0.38	4.61	± 0.09
Cr_2O_3	0.29	± 0.02	0.47	± 0.06	0.43	± 0.08	0.43	± 0.05	0.39	± 0.02
FeO_T	6.68	± 0.06	5.81	± 0.18	6.26	± 0.12	6.25	± 0.08	6.46	± 0.06
MnO	0.15	± 0.03	0.14	± 0.01	0.15	± 0.02	0.13	± 0.01	0.15	± 0.01
MgO	32.24	± 0.10	34.73	± 0.32	33.53	± 0.31	33.43	± 0.19	33.16	± 0.02
CaO	0.75	± 0.01	0.60	± 0.03	0.59	± 0.02	0.60	± 0.01	0.64	± 0.01
Na_2O	0.02	± 0.01	0.00	± 0.01	0.01	± 0.01	0.01	± 0.01	0.02	± 0.01
Total	99.55	± 0.24	100.47	± 0.22	99.74	± 0.26	99.46	± 0.29	100.65	± 0.14
Mg#	89.58	± 0.11	91.42	± 0.31	90.52	± 0.22	90.51	± 0.13	90.15	± 0.08

	TM08-B1		TM08-T		TM17-18		TM17-19		TM17-20	
Cpx:	**n = 4**		**n = 6**		**n = 4**		**n = 5**		**n = 7**	
SiO_2	51.26	± 0.44	51.45	± 0.18	51.92	± 0.48	50.39	± 0.51	51.04	± 0.68
TiO_2	0.49	± 0.02	0.53	± 0.02	0.62	± 0.02	0.51	± 0.01	0.49	± 0.02
Al_2O_3	6.81	± 0.19	6.81	± 0.03	6.06	± 0.11	6.86	± 0.09	7.08	± 0.11
Cr_2O_3	0.82	± 0.04	0.74	± 0.03	0.92	± 0.04	0.75	± 0.04	0.63	± 0.04
FeO_T	2.79	± 0.05	3.27	± 0.06	2.47	± 0.08	3.02	± 0.10	3.08	± 0.05
MnO	0.08	± 0.01	0.10	± 0.02	0.07	± 0.01	0.09	± 0.02	0.10	± 0.02
MgO	15.18	± 0.30	15.98	± 0.15	15.23	± 0.07	16.01	± 0.10	15.58	± 0.06
CaO	20.09	± 0.37	19.29	± 0.16	21.24	± 0.10	19.83	± 0.13	20.09	± 0.14
Na_2O	1.72	± 0.04	1.50	± 0.05	1.65	± 0.07	1.53	± 0.02	1.76	± 0.04
Total	99.24	± 1.12	99.67	± 0.30	100.18	± 0.50	99.03	± 0.47	99.84	± 0.93
Mg#	90.66	± 0.17	89.72	± 0.09	91.66	± 0.24	90.42	± 0.35	90.01	± 0.14
Opx:										
SiO_2	55.15	± 0.20	54.34	± 0.21	55.65	± 0.45	52.94	± 0.60	53.84	± 0.53
TiO_2	0.10	± 0.01	0.15	± 0.01	0.10	± 0.01	0.13	± 0.02	0.12	± 0.01
Al_2O_3	4.45	± 0.30	5.01	± 0.05	3.28	± 0.06	5.04	± 0.09	4.93	± 0.14
Cr_2O_3	0.38	± 0.03	0.42	± 0.03	0.32	± 0.03	0.40	± 0.03	0.33	± 0.02
FeO_T	6.59	± 0.05	6.58	± 0.05	6.39	± 0.03	6.35	± 0.11	6.75	± 0.07
MnO	0.16	± 0.02	0.14	± 0.01	0.14	± 0.02	0.15	± 0.01	0.14	± 0.02
MgO	33.19	± 0.15	32.25	± 0.11	33.40	± 0.18	32.83	± 0.14	32.66	± 0.11
CaO	0.59	± 0.01	0.97	± 0.05	0.47	± 0.01	0.84	± 0.01	0.75	± 0.01
Na_2O	0.03	± 0.02	0.06	± 0.01	0.01	± 0.01	0.04	± 0.02	0.05	± 0.03
Total	100.64	± 0.19	99.92	± 0.35	99.76	± 0.57	98.73	± 0.73	99.55	± 0.73
Mg#	89.98	± 0.07	89.74	± 0.06	90.30	± 0.08	90.21	± 0.13	89.61	± 0.08

	TM17-21		TM17-22		TM17-25	
Cpx:	**n = 4**		**n = 5**		**n = 4**	
SiO_2	51.15	± 0.49	50.44	± 0.55	52.10	± 0.17
TiO_2	0.41	± 0.02	0.53	± 0.03	0.02	± 0.01
Al_2O_3	6.29	± 0.09	6.89	± 0.08	2.66	± 0.09
Cr_2O_3	0.88	± 0.02	0.99	± 0.05	1.05	± 0.06
FeO_T	2.62	± 0.04	2.81	± 0.04	2.03	± 0.05
MnO	0.09	± 0.01	0.08	± 0.02	0.07	± 0.01
MgO	15.45	± 0.04	15.32	± 0.10	17.98	± 0.03
CaO	20.99	± 0.06	19.77	± 0.10	23.05	± 0.11
Na_2O	1.59	± 0.04	1.89	± 0.04	0.54	± 0.05
Total	99.47	± 0.52	98.70	± 0.60	99.51	± 0.31
Mg#	91.31	± 0.12	90.68	± 0.11	94.05	± 0.13
Opx:						
SiO_2	54.25	± 0.35	53.13	± 0.63	55.33	± 0.26
TiO_2	0.07	± 0.01	0.12	± 0.01	0.01	± 0.01
Al_2O_3	4.30	± 0.15	4.47	± 0.15	2.47	± 0.06
Cr_2O_3	0.38	± 0.01	0.45	± 0.03	0.62	± 0.03
FeO_T	6.38	± 0.07	6.46	± 0.05	5.40	± 0.13
MnO	0.14	± 0.02	0.15	± 0.02	0.13	± 0.02
MgO	33.38	± 0.08	33.01	± 0.16	34.72	± 0.10
CaO	0.54	± 0.02	0.66	± 0.02	0.66	± 0.01
Na_2O	0.01	± 0.01	0.03	± 0.02	0.00	± 0.00
Total	99.46	± 0.39	98.48	± 0.71	99.37	± 0.40
Mg#	90.32	± 0.11	90.11	± 0.08	91.97	± 0.17

APPENDIX B – ADDITIONAL XENOLITH GEOCHEMISTRY

Table B.1 – Trace and rare earth element concentrations for xenoliths from Mt. Timothy (TM) and Summit Lake (SL) from the original Activation Laboratories dataset (all figures and tables in the main text that involve bulk xenolith trace or rare earth element compositions use the nanoparticulate pressed powder pellet data collected by Chris Lawley).

	TM08-00	**TM08-48**	**TM08-54**	**TM08-63**	**TM08-64**	**TM08-A2A**	**TM17-20**	**TM17-25A**	**SL17-02**
Sc	8	16	14	16	7	13	13	7	25
Be	< 1	< 1	< 1	< 1	< 1	< 1	< 1	< 1	2
V	46	79	66	77	36	61	68	36	192
Cr	1630	2740	3820	2940	1180	2430	3020	1180	150
Co	122	102	100	102	109	107	111	109	25
Ni	2390	1960	1910	2010	2140	2100	2270	2140	80
Cu	< 10	20	< 10	< 10	< 10	20	20	< 10	70
Zn	60	50	60	50	< 30	60	60	< 30	110
Ga	3	3	3	3	2	3	3	2	18
Ge	0.8	0.9	0.9	0.8	0.6	0.8	0.9	0.6	1.7
As	< 5	< 5	< 5	< 5	< 5	< 5	< 5	< 5	10
Rb	< 1	1	< 1	< 1	< 1	< 1	< 1	< 1	< 1
Sr	23	16	7	2	16	30	5	16	579
Y	2.8	3.8	2.6	3	1.2	3.1	2.7	1.2	21.6
Zr	9	7	5	4	6	9	6	6	223
Nb	1.4	< 0.2	< 0.2	< 0.2	0.8	1.1	< 0.2	0.8	24.9
Mo	3	< 2	< 2	3	< 2	< 2	< 2	< 2	< 2
Ag	< 0.5	< 0.5	< 0.5	< 0.5	< 0.5	< 0.5	< 0.5	< 0.5	0.6
In	< 0.1	< 0.1	< 0.1	< 0.1	< 0.1	< 0.1	< 0.1	< 0.1	< 0.1
Sn	< 1	< 1	< 1	1	< 1	< 1	< 1	< 1	3
Sb	< 0.2	< 0.2	< 0.2	< 0.2	< 0.2	< 0.2	< 0.2	< 0.2	< 0.2
Cs	< 0.1	< 0.1	< 0.1	< 0.1	< 0.1	< 0.1	< 0.1	< 0.1	< 0.1
Ba	22	10	8	5	9	33	4	9	134
Bi	< 0.1	< 0.1	< 0.1	< 0.1	< 0.1	< 0.1	< 0.1	< 0.1	< 0.1
Hf	0.2	0.1	< 0.1	< 0.1	< 0.1	0.2	< 0.1	< 0.1	5.1
Ta	0.1	< 0.01	0.03	< 0.01	0.02	0.14	< 0.01	0.02	3.25
W	9.8	< 0.5	< 0.5	< 0.5	8.4	< 0.5	9.8	8.4	< 0.5
Tl	< 0.05	< 0.05	< 0.05	< 0.05	< 0.05	< 0.05	< 0.05	< 0.05	< 0.05
Pb	< 5	< 5	< 5	< 5	< 5	< 5	< 5	< 5	< 5
Th	0.16	< 0.05	< 0.05	0.06	0.08	0.19	< 0.05	0.08	11.3
U	0.05	0.02	< 0.01	< 0.01	0.02	0.06	0.03	0.02	0.92
La	1.87	0.54	0.35	0.18	0.67	1.75	0.26	0.67	46.7
Ce	3.33	1.07	0.67	0.63	1.31	3.82	0.66	1.31	107
Pr	0.43	0.17	0.09	0.07	0.15	0.44	0.11	0.15	13.1
Nd	1.76	1.03	0.5	0.4	0.64	1.9	0.58	0.64	50.2
Sm	0.43	0.34	0.15	0.18	0.15	0.48	0.17	0.15	8.74
Eu	0.11	0.135	0.085	0.081	< 0.005	0.161	0.097	< 0.005	1.87
Gd	0.41	0.46	0.29	0.36	0.17	0.45	0.31	0.17	5.8
Tb	< 0.01	0.09	0.05	< 0.01	< 0.01	0.07	< 0.01	< 0.01	0.81
Dy	0.47	0.58	0.4	0.49	0.19	0.45	0.42	0.19	4.47
Ho	< 0.01	0.13	0.09	0.11	< 0.01	0.09	< 0.01	< 0.01	0.78
Er	0.28	0.39	0.3	0.34	0.14	0.27	0.31	0.14	2.12
Tm	< 0.005	0.06	0.05	0.053	< 0.005	0.044	< 0.005	< 0.005	0.291

	SL17-36	SL17-41	SL17-43	SL17-47	SL17-48	SL17-49	SL17-57	SL17-74	SL17-80
Sc	16	17	15	8	17	16	17	8	13
Be	< 1	< 1	< 1	4	< 1	< 1	< 1	< 1	3
V	83	80	83	54	83	81	94	39	93
Cr	2530	2340	2590	60	2130	2310	3260	1960	120
Co	101	100	106	12	119	99	111	115	19
Ni	1980	1960	1950	40	1710	1880	1820	2190	60
Cu	20	40	40	100	10	40	20	< 10	230
Zn	50	50	60	60	60	50	70	50	70
Ga	4	3	4	20	4	3	5	1	23
Ge	0.9	1	1.2	1.3	0.8	1	1.1	0.6	1.4
As	< 5	< 5	< 5	< 5	< 5	< 5	< 5	6	< 5
Rb	2	< 1	< 1	< 1	< 1	< 1	< 1	< 1	2
Sr	17	14	15	1203	24	11	25	3	916
Y	4	3.9	3.8	9.6	5.6	3.7	4.9	< 0.5	13.4
Zr	10	6	8	121	17	6	9	2	134
Nb	< 0.2	0.3	0.8	70.7	1.3	< 0.2	< 0.2	< 0.2	22.4
Mo	3	< 2	< 2	< 2	2	< 2	< 2	< 2	< 2
Ag	< 0.5	< 0.5	< 0.5	< 0.5	< 0.5	< 0.5	< 0.5	< 0.5	< 0.5
In	< 0.1	< 0.1	< 0.1	< 0.1	< 0.1	< 0.1	< 0.1	< 0.1	< 0.1
Sn	< 1	< 1	< 1	1	< 1	< 1	< 1	< 1	2
Sb	< 0.2	< 0.2	< 0.2	< 0.2	< 0.2	< 0.2	< 0.2	< 0.2	< 0.2
Cs	< 0.1	< 0.1	< 0.1	< 0.1	< 0.1	< 0.1	0.2	< 0.1	< 0.1
Ba	17	24	28	447	18	13	5	5	274
Bi	< 0.1	< 0.1	< 0.1	< 0.1	< 0.1	< 0.1	< 0.1	< 0.1	< 0.1
Hf	0.2	< 0.1	0.2	2.6	0.4	0.1	0.2	< 0.1	3.3
Ta	< 0.01	0.06	0.07	4.16	0.14	< 0.01	< 0.01	< 0.01	1.93
W	< 0.5	0.8	< 0.5	< 0.5	< 0.5	6.7	< 0.5	4	< 0.5
Tl	0.27	0.21	< 0.05	0.08	0.06	< 0.05	< 0.05	< 0.05	< 0.05
Pb	< 5	< 5	< 5	< 5	< 5	< 5	< 5	< 5	< 5
Th	0.47	0.09	0.1	8.29	0.27	< 0.05	< 0.05	< 0.05	3.99
U	0.02	0.02	0.04	1.34	0.09	0.01	0.01	0.02	0.67
La	1.46	0.56	0.93	46.3	2.05	0.4	1.26	0.16	56
Ce	3.88	1.44	2.21	84.4	5.8	0.81	4.22	0.26	103
Pr	0.54	0.21	0.28	8.93	0.85	0.12	0.65	0.03	10.8
Nd	2.31	1.05	1.55	30.1	3.96	0.63	3.48	0.21	37.4
Sm	0.52	0.37	0.41	4.12	1.08	0.41	1.06	0.03	5.57
Eu	0.185	0.166	0.203	1.11	0.315	0.13	0.265	< 0.005	1.36
Gd	0.53	0.46	0.39	2.61	1.02	0.39	0.93	0.04	3.71
Tb	< 0.01	0.1	0.09	0.37	0.17	0.07	0.15	< 0.01	0.5
Dy	0.69	0.65	0.66	2.08	0.97	0.56	0.9	0.05	2.66
Ho	0.15	0.15	0.13	0.35	0.2	0.13	0.17	< 0.01	0.49
Er	0.46	0.47	0.38	1	0.57	0.4	0.49	0.03	1.42
Tm	0.07	0.07	0.055	0.147	0.084	0.058	0.069	0.006	0.19
Yb	0.48	0.4	0.43	0.96	0.55	0.37	0.45	0.07	1.36
Lu	0.071	0.056	0.062	0.164	0.086	0.054	0.064	0.017	0.224
Yb	0.25	0.38	0.3	0.33	0.16	0.28	0.28	0.16	1.82
Lu	0.041	0.063	0.052	0.05	< 0.002	0.046	0.042	< 0.002	0.274

	SL17-81B	SL17-81C	SL17-82	SL17-84	SL17-85	SL17-97	TL17-01	TL17-12
Sc	15	14	14	15	11	8	7	6
Be	< 1	< 1	< 1	< 1	< 1	< 1	< 1	< 1
V	78	64	68	72	55	37	29	26
Cr	2520	2240	2770	2940	2570	2460	3700	3950
Co	105	108	107	102	105	121	122	129
Ni	1900	2070	2200	2020	2160	2410	2610	2470
Cu	40	30	20	30	20	< 10	< 10	< 10
Zn	60	50	50	50	60	60	60	50
Ga	3	3	3	3	2	2	1	1
Ge	1	0.9	0.9	0.8	0.7	0.8	0.8	0.6
As	< 5	< 5	< 5	< 5	< 5	< 5	< 5	< 5
Rb	5	< 1	< 1	< 1	< 1	< 1	< 1	1
Sr	14	15	5	11	5	8	2	13
Y	3.5	3.1	2.9	3.8	1.9	0.6	< 0.5	0.6
Zr	10	5	8	12	6	5	5	4
Nb	< 0.2	< 0.2	< 0.2	< 0.2	< 0.2	< 0.2	< 0.2	0.3
Mo	< 2	< 2	< 2	< 2	< 2	< 2	2	< 2
Ag	< 0.5	< 0.5	< 0.5	< 0.5	< 0.5	< 0.5	< 0.5	< 0.5
In	< 0.1	< 0.1	< 0.1	< 0.1	< 0.1	< 0.1	< 0.1	< 0.1
Sn	< 1	< 1	< 1	< 1	< 1	< 1	< 1	< 1
Sb	< 0.2	< 0.2	< 0.2	< 0.2	< 0.2	< 0.2	< 0.2	< 0.2
Cs	< 0.1	< 0.1	< 0.1	< 0.1	< 0.1	< 0.1	< 0.1	< 0.1
Ba	21	13	4	24	7	5	4	28
Bi	< 0.1	< 0.1	< 0.1	< 0.1	< 0.1	< 0.1	< 0.1	< 0.1
Hf	0.2	< 0.1	0.1	0.3	< 0.1	< 0.1	< 0.1	< 0.1
Ta	< 0.01	0.03	< 0.01	0.03	< 0.01	0.03	0.02	0.05
W	< 0.5	< 0.5	< 0.5	< 0.5	< 0.5	1.5	3.6	< 0.5
Tl	< 0.05	< 0.05	0.07	0.1	< 0.05	< 0.05	< 0.05	< 0.05
Pb	< 5	< 5	< 5	< 5	< 5	< 5	< 5	< 5
Th	< 0.05	< 0.05	< 0.05	0.18	< 0.05	< 0.05	< 0.05	0.05
U	0.01	< 0.01	< 0.01	0.02	< 0.01	< 0.01	< 0.01	0.01
La	0.48	0.53	0.12	0.53	< 0.05	0.84	0.21	0.59
Ce	1.21	1.3	0.34	1.28	0.18	1.6	0.47	1.15
Pr	0.23	0.2	0.06	0.16	0.04	0.17	0.06	0.14
Nd	1.45	0.94	0.43	0.99	0.32	0.51	0.22	0.74
Sm	0.36	0.26	0.18	0.28	0.13	< 0.01	< 0.01	0.11
Eu	0.127	0.117	0.089	0.102	0.046	< 0.005	< 0.005	0.03
Gd	0.38	0.42	0.32	0.44	0.18	< 0.01	< 0.01	0.08
Tb	0.09	0.08	< 0.01	0.1	0.04	< 0.01	< 0.01	0.02
Dy	0.61	0.52	0.45	0.63	0.29	< 0.01	< 0.01	0.12
Ho	0.14	0.11	0.11	0.13	0.06	< 0.01	< 0.01	0.02
Er	0.36	0.32	0.3	0.4	0.2	< 0.01	< 0.01	0.07
Tm	0.05	0.055	< 0.005	0.061	0.033	< 0.005	< 0.005	0.012
Yb	0.33	0.37	0.3	0.42	0.26	0.11	< 0.01	0.08
Lu	0.052	0.056	0.045	0.064	0.049	< 0.002	< 0.002	0.015

APPENDIX C – MODAL MINERALOGY

Modal mineralogies of all ultramafic xenoliths were determined via a point counting code written in MatLab. The code – outlined below – was created when it was determined that more widely used techniques for calculating modal mineralogies would be either ineffective or overly arduous for the available sample collection.

Manual point counts using a microscope and a physical point counter would have been limited in their usefulness largely due to how coarse-grained and heterogenous many of the peridotite samples are. Effectively, a single, or a handful of, transects across a given thin section would not be guaranteed to accurately represent the mineralogy of the section as a whole. Taking enough transects to obtain an accurate representation of each sample would have taken more time and effort than was necessary for these analyses.

The other suggested method for obtaining these modal mineralogies was by using the color thresholding functions available with the ImageJ image processing software. Here, the software would load a scan of a thin section and would determine the percentages of the scan occupied by different colors. This would be made possible by the thicker-cut 100 um sections showing clearer distinctions between different minerals than would more standard 30 um sections. This was found to be somewhat effective for determining olivine abundances in the samples but differentiating between orthopyroxene and clinopyroxene grains proved much more difficult for ImageJ to do with any level of precision. Additionally, the abundance of dark grain fractures boundaries and spotty alteration in many samples made color thresholding an ineffective technique for these samples.

The MatLab point counting code written to solve these issues, like the image thresholding method, is possible due to the clearer mineral distinctions of the thick-cut sections and runs according to the following outline:

1. Import thin section scan
2. Read image dimensions
3. Create list of *n* randomly generated coordinate pairs, with *n* determined by user input, based on image dimensions
4. Zoom to the first coordinate pair on the thin section scan (point marked by an X)
5. Request user input for mineral marked by point (i.e. olivine, orthopyroxene, clinopyroxene, spinel, other, or blank space)
6. Repeat steps 4 and 5 until mineral types are saved for all *n* coordinate pairs
7. Determine modal mineralogy and rock type of section based on the entered values

A series of trials were run on sample TM08-25B to determine the number of randomized coordinate pairs necessary to record satisfactorily precise counts for olivine, orthopyroxene, and clinopyroxene. Here, the script was run five times each for random selections of 50, 100, 250, 500, and 1000 points on this sample, with the averages and standard deviations being recorded for each set of five runs (displayed in Figure C.1). It was found that repeated runs of 1000 points produced highly precise, very repeatable modal percentages for the three minerals: thus, 1000 runs was determined to be the minimum number of trials required for point counts on each sample.

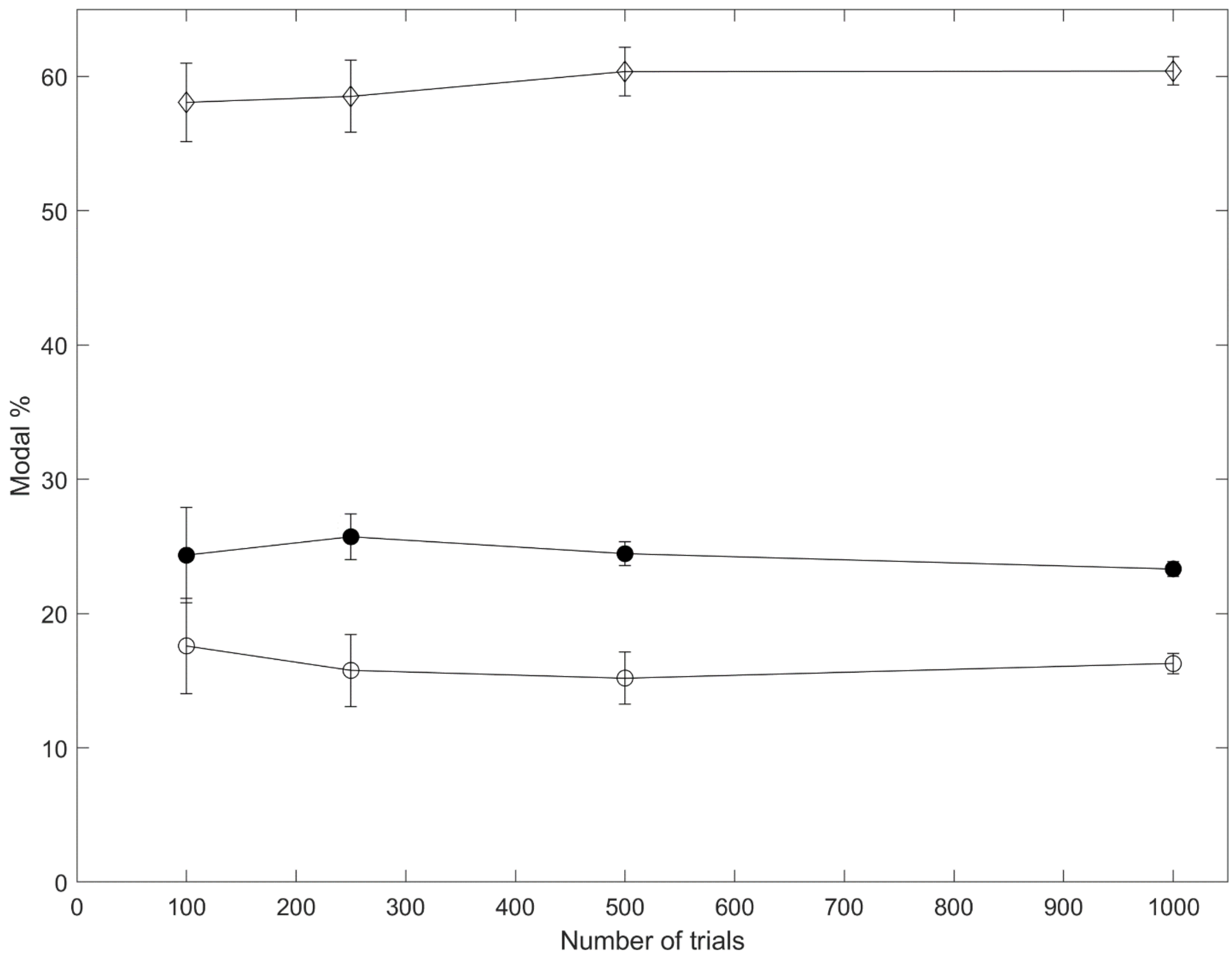

Figure C.1 – Statistics on 5-run trials of the point counter script for olivine (open diamonds), orthopyroxene (filled circles), and clinopyroxene (open circles). Error bars are +/- one standard deviation, and points are averages, each for 5 runs at that Number of Trials.